UNIVERSITY OF OKLAHOMA

GRADUATE COLLEGE

MODELING AND ANALYSIS OF THE INTERACTION BETWEEN ROLLER DRUM AND PAVEMENT MATERIAL DURING COMPACTION

A DISSERTATION

SUBMITTED TO THE GRADUATE FACULTY

in partial fulfillment of the requirements for the

Degree of

DOCTOR OF PHILOSOPHY

By

SYED ASIF IMRAN
Norman, Oklahoma
2016

MODELING AND ANALYSIS OF THE INTERACTION BETWEEN ROLLER DRUM AND PAVEMENT MATERIAL DURING COMPACTION

A DISSERTATION APPROVED FOR THE
SCHOOL OF ELECTRICAL AND COMPUTER ENGINEERING

BY

_____
Dr. Sesh Commuri, Chair

_____
Dr. Musharraf Zaman

_____
Dr. James Sluss

_____
Dr. Thordur Runolfsson

_____
Dr. Choon Yik Tang

_____
Dr. Fares Beainy

This Dissertation is dedicated to my family, my father, Dr. S. M. Ebad Ullah, my mother, Roksana Begum, my sister, Tanzima Sultana, my brother, Abid Sahdman, and last but not the least, my wife, Shahida Chowdhury

for they mean everything to me.

Acknowledgements

I would like to start by expressing my sincere gratitude and appreciation to my advisor, Dr. Sesh Commuri, for his cordial support, guidance, and encouragement throughout my graduate studies. His inspirational and motivational presence as a mentor helped me to grow as a researcher. I always found him extremely supportive during the difficult days of my academic and personal life.

I am grateful to my committee member, Dr. Musharraf Zaman, for all his support during the course of my graduate studies. His insightful comments and advices had a significant impact on the quality of my research. I would also like to thank my other committee members, Dr. James Sluss, Dr. Thordur Runolfsson, Dr. Choon Yik Tang, and Dr. Fares Beainy for their cordial support in the completion of my dissertation.

I would also like to extend my heartiest thanks to my colleagues Dr. Manik Barman and Mr. Moeen Nazari. Their courteous and valuable cooperation and expertise in pavement engineering helped me conduct my research in an interdisciplinary area. I was fortunate enough to have them in my team. We performed numerous field investigations during the red, hot summers of Oklahoma over the past several years. I would also like to acknowledge the contributions of my other co-workers, Dr. Fares Beainy, Dr. Amir Arshadi, and Dr. Anh Mai in the process of my graduate studies.

I would like to thank the Volvo Construction Equipment (VCE), Oklahoma Department of Transportation, Oklahoma Transportation Center (OkTC), and Southern Plains Transportation Center for providing me with all the financial and logistic support needed for this research. The field investigations demonstrated in this research would

not have been possible without the support of Haskell Lemon Construction Co. at Oklahoma City, and Silver Star Construction Company at Moore, Oklahoma.

At the end of my academic journey as a student, I would like to pay my deepest respect and gratitude to all my teachers and mentors throughout my academic life. I am indebted to my family for everything I achieved in my life. I cannot express in words how grateful I am for all the sacrifices they made for me. Finally, a special thanks to all my friends for their precious support, company, and friendship in my life.

Table of Contents

List of Tables

List of Figures

Abstract

The problem of ensuring real time control of compaction quality during pavement construction is considered in this dissertation. Asphalt pavements are complex, multilayer, heterogeneous structures where different layers of asphalt mixes are often placed on top of and supported by a base subgrade layer. In order to ensure long term performance of these pavements, it is imperative to ensure proper quality in both the subgrade and the asphalt layer during their construction. Compaction is one of the important steps in pavement construction that significantly affects the quality and long term performance of the pavement. Proper and uniform compaction of the subgrade and asphalt layers during construction is necessary for the pavement to support the expected traffic load over its lifetime. Inadequate compaction of asphalt layers could result in a pavement with insufficient stiffness leading to problems such as reduced fatigue life, accelerated aging/decreased durability, rutting, raveling, and moisture damage. The underlying subgrade also needs sufficient compaction to ensure adequate load bearing capacity of the pavement and reduce its susceptibility to moisture and other weather-related distresses.

Although the impact of compaction on the performance and longevity of pavements is well understood, addressing compaction issues during construction is not easy given the limitations in the available quality control tools. The traditional QC methods rely on in situ measurement devices that provide an estimate of compaction quality at discrete test locations and generally cover less than 1% of the entire pavement area. Therefore, it is not possible to address under-compaction in areas other than those identified at the test locations. Besides, the tests are time consuming, expensive, and often destructive

in nature. In order to overcome these limitations, 'Intelligent Compaction (IC)' methods have been proposed to provide 100% coverage of the pavement surface during compaction. These methods analyze the vibrations of roller drum and provide an estimate of the stiffness of the compacted pavement material. Further, these systems have integrated Global Position Sensors (GPS) and computational devices that record the spatial location of the roller and the stiffness values continuously during compaction. One major limitation in the available IC technologies is that they provide the estimation of pavement quality in terms of vendor specific values and do not provide estimates in terms of any of the parameters used in the design of the pavement. The relationship between these measurement values and accepted measures such as modulus or pavement density is also not well established. Limitations in the understanding on the coupled dynamics between a vibratory roller and lack of mathematical framework hamper the research and validation of the IC technologies.

In this dissertation, the limitations of the IC technologies in quality control of asphalt compaction are addressed through the development of a mathematical model to study and analyze the interaction between a moving vibratory roller and the underlying asphalt pavement. A lumped element modelling approach is adopted and the vibration of the roller drum, its movement along and interaction with the pavement are formulated by mathematical equations. The asphalt pavement is represented by a collection of blocks of mechanical elements arranged in a grid wise manner with each block exhibiting visco-elastic and plastic properties. The asphalt model parameters are estimated from the results of standard laboratory complex modulus test. These parameters account for the effect of pavement temperature, layer thickness, loading

frequency and volumetric properties of asphalt mix. Numerical simulations are performed to study the ability of the model to replicate the results of field compaction. Comparison of the model simulation results with field compaction data shows that the model can emulate the salient characteristic vibratory response of the drum observed during field compaction. The results also indicate that the model is able to replicate the pass by pass densification process during field compaction. Analyses of the results show that the model can be used to account for the asphalt-roller interaction in both the vertical and the horizontal directions.

The development of an intelligent compaction technology for real time control of subgrade quality is also addressed in this dissertation. An Artificial Neural Network (ANN) based intelligent compaction system is developed to estimate the stiffness of the subgrade during compaction. The ANN classifies the vibrations of the roller drum during compaction into known patterns. Details of the pavement under compaction and the classified patterns are then used together to estimate the stiffness of the layer. A calibration procedure is developed that can adjust the IC parameters to minimize the error between the IC estimated stiffness values and in-situ measurements taken after the pavement is fully compacted. The system was tested and validated during four different construction projects. The results indicate that the system is capable of real time estimation of subgrade stiffness with accuracy suitable for contractor's quality control operations. Field investigations also indicate that the system can be used for detecting under-compacted regions of subgrade in real time, thereby allowing remedial actions to be performed.

Improving the overall quality of pavement during construction will improve its performance and service life and reduce the cost to maintain it over its lifetime. It will help to improve driver safety by providing a smooth, stable and skid resistant surface for the vehicle. Sustainable pavements will also reduce the impact of road construction on the environment.

CHAPTER 1 Introduction

Asphalt pavements constitute an important part of the transportation infrastructure and play a significant role in the economy of the United States. Pavements are designed to accommodate current and predicted traffic needs in a safe, durable, and cost effective manner (FHWA, 1999). Asphalt pavements are complex, multilayer, heterogeneous structures constructed on top of a prepared base. A well-designed and well-constructed asphalt pavement can support traffic loads without premature deterioration and provide smooth riding surface over its lifetime. Compaction of the pavement is one of the important steps in its construction and has a direct effect on the quality, longevity and performance of the pavement. In order to ensure long term performance of these pavements, it is imperative to ensure proper quality of both the subgrade and the asphalt layers during construction.

1.1 Importance of the Problem

There are over 2.6 million miles of paved roads (NAPA, 2014) in the country. These roads are an important part of the transportation network and play a vital role in every aspect of human activity from economy to homeland security. In the United States, approximately 24 million children, comprising 55% of the country's kindergarten through high school population, use school buses to commute 180 days each year. More than 60 million trips are made by over 50,000 ambulances every year (over 164,000 trips each day) to transport the sick to the hospitals. Emergency responders and the fire department have to respond to a fire alarm with one or more vehicles every 20 seconds throughout the year (AASHTO, 2009). In 2015 alone, private and commercial vehicles

traversed over 3 trillion vehicle miles on the roadways (FHWA, 2015). Pavements also have a significant role in the transportation of freight. In 2012, more than 8 billion tons of freight, valued over $10 trillion (73% of the total value of all goods shipped), was transported by trucks in the United States (Margreta et al., 2014). Over the next decade, overall freight volume is expected to grow by 29% with a 74.5% increase in revenue to $1.52 trillion (ATA, 2015).

The importance of road infrastructure in everyday life of the American people makes it necessary for the roads to be maintained in good condition. Each year a significant budget outlay is required for maintenance and upkeep of roads and early deterioration of the pavement imposes additional budgetary demands that are hard to meet. According to the Federal Highway Administration (FHWA), more than $46 billion was spent only on highway maintenance in 2011 (FHWA, 2011). This is still not sufficient enough considering the fact that 65 percent of America's major roads are rated in less than good condition (White House, 2014). In the most recent World Economic Forum rankings (White House, 2014), it is shown that in less than a decade the U.S. had fallen from 7th to 18th overall in the quality of roads. The American Society of Civil Engineers gave U.S. infrastructure a dismal D+ rating in its 2013 assessment, which is a marginal and insignificant improvement over its D rating in 2009 (ASCE, 2014). The 2015 AASHTO Transportation Bottom Line Report found that the U.S. currently has a $740 billion backlog in improvements needed to restore the nation's roads, highways and bridges to the level of condition and performance needed to meet the nation's transportation demands (Pisarski and Reno, 2015).

Poor pavement condition has both direct and indirect impact on the nation's economy. The costs of inadequate infrastructure investment are exhibited all around the United States. Americans spend 5.5 billion hours in traffic each year, costing families more than $120 billion in extra fuel and lost time condition (White House, 2014). American businesses pay $27 billion a year in extra freight transportation costs, increasing shipping delays and raising prices on everyday products. It also has an adverse effect on the safety of the people using it. There were more than 33,000 traffic fatalities last year alone and roadway condition is a significant factor in approximately one-third of traffic fatalities. Such fatalities occur disproportionately in rural America, in part because of poor road conditions.

Asphalt pavements constitute 93% of the total pavements in the United States (NAPA, 2014). The durability of these asphalt pavements can be increased to a great extent by ensuring adequate quality during construction. The construction of an asphalt pavement is a multistep process starting with the design of the pavement according to the specifications based on the type of the road, traffic volumes, intended use, condition of the underlying base layer, as well as the seasonal variations that the road has to withstand. The next steps typically include preparation of the base layer to support the asphalt pavement, production of hot mix asphalt according to the design, transportation of asphalt mix from the production facility to the construction site, placement of the mix, and then compaction of the mix using vibratory rollers to achieve the desired density. Compaction is one of the most important steps in pavement construction as it can significantly affect the quality of the constructed pavement. Compaction of asphalt mix increases the interlocking between aggregates and thereby reduces the air void

content between aggregates. Studies suggest that for optimal performance of asphalt pavement, the air void content is required to be between 3% and 5% (Scherocman, 2000). Under-compacted pavements lead to early deterioration by reducing the fatigue life. Experiments show that reducing the air-void content of a given asphalt-concrete mix from 8% to 5% can improve the fatigue life of pavements by 100%. Proper compaction also reduces pavement deterioration due to rutting, oxidization, moisture damage, distortion, and disintegration or raveling of the pavement (Scherocman and Dwight, 2008). Adequate compaction is also important in preparation of subgrade layers. A well compacted and good quality subgrade increases the load bearing capacity of the pavement and reduces susceptibility to moisture and other weather condition-related distresses.

1.2 Motivation

The importance of adequate compaction of the pavement layer during construction is widely accepted. During compaction with a vibratory roller, both the static weight of the roller and the vibrating force generated by an assembly of rotating eccentric masses in the roller drum are used to compact the underlying pavement. The magnitude and frequency of vibratory force is controlled by changing the rotational frequency and the eccentricity of the unbalanced eccentric masses around the axle of the drum. In the traditional compaction method, constant amplitude and loading frequency are used throughout the process while maintaining a constant roller speed. Thus, assuming that the field conditions and the properties of the pavement are unchanged, a constant compacting force will result in a constant level of compaction over the entire pavement. However, this is not the case in general as the environmental and pavement conditions

vary during compaction. During compaction of asphalt layer, the quality achieved is influenced by several factors such as ambient temperature, wind-velocity and relative humidity, solar radiation, stiffness of the underlying layer, rheological and volumetric properties of the asphalt mix at laydown and thickness of asphalt mat (Brown et al., 2009). Variations in any of these factors during construction may result in non-uniform compaction. The compaction quality also varies laterally from the central portion of a stretch to the unconfined edges. Investigations carried out during field compaction have shown as much as 2% variation in density in locations less than a meter apart from each other (Beainy et al., 2012). In the case of subgrade, the compaction quality is affected by factors such as the properties of the soil, the moisture content and amount and type of additives mixed with the subgrade.

The variations in field and pavement conditions necessitate the use of continuous quality control techniques during compaction. Unfortunately, existing quality control (QC) procedures only test the pavement at discrete number of locations after the construction is complete. Further, these tests are time consuming and in some cases, destructive in nature. A brief description the existing QC procedures is provided to highlight the motivation for this research.

1.2.1 Quality Control Procedures during Field Compaction

The long term performance of asphalt pavement depends, to a large extent, on its ability to support rated vehicular traffic without undergoing deterioration. Therefore, the pavement structure has to have adequate stiffness to support the load. While stiffness is one of the criteria considered during the design of pavements (ARA, 2004), this

quantity is seldom measured during the construction process. Instead, density of asphalt layer (dry density and moisture content, in case of subgrades) is measured with the implicit understanding that the measured values are directly related to the stiffness as long as all other parameters are held constant.

Today, most of the state departments of transportation (DOTs) in the United States use density to assess the quality of construction of asphalt pavement (FHWA, 2014). A widely accepted method of assessing quality is the extraction of field cores at several locations and evaluating their densities in the laboratory as specified in AASHTO T-166. Although this test method is very reliable, it is time consuming, expensive, destructive, and provides quality at a few discrete locations. Alternative methods for in-place measurement of density of hot mix asphalt (HMA) layers include both nuclear density gauges and nonnuclear density gauges (Allen et al., 2003; Sebesta et al., 2006; Herbert and Jennette, 2011) which are also spot testing methods.

The traditional quality control (QC) method used during subgrade compaction is limited to in-situ testing of density and moisture content, preferably using a Nuclear Density Gauge (NDG) (Rahman et al. 2008). Several other test methods using devices, such as California Bearing Ratio (CBR), Dynamic Cone Penetration (DCP) (Davisch et al., 2006; Siekmeier et al., 2000; Burnham, 1997), Light Weight Deflectometer (LWD), Falling Weight Deflectometer (FWD) (Nazzal and Mohammad, 2010; Russell and Hossain, 2000) are also used to determine the strength and stability of the soil subgrade.

One of the major limitations of these traditional QC methods for both asphalt as well as subgrade layers are that they are spot testing methods which generally covers less than

1% of the entire pavement area and do not evaluate the entire pavement. The tests are also time consuming and can be conducted only post compaction. Therefore, there is an urgent need to develop alternate QC methods that can provide accurate estimates of quality of the entire pavement in real time.

1.2.2 Intelligent Compaction for Continuous Control of Pavement Quality

Limitations of the traditional field testing methods in ensuring continuous control have motivated the development of advanced technologies such as Intelligent Compaction. Intelligent Compaction research is a method that integrates accelerometers, global positioning system (GPS) sensors, and computational units to estimate the stiffness of the pavement during vibratory compaction. Further, these systems provide real-time coverage of the entire pavement surface thereby enabling the detection of over/under compaction of the material. Intelligent compaction is based on the hypothesis that the vibratory roller and the underlying pavement form a coupled system whose response characteristics are influenced by the stiffness of the pavement layers underneath the roller. Therefore, any change in the stiffness of the pavement layer will affect the roller response (Commuri and Zaman, 2008 & 2010). Researchers have attempted to analyze the drum vibrations as a means of developing techniques for estimating the quality of compaction (Thurner and Sandström, 2000; Anderegg and Kaufmann, 2004; Åkesson, 2008; Connolly, 2008; Rakowski, 2008; Rawls and Potts, 2008). Several IC systems have also been introduced in recent years by the manufacturers of vibratory compactors (Arasteh, 2007; Briaud and Seo, 2003; Camargo et al., 2006; CTC, 2006; Wisdom, 2009; Moore, 2006; Petersen, 2005; Peterson and Petersen, 2006; Thompson, 2006).

Geodynamik (FHWA, 2014) uses a dimensionless compaction parameter called 'Compaction Meter Value' (CMV) to indicate the level of compaction. This parameter is based on the assumption that the harmonic components of drum vibration are influenced by the stiffness of the underlying material. CMV is calculated as a ratio of the amplitude of 2^{nd} harmonic to the amplitude of fundamental frequency (Sandstrom and Pettersson, 2004). Sakai (2016) utilized the concept of jumping motion of the roller with the increase of stiffness of pavement material. The changes in amplitude spectrum with increase of ground stiffness are studied and a parameter named 'Compaction Control Value' is proposed which is dependent on the amplitude of different spectral components. BOMAG (2016) reports a modulus value, E_{Vib}, based on the one degree of freedom lumped parameter model and Lundeberg's theoretical solution for a rigid cylinder sitting on an elastic half space (Hertz, 1895; Lundberg, 1939; Krober et al., 2001). Caterpillar introduced machine drive power (MDP) as a parameter that evaluates the rolling resistance as an indicator of stiffness. These IC technologies perform as real time indicators of pavement quality and facilitate the quality control procedures. These devices provide continuous real time quality control during compaction. However, there are many limitations in the use of these IC devices to control pavement stiffness during construction. Most of the IC devices provide their device specific measurement values commonly known as Intelligent Compaction Measurement Values (ICMV) as an indicator of the pavement quality. Although these technologies are an encouraging addition to the quality control methods of pavement construction, the relationship between these device-specified ICMV values and the in situ measurement results are yet to be established. The correlation between the ICMV values and the design quality

parameters such as pavement density and resilient modulus is also under investigation (Maupin, 2007; Chang et al., 2011; Chang et al., 2014).

In recent years, researchers at the University of Oklahoma have developed and successfully demonstrated the Intelligent Asphalt Compaction Analyzer (IACA) for real time estimation of pavement density during compaction of asphalt pavement (Commuri and Zaman, 2008 & 2010). Success of IACA in estimation of asphalt density has also encouraged the researchers to extend this technology for estimation of subgrade quality.

While commercially available IC techniques are useful for quality control during construction, they do not provide any insight into the behavior of the mix during the compaction process. Limited research in the dynamics of field compaction and lack of mathematical framework to express the coupled interaction between a moving vibratory roller and the underlying pavement hampers the validation of such IC technologies and their use in understanding the compaction process.

1.2.3 Modeling the Compaction of Asphalt Pavement

Compaction has an important effect on the long term performance of asphalt pavement. Inadequate compaction can potentially expose the pavement to several types of distresses notably, moisture and oxygen diffusion, rutting, raveling, cracking and low fatigue life. Therefore, studies of asphalt materials are predominantly focused on developing models to understand the long term behavior and the deterioration it experiences during its life span (Bonaquist and Christensen, 2005; Cominsky et al., 1998; Chen and Huang, 2000; Pellinen and Witczak, 2002; Shenoy and Romero, 2002; Witczak, 2002; Zapata and Houston, 2008; Loulizi et al., 2007; Desai, 2008; Zapata and

Houston, 2008; Woo et al., 2008; Goh et al., 2011). Very few attempts have been made to study the behavior of asphalt material during compaction. Krishnan and Rao (2000) utilized the theory of mixes to study the reduction of air voids in asphalt mixes during compaction. Asphalt concrete was modeled as a mixture of asphalt, aggregates and initial air voids. The response of this model was then simulated under quasi static load assuming isothermal conditions. Guler et al. (2002) developed a porous elasto-plastic material model with a modified Gurson-Tvergaard yield function. Simple linear models were then developed to predict the model parameters based on the mix properties. In order to accomplish this, a parameter estimation algorithm was proposed and implemented for selected constitutive relations. This model was used to estimate the volume change of mix specimen under continuous gyratory compaction by the Superpave gyratory compactor. Huerne (2004) proposed a constitutive model of asphalt mix using critical state theory adopted from the soil mechanics. The asphalt mix was considered as a granular material whose behavior was characterized as elastic (until the particles start to move) and plastic (when the particles move). The critical state theory was used to expresses a relationship between the specific volume of the material and the stress situation inside the material based on the particle movements. The model was used to study compaction using a static roller. The effect of mix properties such as temperature was not taken into account. Shen and Lin (2008) introduced an asymmetric hysteresis model based on Bouc-Wen differential equation (Bouc, 1967; Wen, 1976) to investigate the dynamic characteristics of a vibratory compaction system. An asymptotic method combining Krylov-Bogolyubov-Mitropolsky method with harmonic balance method was used to study the steady state response of the system under

harmonic excitation. The model was able to address the response of the drum. However, the properties of the asphalt mix and their effect on the dynamics was not taken into account. Koneru et al. (2008) developed a constitutive model using a thermodynamic framework to study the compaction of asphalt mixes. In this method, the notion of multiple natural configurations assumed by a body was used to analyze compaction of asphalt mixes using laboratory equipment.

Micaelo et al. (2009) used a micromechanical Discrete Element Method (DEM) to study the evolution of particle structure during field compaction. Masad et al (2010) used a thermodynamics based nonlinear viscoelastic model of the asphalt mix. A finite element based numerical scheme was developed to simulate the response during laboratory and field compaction. This model was used to demonstrate the influence of material properties such as binder viscosity, aggregate shape characteristics, and aggregate gradation on the static compaction of asphalt specimen. Chen (2011) formulated a Discrete Element Method based model of asphalt compaction considering the viscoelastic property of the mix as well as the slippage and interlocking of the aggregates during compaction. Kassem at al. (2012) performed a comprehensive evaluation of compaction of asphalt pavements and developed software for monitoring field compaction in real time. The research was aimed at understanding the effects of compaction temperature, compaction method, mix design, and base type on the compaction quality of asphalt mixes. The results suggested that vibratory rollers can reduce the air void content of the pavement better than a static steel drum roller for the same number of passes. Their investigations also showed that there was a 10 percent

increase in the measured percent air voids per 30°F reduction in the compaction temperature.

Researchers have also looked at analytical models such as Maxwell, generalized Maxwell, Kelvin–Voigt, generalized Kelvin, Huet–Sayegh, and Burger models to represent asphalt pavement as a combination of springs and dashpots (Nillson et al., 2002; Pronk, 2005; Dave et al., 2006; Xu and Solaimanian, 2009). These models were mostly used to study and understand the long term behavior of the pavement under traffic loads. Their use in representing the pavement during field compaction is not widely studied.

Although, the results reported in literature have provided significant insight into the relationship between mix parameters and long term behaviour of pavements, most of the research is focussed on studying the behaviour of the asphalt mix under laboratory compaction. The interaction between a vibratory roller and asphalt mix has not been widely studied. The difficulty in modelling the contact between hot asphalt layer and the roller drum and determining the relevant parameters make such modelling even more difficult to accomplish. Beainy et al. (2014) showed that a lumped element based model can be used to study the interaction between a vibratory roller and underlying asphalt pavement during compaction. The Burger's model (Chang and Meegoda, 1997) was used in their research to capture the visco-elastic-plastic behaviour of the asphalt mix. The model parameters were shown to depend on the properties of the asphalt mix and the compactor and can be obtained from standard laboratory testing.

1.3 Scope of the Dissertation

The focus of Intelligent Compaction technology is to analyze the interaction between the roller and the pavement during compaction and provide an estimation of the pavement quality during the construction process. Therefore, it is imperative to understand the dynamics of the combined roller-pavement system. One of the aims of this dissertation is to study the vibratory compaction of asphalt pavement through the development of a mathematical framework. In order to accomplish this goal, the dynamics of interaction of a moving vibratory roller and the underlying asphalt pavement is examined and a lumped element based model is developed to capture the coupled dynamics of interaction. The viscoelastic and plastic properties of the asphalt mix are considered and represented as Burger's material. The model parameters account for volumetric and rheological properties of the asphalt pavement such as gradation, temperature and air void content of the mix, type of the binder, frequency of loading as well as thickness of the pavement during compaction. The ability of the model to represent the vibrational characteristics of the roller drum in both the vertical and the horizontal direction is studied. The dynamical equations that represent the behaviour of the model are shown to be computationally tractable. The model is first verified using data collected during construction of asphalt pavement. Numerical simulations are then performed to study the response of the model during different passes of the roller on the pavement. The ability of the model to represent the pass by pass densification process during field compaction is examined. The ability of the model to represent field compaction of different asphalt mixes using different rollers is also studied.

The research in this dissertation also focuses on the development of an Intelligent Compaction system for real time estimation of the resilient modulus of subgrade during compaction. A calibration procedure is developed that takes into account the properties of the soil and the modifier used (if any). The verification of the system is demonstrated through field investigations at different construction projects in Oklahoma.

1.4 Contributions of this Dissertation

In this dissertation, a theoretical framework is developed to provide insight into the interaction between the moving vibratory roller and the asphalt pavement during construction. A model is developed that can effectively represent the visco-elastic plastic properties of the asphalt pavement. A procedure is also developed to determine the parameters of this model from standard laboratory tests using the asphalt mix. The asphalt layer is represented by a grid of asphalt blocks, with each block capable of visco-elastic and plastic deformations. Mathematical equations governing the interaction of the roller with the pavement are developed and numerical simulations are performed to study the ability of this model to replicate the field compaction process. The simulations examples show that the model can be used to emulate the salient characteristic vibratory response of the drum observed during field compaction. The results also indicate that the model is able to replicate the pass by pass densification process during field compaction. Verification of the model using field compaction data collected at two different construction projects also demonstrates its ability to address site specific and environmental changes that are encountered during compaction of pavements.

An Artificial Neural Network (ANN) based Intelligent Compaction system named as Intelligent Compaction Analyzer (ICA) for real time estimation of subgrade quality is also demonstrated in this dissertation. This system is an extension of the IC system named IACA that was developed by the researchers at the University of Oklahoma for estimation of pavement density. The system comprises an accelerometer for measuring the vibration of the drum, a GPS receiver to record the roller location, a data acquisition system, and rugged tablet pc which runs a Simulink model in real time. The Simulink model performs the signal processing and implements an artificial neural network based classifier. The system was validated during four different field investigations in Oklahoma. Comparison of ICA results with an in situ subgrade quality measurement method namely Falling Weight Deflectometer (FWD) shows that the ICA can be used as a good indicator of the subgrade quality during compaction. Encouraging correlation has also been found between the ICA estimated moduli and the corresponding laboratory resilient moduli that are obtained from the soil properties and the in situ density and moisture content values of the subgrade. The system was also able to identify under-compacted regions in real time which was helpful in providing remedial actions to improve the quality of subgrade.

1.5 Organization of the Dissertation

In Chapter 2, a mathematical model of the interaction between a moving vibratory roller and asphalt pavement underneath is introduced. Lumped element based models representing both the roller and the asphalt pavement are used and the dynamics of interaction is expressed in terms of mathematical equations. In Chapter 3, verification of the model in representing compaction dynamics is performed. The parameters in the

interaction model are determined from experimental data. Simulation results are then obtained for two different compaction scenarios and their comparison with field compaction data are presented and discussed. In Chapter 4, an Intelligent Compaction system is proposed for real time estimation of subgrade quality during compaction. The working principal of the system is described and its hypothesis is verified by field compaction results. In Chapter 5, a detailed description of examination of the proposed Intelligent Compaction system during field investigations is presented. The use of this system as a Quality Control method during subgrade construction is discussed. Finally, conclusions of the research and scope of future work are presented in Chapter 6.

CHAPTER 2 Modeling the Interaction between a Moving Vibratory Roller and the Underlying Asphalt Pavement during Compaction

2.1 Introduction

In this Chapter, a dynamical model of the interaction between a moving vibratory roller and the underlying asphalt pavement is presented. A lumped element based visco-elastic-plastic model developed by Beainy et al. (2014) is used to characterize the behavior of asphalt mix during compaction. The vibratory compactor is modeled as a series-parallel combination of spring, mass, and damper elements. This model is integrated with that of the asphalt pavement to derive the interaction dynamics. The movement of the roller along the pavement is considered and the vibration of the drum in the vertical as well as horizontal direction is taken into consideration. The use of this coupled model in representing the compaction process is studied through numerical examples.

2.2 Development of the Asphalt-Roller Interaction Model

2.2.1 Assumptions of the Model

The model presented in this chapter is based on the assumption that the dynamics of the roller and underlying pavement material are coupled and the vibratory response of the roller is influenced by the stiffness of the material. Further, the roller is considered to be in continuous contact with the asphalt pavement and the dynamics due to bouncing or loss of contact of the drum with the pavement is not considered in this research. In this

research, the compaction of a single layer of asphalt pavement is considered. The asphalt layer is assumed to be placed on top of a rigid, uniform base that does not undergo further compaction during the rolling process. In the first phase of the development, only the dynamics in the vertical direction are considered and lateral and longitudinal shear flows are ignored. In the second phase, the effect of longitudinal shear flow is also considered.

2.2.2 Modeling of Vibratory Compactor

Smooth drum vibratory compactors are commonly used for compaction of asphalt pavement. The rollers use a combination of static force i.e. the weight of the drum and the frame and vibratory force to compact asphalt mix. The vibratory force is generated by the rotation of unbalanced eccentric mass around the axle of the drum (Mitsui, 2007). The force imparted by the drum to the pavement depends on the geometry of the eccentric mass and its rotational speed. The frequency and the amplitude of the centrifugal forces generated by the rotating mass are used to quantify the compactive effort of the roller (Lavin, 2003). This vibratory force and can be mathematically expressed as

$$F_{ec} = m_{ec} r_{ec} {\omega_{ec}}^2 \tag{2.1}$$

where, F_{ec} is the vibratory force imparted to the pavement layer; $m_{ec} r_{ec}$ is the moment of the eccentric mass and ω_{ec} is the angular frequency of rotation.

In the lumped element representation considered in this dissertation, the vibratory compactor is represented as a combination of mass of the drum, mass of the frame, and

coupling between the drum and the frame. This coupling is further represented as a parallel combination of spring and dashpot. This type of model had been used effectively to model the dynamics of soil compaction (Anderegg et al., 2006; Susante and Mooney, 2009; Dubravka and Davor, 2008). Beainy et al. (2014) used this model to study the in-place compaction of asphalt mix.

2.2.3 Modeling of Asphalt Pavement

Asphalt mixes are complex, heterogeneous, viscoelastic materials whose mechanistic properties depend on volumetric properties such as air void content, effective binder content, the gradation, shape, and texture of the aggregates, rheological properties such as binder viscosity, the magnitude and frequency of the applied load, and its temperature during compaction. Several mathematical models had been formulated to describe the viscous, elastic, and plastic behaviors of an asphalt mix. Maxwell, generalized Maxwell, Kelvin–Voigt, generalized Kelvin, Huet–Sayegh, and Burger are some of the more commonly used models (Xu and Solaimanian, 2009). Among these models, the Burger's model is simple and can effectively represent the visco-elastic-plastic behavior of asphalt mix. In addition, the process of obtaining the parameter values for this model is simple and straight forward.

In this research, the asphalt pavement is modeled as a collection of block elements of Burger's material placed in a grid wise manner adjacent to each other (Figure 2.1). Each grid element is treated as a Burgers material and represented by a combination of lumped elements that depict instantaneous elastic response, the delayed (viscous) response, and the permanent deformation (Figure 2.2).

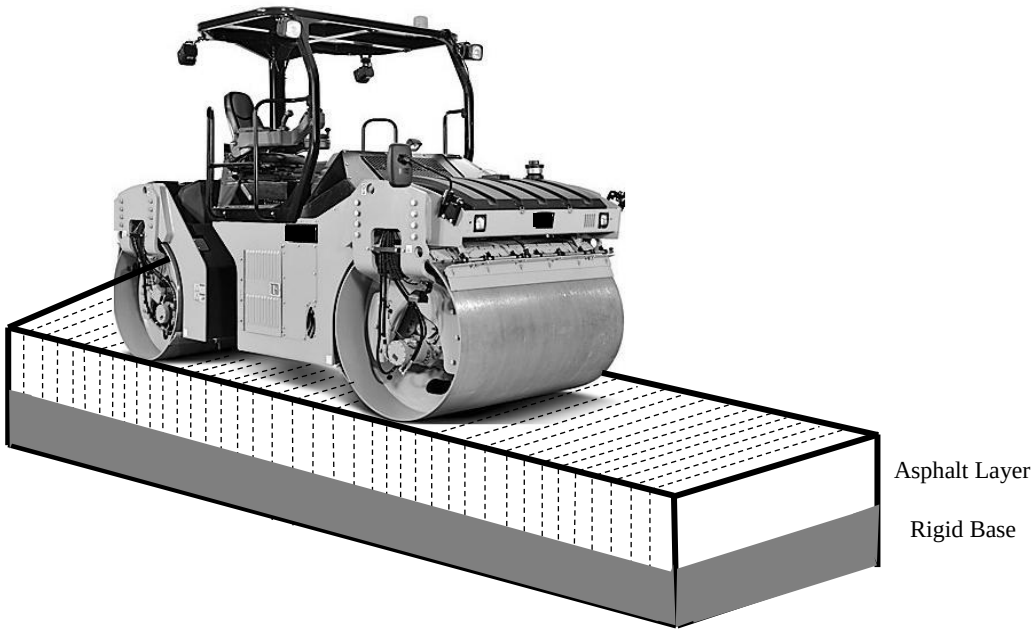

Figure 2.1 Grid wise representation of asphalt layer in an asphalt-roller interaction model.

The determination of the rolling contact of a rigid cylindrical drum on a viscoelastic asphalt pavement is a nontrivial problem due to the geometry and mechanical properties of the drum and the asphalt pavement. During compaction, different locations along the direction of travel of the drum experience different magnitudes of compressive force. In order to study the dynamics of the roller-asphalt combination at different contact locations while keeping the computational complexity to an implementable level, the contact area is divided into three parts of equal contact area with the roller drum - the leading section in the direction of travel of the drum, the central section directly underneath the drum, and the trailing section (Figure 2.2). In order to represent the interaction between the roller and the pavement at an instant in time, the roller drum is assumed to be in contact with three adjacent identical grids of same width as the drum.

The total force exerted by the drum is distributed among these three grid elements. The amount of force on each element depends on the position of the grid elements with respect to the drum.

Consider the action of the roller on the pavement at an instant 't_i'. At this instant, suppose the drum is vertically above the grid element 'i'. The grid element 'i' experiences three types of vertical deformation due to the compressive force σ_i applied by the roller. The total vertical deformation consists of an instantaneous elastic deformation 'ε_{ei}', a delayed viscoelastic deformation 'ε_{vi}', and a permanent deformation 'ε_{pi}'.

The viscoelastic behaviour is characterized by a spring constant, K_{avi}, and a coefficient of viscosity, η_{avi} . The equation for viscoelastic deformation can now be expressed as

$$\sigma_i = \varepsilon_{vi} K_{avi} + \dot{\varepsilon}_{vi} \eta_{avi} \tag{2.2}$$

The general solution of this equation is

$$\varepsilon_{vi} = \left(\frac{1}{\eta_{avi}} \int \sigma_i e^{\frac{K_{avi}}{\eta_{avi}} t} \, dt + C_{1i} \right) e^{-\frac{K_{avi}}{\eta_{avi}} t} \tag{2.3}$$

where, C_{1i} is constant of integration that is obtained by setting the appropriate boundary conditions.

The elastic response of the grid element 'i' is determined by its spring constant, K_{aei}, and the instantaneous elastic deformation can be written as

$$\varepsilon_{ei} = \frac{\sigma_i}{K_{aei}} \tag{2.4}$$

The permanent deformation of the grid element 'i' is characterized by its coefficient of viscosity, η_{api} and is given by

$$\sigma_i = \dot{\varepsilon}_{pi}\eta_{pi} \tag{2.5}$$

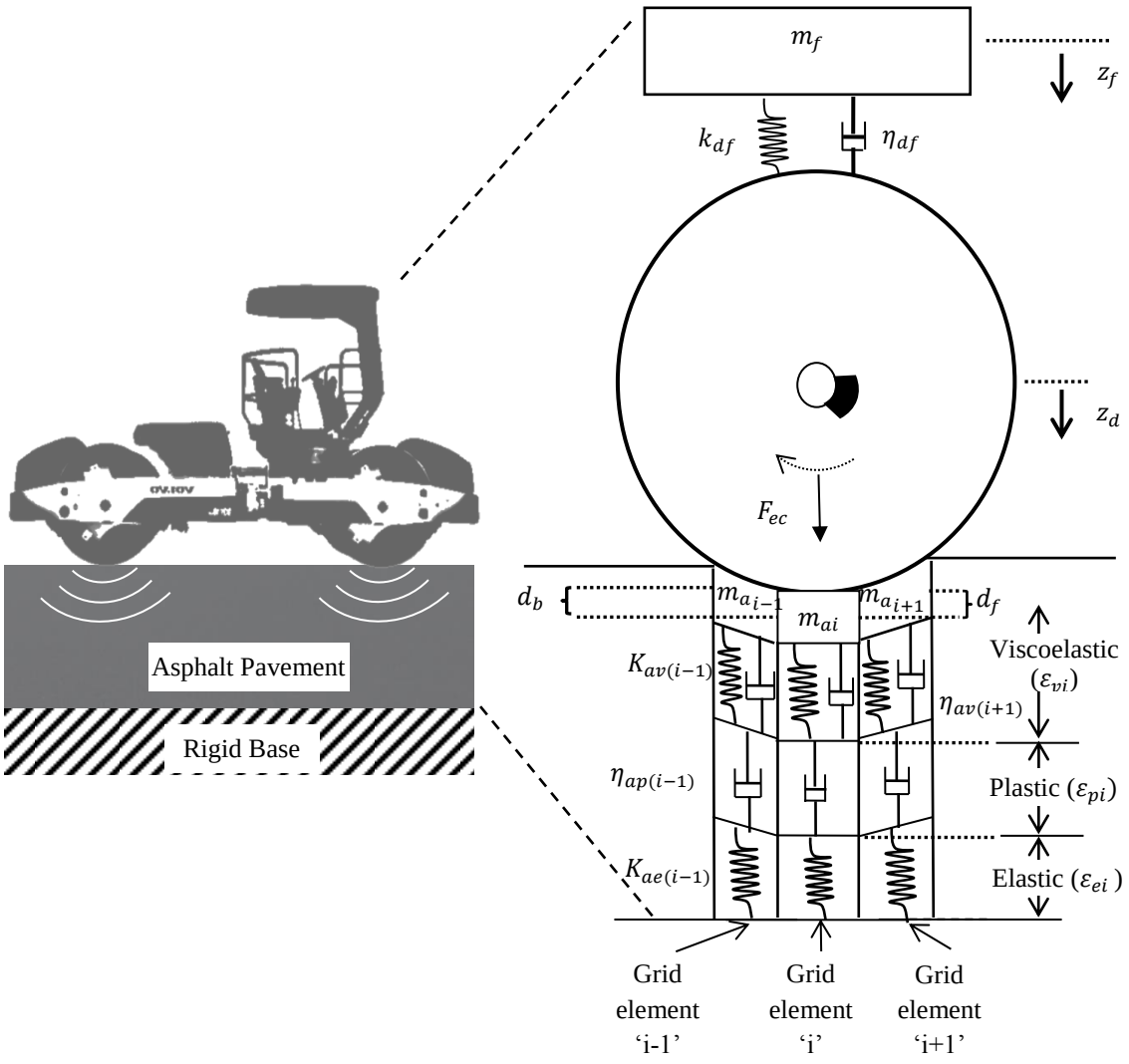

Figure 2.2 Lumped elements based representation of a combined vibratory roller - asphalt layer system.

The general solution to this equation is

$$\sigma_i = \frac{\int \sigma_i \, dt + C_{2i}}{\eta_{api}} \tag{2.6}$$

where, C_{2i} is constant of integration that is obtained by specification of appropriate boundary conditions.

The total deformation is a sum of elastic, viscoelastic and plastic deformations and can be expressed as

$$\begin{aligned} \varepsilon_i(t) &= \varepsilon_{vi} + \varepsilon_{ei} + \varepsilon_{pi} \\ &= \left(\frac{1}{\eta_{avi}} \int \sigma_i e^{\frac{K_{avi}}{\eta_{avi}} t} \, dt + C_{1i} \right) e^{-\frac{K_{avi}}{\eta_{avi}} t} + \frac{\sigma_i}{K_{aei}} + \frac{\int \sigma_i \, dt + C_{2i}}{\eta_{api}} \end{aligned} \tag{2.7}$$

2.2.4 Governing Equations of the Model

The constitutive equations of the asphalt grid elements are used in conjunction with the dynamical equations of a moving vibratory roller to derive the interaction between roller and asphalt mix. During field compaction, the roller imparts a vibratory force of constant amplitude and frequency and moves at rated speed. Since the grid elements are assumed to be identical, the duration of their interaction with the roller is also equal. As the roller in the model interacts with three adjacent grid elements at any given instance, the interaction dynamics of each grid element underneath the roller, as well as the transition of the roller from one grid to another has to be addressed through proper boundary conditions.

The vibration dynamics of the roller drum and the frame can be expressed in terms of the following equations (Figure 2.3).

Vibrations of the Drum:

$$(m_d + m_a)\ddot{z}_d = m_{ec} r_{ec} {\omega_{ec}}^2 \sin(\omega_{ec} t) + m_d g + m_a g - k_{df}\left(z_d - z_f\right) - \eta_{df}\left(\dot{z}_d - \dot{z}_f\right) - F_a \tag{2.8}$$

Vibrations of the Frame:

$$m_f \ddot{z}_f = m_f g + k_{df}\left(z_d - z_f\right) + \eta_{df}\left(\dot{z}_d - \dot{z}_f\right) \tag{2.9}$$

where, z_d is the displacement of the drum; F_a is the reaction force of the asphalt layer; z_f is the displacement of the frame; k_{df} is the drum-frame stiffness coefficient; η_{df} is the drum-frame damping coefficient; $\dot{z}_d$ is the velocity of the drum; $\dot{z}_f$ is the velocity of the frame; m_a is the asphalt mass; m_d is the mass of the drum; m_f is the mass of the frame; $\ddot{z}_d$ is the vertical acceleration of the drum; $\ddot{z}_a$ is the vertical acceleration of the asphalt pavement; and $\ddot{z}_f$ is the acceleration of the frame.

The reaction force F_a is the summation of the reaction forces of the three adjacent grid elements underneath the drum.

$$F_a = \sum_{i=1}^{3} \sigma_i = \sum_{i=1}^{3} K_{aei}\varepsilon_{ei} = \sum_{i=1}^{3} K_{aei}(\varepsilon_i - \varepsilon_{vi} - \varepsilon_{pi}) \tag{2.10}$$

$$= \sum_{i=1}^{3} K_{aei}\left[\varepsilon_i - \left\{\left(\frac{1}{\eta_{avi}}\int \sigma_i e^{\frac{K_{avi}}{\eta_{avi}}t}\, dt + C_{1i}\right)e^{-\frac{K_{avi}}{\eta_{avi}}t} + \frac{\int \sigma_i\, dt + C_{2i}}{\eta_{api}}\right\}\right]$$

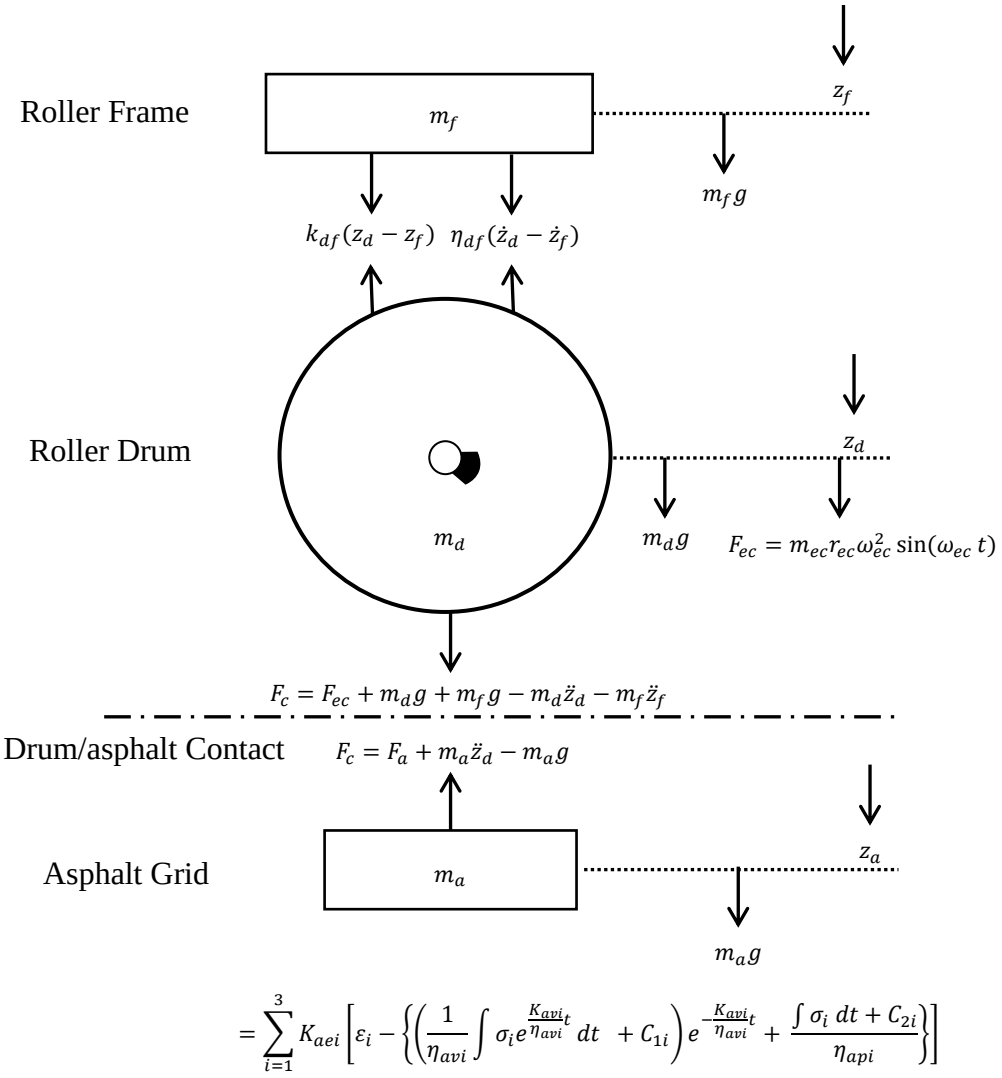

Figure 2.3 Free body diagram of interaction between a vibratory roller and asphalt layer.

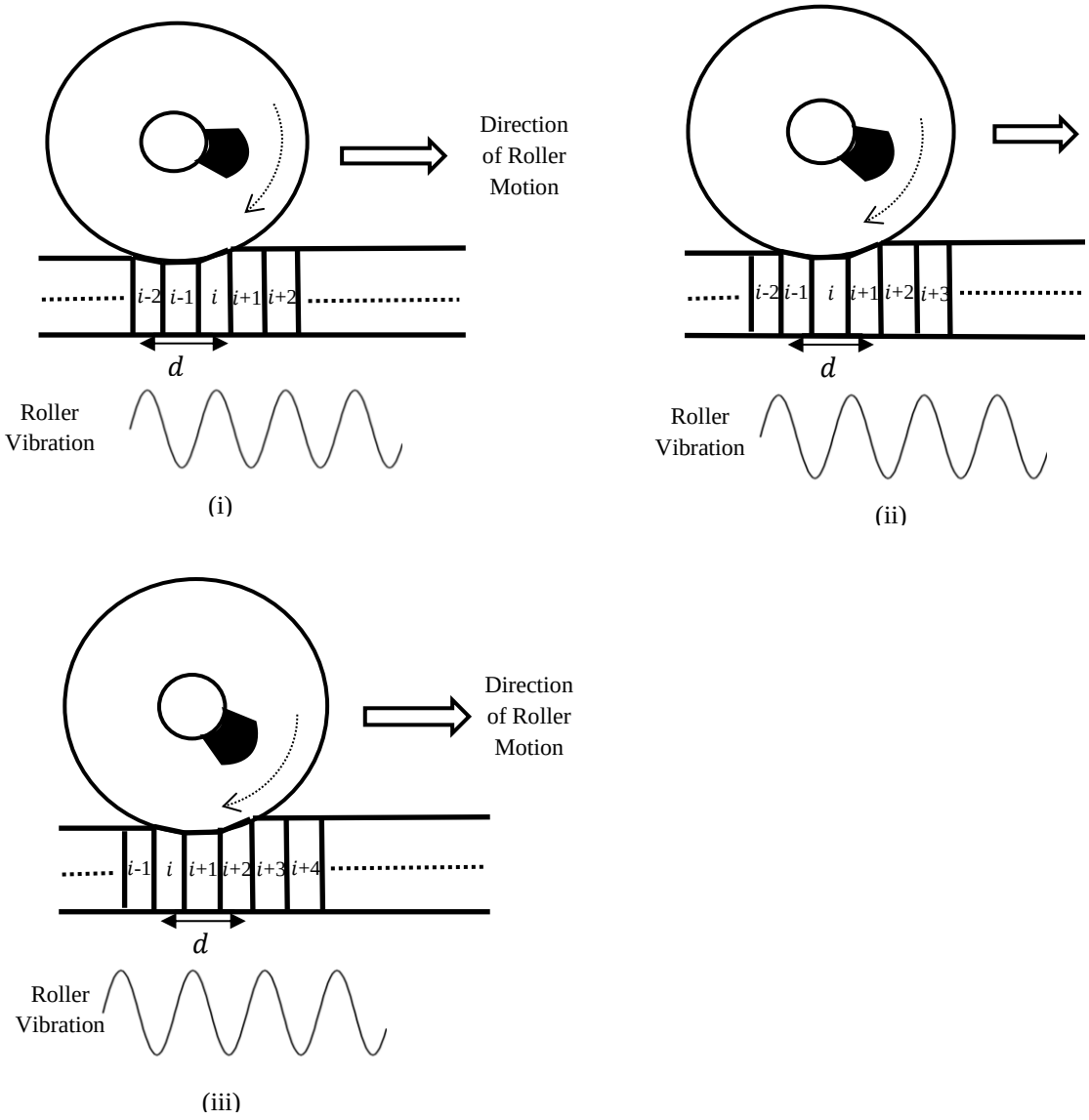

Figure 2.4 Stepwise representation of contact between a moving roller and asphalt layer grid elements.

2.2.5 Boundary Conditions

The reaction force of each grid element depends on its position with respect to the roller drum. As a result of the geometry of the drum, each element experiences different contact force when it is directly underneath the drum in comparison to when it is in

contact with the leading or trailing part of the drum. The transition of contact force experienced by each grid element starting from the initial to the final contact has to be expressed by proper boundary conditions.

Step 1

Each grid element undergoes three steps of compaction during each pass of the roller. In the first step the element is initially at rest and comes in contact with the leading part of the roller drum (Figure 2.4(i)). During this step, the total compaction force is spread over the ith grid element and previous two elements (Figure 2.4(i)). The viscoelastic and plastic deformations of the ith element in this step start at time instant τ, can be represented as,

$$\varepsilon_{vi} = \left(\frac{1}{\eta_{avi}}\int_{\tau}^{\tau+T/3} \sigma_i e^{\frac{K_{avi}}{\eta_{avi}}t}\, dt \; + C_{vi}\right) e^{-\frac{K_{avi}}{\eta_{avi}}t} \tag{2.11}$$

$$\varepsilon_{pi} = \frac{\int_{\tau}^{\tau+T/3} \sigma_i dt + C_{pi}}{\eta_{api}} \tag{2.12}$$

where, the drum grid elements contact period is represented as T. The contact period depends on the speed of the roller and the length of the asphalt material in contact with the drum. Since it is assumed that three grid elements are in contact with the drum at any given instant, it is assumed that each element is in contact with the drum for T/3 seconds.

The reaction force of the ith grid element can be represented by the following equation.

$$F_{a_i} = K_{aei}\varepsilon_{ei} = K_{aei}(z_{a_i} - \varepsilon_{vi} - \varepsilon_{pi}) \tag{2.13}$$

$$= K_{aei}\left[z_{a_i} - \left\{\left(\frac{1}{\eta_{avi}}\int_{\tau}^{\tau+T/3}\sigma_i e^{\frac{K_{avi}}{\eta_{avi}}t}\,dt \;+ C_{vi}\right)e^{-\frac{K_{avi}}{\eta_{avi}}t} + \frac{\int_{\tau}^{\tau+T/3}\sigma_i dt + C_{pi}}{\eta_{api}}\right\}\right]$$

Since each grid element is independent and is initially at rest condition, the initial displacement of the viscoelastic and delayed parts of the grid element can be considered as,

$$C_{vi} = 0 \tag{2.14}$$

$$C_{pi} = 0 \tag{2.15}$$

z_{a_i} is the total displacement of the ith grid element and can be written as,

$$z_{a_i} = z_d - d_f \tag{2.16}$$

Here, d_f is a constant that depends on the diameter and geometric property of the drum and the mechanical (elastic and viscous) property of the mix.

Step 2

The second step deals with the forward movement of the drum by one grid element. Now, the drum is directly on top of the ith grid element (Figure 2.4(ii)). In this case, the total compaction load is distributed between ith element and (i-1)th and (i+1)th elements (Figure 2.4(ii)).

$$F_{a_i} = K_{aei}\varepsilon_{ei} \tag{2.17}$$

$$= K_{aei}\left[z_{a_i} - \left\{\left(\frac{1}{\eta_{avi}}\int_{\tau+T/3}^{\tau+2T/3}\sigma_i e^{\frac{K_{avi}}{\eta_{avi}}t}\,dt \;+ C_{vi}\right)e^{-\frac{K_{avi}}{\eta_{avi}}t} + \frac{\int_{\tau+T/3}^{\tau+2T/3}\sigma_i dt + C_{pi}}{\eta_{api}}\right\}\right]$$

Here, the initial conditions are expressed as,

$$C_{vi} = \varepsilon_{vi_1} \tag{2.18}$$

$$C_{pi} = \varepsilon_{pi_1} \tag{2.19}$$

where, ε_{vi_1} and ε_{pi_1} are the visco-elastic and permanent deformation of the grid element after the first step. The displacement of the i[th] grid element z_{a_i} in this step is equal to the displacement of the drum.

$$z_{a_i} = z_d \tag{2.20}$$

It should be noted that, in this time period the dynamics of the (i+1)[th] grid element is similar to that of i[th] grid element in step one.

Step 3

In the third and final step the roller moves another grid element forward and as a result the i[th] grid element is now underneath the trailing part of the drum. The total load in this case is distributed over the i[th] grid element and (i+1)[th] and (i+2)[th] grid element (Figure 2.4(iii)).

$$F_{a_i} = K_{aei}\varepsilon_{ei} \tag{2.21}$$

$$= K_{aei}\left[z_{a_i} - \left\{\left(\frac{1}{\eta_{avi}}\int_{\tau+2T/3}^{\tau+T} \sigma_i e^{\frac{K_{avi}}{\eta_{avi}}t}\, dt \;+ C_{vi}\right)e^{-\frac{K_{avi}}{\eta_{avi}}t} + \frac{\int_{\tau+2T/3}^{\tau+T}\sigma_i dt + C_{pi}}{\eta_{api}}\right\}\right]$$

$$C_{vi} = \varepsilon_{vi_2} \tag{2.22}$$

$$C_{pi} = \varepsilon_{pi_2} \tag{2.23}$$

where, ε_{vi_2} and ε_{pi_2} are the visco-elastic and permanent deformation of the ith grid element after the second step. The displacement of the ith grid element is less than the displacement of the drum.

$$z_{a_i} = z_d - d_b \tag{2.24}$$

where, d_b is a constant that depends on the diameter of the drum.

2.3 Extension of the Interaction Model to Two Dimensions

The model developed in the previous sections is limited to describing the asphalt-roller interaction in the vertical direction. No longitudinal or lateral shear forces were considered. However, during actual field compaction shear plays an important role in the interaction dynamics as well as the densification of asphalt mix. In this section, the model is extended to incorporate the longitudinal shear force in the asphalt pavement during compaction. The response of the model in both vertical and longitudinal direction is also considered. This model is an extension of the interaction model

developed in the previous sections. However, in order to reduce complexity in the dynamics, some assumptions are made to simplify the model. The key assumptions of this two dimensional models are as follows.

(i) The roller is assumed to be in constant contact with the asphalt layer throughout the compaction process.

(ii) A single layer of asphalt is taken into account and the asphalt layer is assumed to be placed on top of a rigid base.

(iii) In the previous one dimensional model, the roller drum was assumed to be on top of three grid elements. In this simplified model, the drum is considered to be on top of only one grid element. Therefore, at any given cycle of vibration the roller interacts with only one grid element in the vertical direction and its adjacent two grid elements in the horizontal direction.

(iv) The dimension of each element depends on the geometry of the drum and asphalt layer and the velocity of the roller. Its height is equal to the thickness of the pavement layer. The width corresponds to the width of the drum. The length is the distance the roller travels along the pavement for the duration of one impact.

(v) At the beginning of each impact cycle the drum moves on top of a new grid element. The interaction between the roller and a grid element continues for one cycle of the vibration. In the next cycle the roller moves to the next grid element.

(vi) The longitudinal shear is represented by a spring connecting elements adjacent to one another in the longitudinal direction.

(vii) The lateral shear is not considered in this model. Hence the elements in the lateral direction are considered to be independent of one other.

2.1.1 Development of a Two Dimensional Interaction Model

The eccentric vibratory force shown in Equation (2.1) can be divided into two components, a vertical force that acts normal to the asphalt surface and a horizontal component that acts tangentially to it. They are expressed as follows,

Vertical eccentric force,

$$F_{ecZ} = m_{ec} r_{ec} \omega_{ec}{}^2 \sin(\omega_{ec} t) \tag{2.25}$$

Horizontal eccentric force,

$$F_{ecX} = -m_{ec} r_{ec} \omega_{ec}{}^2 \cos(\omega_{ec} t) \tag{2.26}$$

It is considered that the vertical force is responsible for the vertical deformation of the asphalt mix, whereas the horizontal force is responsible for the shear deformation in the longitudinal direction. The frame of the roller is coupled to the drum by an insulating rubber padding which is represented as a parallel combination of a linear spring and a linear dashpot element.

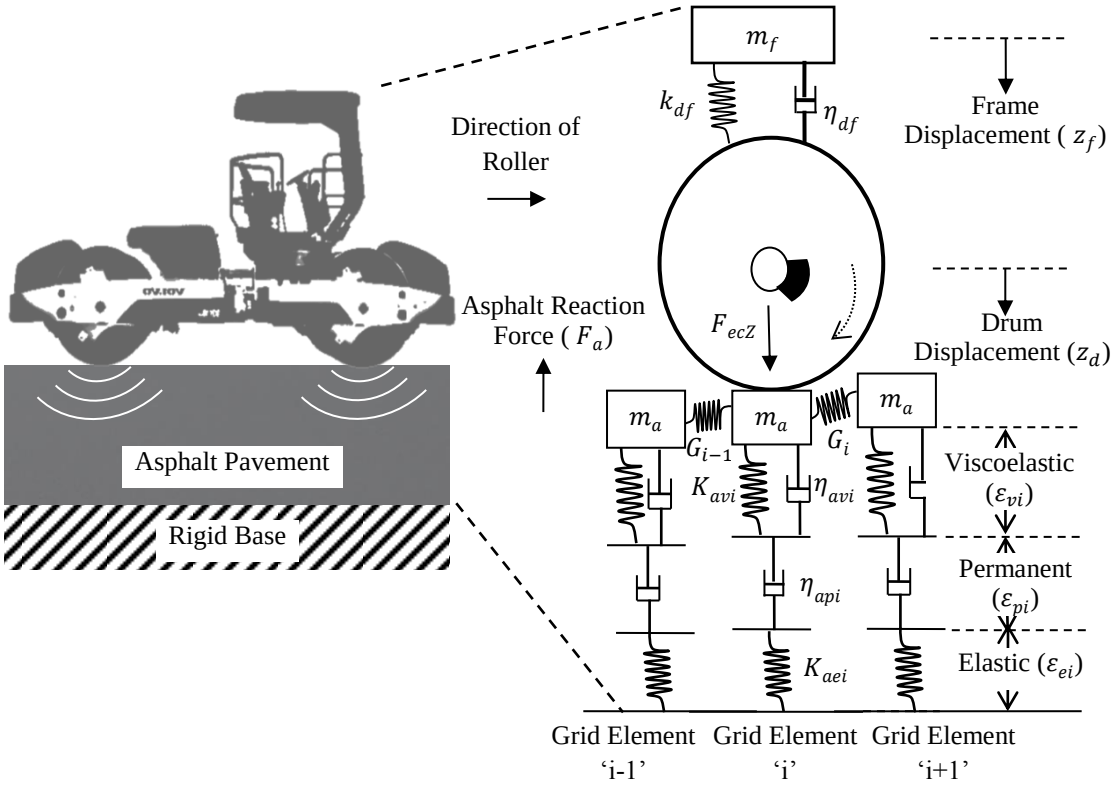

Figure 2.5 Asphalt-roller interaction model in the vertical direction.

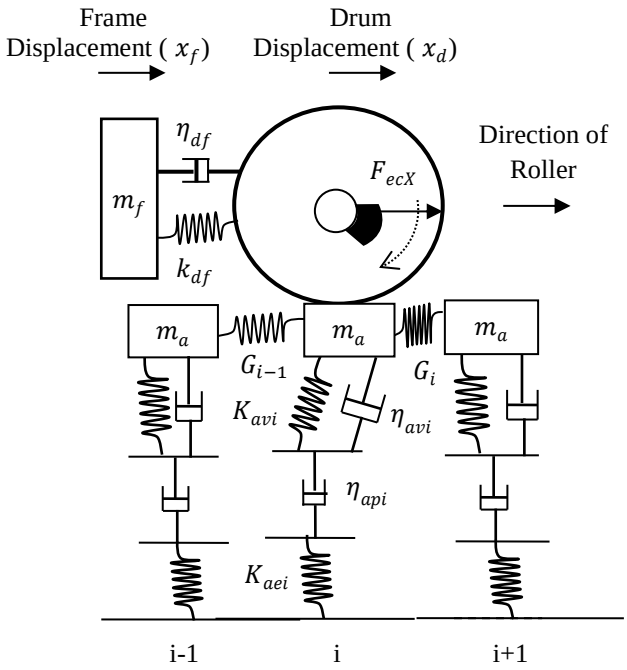

Figure 2.6 Asphalt-roller interaction model in the horizontal direction.

2.3.1 Governing Equations for Vertical Vibration

The total deformation occurring in i^{th} grid element due to the stress applied by the roller is comprised of an instantaneous elastic deformation 'ε_{ei}', viscoelastic deformation 'ε_{vi}', and a permanent deformation 'ε_{pi}'. The constitutive equation of the strain can be expressed as,

$$\begin{aligned}\varepsilon_i(t) &= \varepsilon_{vi} + \varepsilon_{pi} + \varepsilon_{ei} \\ &= \left(\frac{1}{\eta_{avi}}\int \sigma_i e^{\frac{K_{avi}}{\eta_{avi}}t}\, dt \;+ C_{vi}\right) e^{-\frac{K_{avi}}{\eta_{avi}}t} + \frac{\int \sigma_i\, dt + C_{pi}}{\eta_{api}} + \frac{\sigma_i}{K_{aei}}\end{aligned} \tag{2.27}$$

The interaction between the roller and the underlying asphalt grid element due to the vertical component of vibration can be formulated as follows.

Drum Vibration:

$$\begin{aligned}(m_d + m_a)\ddot{z}_d &= (m_d + m_a)\ddot{z}_a \\ &= m_{ec} r_{ec} {\omega_{ec}}^2 \sin(\omega_{ec} t) + m_d g + m_a g - k_{df}\left(z_d - z_f\right) \\ &\quad - \eta_{df}\left(\dot{z}_d - \dot{z}_f\right) - F_a - F_{xi}\end{aligned} \tag{2.28}$$

Frame Vibration:

$$m_f \ddot{z}_f = m_f g + k_{df}\left(z_d - z_f\right) + \eta_{df}\left(\dot{z}_d - \dot{z}_f\right) \tag{2.29}$$

where z_a is the displacement of the asphalt layer; F_a is the vertical reaction force of the asphalt grid element; F_{xi} is the reaction force due to shear component; z_d is the displacement of the drum; z_f is the displacement of the frame; k_{df} is the drum-frame

stiffness coefficient; $\dot{z}_d$ is the velocity of the drum; $\dot{z}_f$ is the velocity of the frame; η_{df} is the drum-frame damping coefficient; m_a is the asphalt weight; $\ddot{z}_d$ is the vertical acceleration of the drum; $\ddot{z}_a$ is the vertical acceleration of the asphalt grid element; and $\ddot{z}_f$ is the acceleration of the frame.

The vertical reaction force of the asphalt grid element F_a is the force exerted by each grid element opposing the compaction force of the roller. It can be expressed as

$$F_a = \sigma_i = K_{aei}\varepsilon_{ei} = K_{aei}\left[z_a - K_{aei}\left\{\left(\frac{1}{\eta_{avi}}\int \sigma_i e^{\frac{K_{avi}}{\eta_{avi}}t}\,dt + C_{1i}\right)e^{-\frac{K_{avi}}{\eta_{avi}}t} + \frac{\int \sigma_i\,dt + C_{2i}}{\eta_{api}}\right\}\right] \tag{2.30}$$

where, F_{xi} is the force generated by the shear spring component G_i between the current ith grid element and the element next to it and can be represented as

$$F_{xi} = G_i z_d \tag{2.31}$$

2.3.2 Governing Equations for Horizontal Vibration

The dynamics of interaction between the roller and the asphalt mat in the longitudinal direction can be formulated as

Drum Vibration:

$$(m_d + m_a)\ddot{x}_d = -m_{ec}r_{ec}{\omega_{ec}}^2\cos(\omega_{ec}t) - k_{df}(x_d - x_f) - \eta_{df}(\dot{x}_d - \dot{x}_f) - (K_{avi} + G_{i-1} + G_i)x_d - \eta_{avi}\dot{x}_d \quad (2.32)$$

Frame Vibration:

$$m_f\ddot{x}_f = k_{df}(x_d - x_f) + \eta_{df}(\dot{x}_d - \dot{x}_f) \quad (2.33)$$

2.3.3 Boundary Conditions

During the compaction of ith grid element, the next element (i+1) experiences a force equal to F_{xi} which is generated by the shear spring component between the two grid elements. Therefore, at the beginning of the compaction cycle of the (i+1)th element it has the initial viscoelastic and permanent displacements of $C_{1(i+1)}$ and $C_{2(i+1)}$. For simplicity of calculation if we consider F_{xi} to be a constant force, then, the constants $C_{1(i+1)}$ and $C_{2(i+1)}$ can be determined.

$$C_{1(i+1)} = \left(\frac{1}{\eta_{avi}}\int_{t_i}^{t_{i+1}} F_x e^{\frac{K_{avi}}{\eta_{avi}}t}\, dt\right) e^{-\frac{K_{avi}}{\eta_{avi}}(t_{i+1}-t_i)} \approx \frac{F_x}{K_{avi}} \quad (2.34)$$

$$C_{2(i+1)} = \frac{\int_{t_i}^{t_{i+1}} F_x dt}{\eta_{api}} = \frac{F_x(t_{i+1}-t_i)}{\eta_{api}} \quad (2.35)$$

2.4 Conclusions of Chapter

In this chapter, a lumped element model was developed to capture the interaction between a moving vibratory roller and the asphalt pavement during field compaction. The properties of asphalt mixes were used to describe three types of deformations

(plastic, instantaneous elastic, and delayed viscoelastic) that an asphalt mat experiences in response to the loading force of the vibratory roller. A lumped element based representation of the vibratory roller was integrated with the grid wise representation of asphalt pavement to develop the governing equations of their interaction. The movement of the roller on the asphalt grid and the response of the drum-asphalt coupled system for both the vertical and longitudinal direction were accounted for. Related boundary conditions were developed to express the transition of interaction between the roller drum and asphalt grid as the roller moves forward at a given speed.

CHAPTER 3 Validation of the Asphalt-Roller Interaction Model

3.1 Introduction

The ability of the Asphalt-Roller Interaction model developed in the previous chapter to emulate the compaction of asphalt pavement is studied in this chapter. The procedures to determine the parameter values for the vibratory roller and the asphalt pavement are described. Numerical simulations are performed to examine the response of the model for different compaction scenarios. The responses of the model are compared with data recorded during field compaction to study the effectiveness of the model in replicating field compaction process.

3.2 Determination of Model Parameters

The development of mathematical equations of asphalt–roller interaction model requires the identification of the parameters of the vibratory roller as well as the asphalt pavement. The parameters of the vibratory roller are dependent on the make and model of the roller. The parameters of the asphalt layer are dependent on the type of asphalt mix, gradation of aggregates, temperature, loading frequency, thickness of the pavement etc. A brief description of the problem to obtain the model parameters is given below.

3.2.1 Roller Parameters

The dynamics of the interaction model depends largely on several roller parameters including mass of the drum, mass of the frame, drum-asphalt contact area, width and diameter of the drum, stiffness coefficient and damping coefficient of drum-frame interaction, rotational frequency of eccentrics and the eccentric moment etc. Most of

these parameters can be obtained from the manufacturer's specifications of the selected roller. The damping coefficient and stiffness coefficient of the frame-drum coupling are usually not found in the specifications. These values are assumed based on the feedback from the manufacturers and earlier researches (Beainy et al., 2014; Susante and Mooney, 2008; Pietzsch and Poppy, 1992). It was found that the model is robust to the variations of these parameter values. Therefore, errors in the assumed values are not expected to have a big influence on the results of this research.

Determination of the drum-asphalt contact area is a non-trivial problem. The contact geometry is mostly dependent on the stiffness and dimension of the drum, weight of the compactor, stiffness of asphalt pavement, and total eccentric force applied to the pavement (Kröber et al. 2001). In order to avoid complexity in the computation, the contact area in this research is assumed to be fixed during each roller pass and is estimated based on the interaction of the static drum and pavement material. However, in reality, the contact area is dependent on the stiffness of the material and generally reduces as the asphalt material is compacted. Since, the drum is considered to be in contact with 3 blocks of equal dimensions, the surface area of each block is one third of the contact area. The contact area between the drum and asphalt blocks is calculated according to the following equation,

$$A_c = w \times 3\mathrm{d} \tag{3.1}$$

where, A_c is the contact area of three asphalt blocks and drum , w is the width of the drum, and d is the length of each block underneath the drum. Since the length of each block is the distance the roller travels in one third of its loading cycle and the width of

the blocks is equal to the width of the roller, the contact area can be calculated from the surface area of each block. The mass of the blocks in contact with the roller can then be determined using the contact area and the thickness of the pavement layer as well as the properties of the asphalt mix.

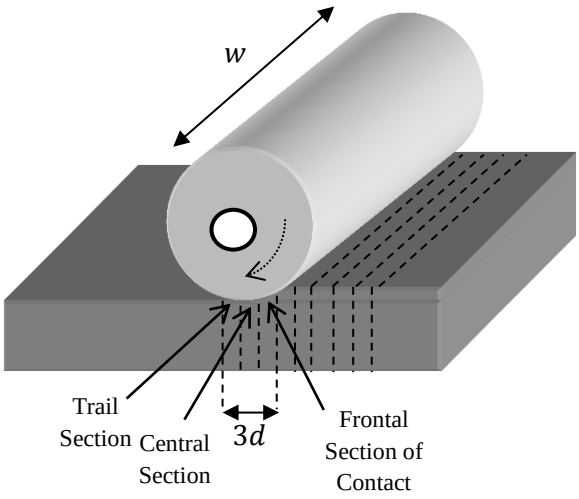

Figure 3.1 Roller-Asphalt contact area.

3.2.2 Asphalt Layer Parameters

The viscoelastic-plastic properties of the asphalt pavement are represented in the interaction model using the four parameters $K_{ae}, \eta_{ap}, K_{av},$ and η_{av}. These parameter values are estimated indirectly from laboratory dynamic modulus test performed on the asphalt mixes (Beainy et al., 2013a, Beainy et al., 2013b). The estimation of parameters involves laboratory testing according to AASHTO TP-62 Standard Method of Test for Determining Dynamic Modulus of Hot-Mix Asphalt Concrete Mixtures (AASHTO, 2007). The tests are performed to determine the complex modulus of asphalt mix at different temperatures, air void contents, and loading frequencies. The relationship

between the dynamic modulus |E* | and phase angle ϕ of the mix and the model parameters can be expressed as follows (Xu and Solaimanian, 2009; Liu et al. 2009).

$$1/E^* = \Delta\varepsilon/\Delta\sigma \tag{3.2}$$

$$= \sqrt{1/K_{ae}^2 + 1/\eta_{ap}^2\omega^2 + \left(1 + 2(K_{av}/K_{ae} + \eta_{av}/\eta_{ap})\right)/\left(K_{av}^2 + \eta_{av}^2\omega^2\right)}$$

$$\tan(\phi) = 1/\tan(\theta) \tag{3.3}$$

$$= K_{ae}[K_{av}^2 + \eta_{av}(\eta_{ap} + \eta_{av})\omega^2]/\eta_{ap}\omega(K_{av}^2 + K_{ae}K_{av} + \eta_{av}^2\omega^2)$$

$$K_{ae} = \lim_{\omega\to\infty} |E^*| \tag{3.4}$$

and

$$\eta_{ap} = \lim_{\omega\to 0} |E^*|/\omega. \tag{3.5}$$

An iterative procedure developed by Liu et al. (2009) was employed to estimate the asphalt model parameters for different frequency, air void contents and temperature for each asphalt mix. The dynamic modulus and phase angle calculated using these parameters in equations 3.2-3.5 were verified against the laboratory test data for all test frequencies, temperature, and air voids. Finally, a nonlinear regression analysis was performed to develop empirical equations of the model parameters as functions of the

temperature and air void contents for a frequency that is used by the roller during field compaction. The empirical equations for the parameters are then used to determine the parameter values of the asphalt mix for any temperature and air void contents encountered during the simulation process. A detailed description of the parameter estimation procedure can be found in Imran et al., (2014, 2015) and Beainy et al., (2013a, 2013b). A generic form of the empirical equations are expressed as follows

$$f(V_a, T) = p_{00} + p_{10}V_a + p_{01}T + p_{20}V_a^2 + p_{11}V_aT + p_{02}T^2 + p_{30}V_a^3 + p_{21}V_a^2T + p_{12}V_aT^2 + p_{03}T^3 \quad (3.6)$$

where, V_a is the air void content and T is the temperature and p_{ij} 's are the coefficients that need to be determined for all four parameters.

One important parameter of the two dimensional extension of the Interaction model is the shear component G_i. Unfortunately, due to limitations in the resources, it was not possible to obtain estimates of the shear stiffness as a function of asphalt material properties. However, studies found in the literature indicate that the shear modulus values are approximately 30-40% of the dynamic modulus values for asphalt cores (Pellinen and Xiao, 2006). In this research, the shear stiffness is considered to be 35% of the stiffness of Burger's material at the corresponding compaction temperature and air void content.

3.3 Validation of the Interaction Model

The model developed in this dissertation is aimed to replicate the field compaction process which can be helpful in the research of understanding the compaction dynamics

and improvement of the Intelligent Compaction technologies. The model should be able to capture the effect of several important factors that affect the compaction such as type of asphalt mix, temperature and thickness of the pavement during compaction, amplitude and frequency of the compaction force exerted by the roller etc. The model should also be able to be used to represent compaction involving different models of rollers and different types of asphalt mixes. In order to examine the ability of the model to represent field compaction, the numerical equations are implemented and simulated in Matlab Simulink platform (Matlab, 2013). The model's sensitivity to temperature of asphalt pavement is analyzed first. The vibratory response characteristics of the model at different harmonic frequencies are studied next. The densification of the asphalt pavement at different roller passes is also examined. Field data are collected from two different construction projects. The model was validated with both the field compaction results. The effect of base layer on the compaction of asphalt pavement is also studied in this section. A brief description of the two construction projects and the determination of model parameters is given below.

3.3.1 Description of Construction Projects

Test Project I

The first field data were collected during the compaction on a stretch of Interstate I-35 in Norman, Oklahoma. In this project, 76.2 mm thick asphalt layer prepared with a nominal maximum aggregate size of 12.5mm and PG 76 -28 binder was placed. An IR DD 118HF smooth drum vibratory roller was used to compact the asphalt layer. The field compaction data contains the vibration of the drum, the location and movement of

the roller, and, surface temperature and real time density of the pavement during compaction. In order to collect these data, the roller was instrumented with accelerometers and global positioning system (GPS) receiver and a proprietary Intelligent Asphalt Compaction Analyzer (IACA). The IACA was used for real time estimation of pavement density.

Test Project II

The second field investigation was performed during full depth construction on a section of Interstate I-35 near Main Street I-35 intersection at Norman, Oklahoma. In this project, a Dynapac CC 422V smooth drum roller was used to compact an 88.9mm (3.5 inch) of asphalt layer with nominal maximum aggregate size of 19mm. The asphalt mix was comprised of PG 64 -22 OK asphalt binder. It also contained 25% reclaimed asphalt pavement materials. The GPS location of the roller, surface temperature of the asphalt mat, and the density of the pavement estimated by the IACA were recorded during the entire compaction process.

3.3.2 Determination of Model Parameters for Test Project I and II

Parameters of the Roller

The parameters of the IR DD 118HF and Dynapac CC 422V vibratory rollers were obtained using the method described in previous section ((Ingersoll Rand, 2007; Dynapac, 2009). The parameters and their values used in the model simulations are shown in Table 3.1.

Table 3.1 Parameters of IR DD 118HF and Dynapac CC 422V vibratory compactors.

Parameter	Symbol	Value		Unit	Source
		IR DD 118HF	Dynapac CC 422V		
Mass of Drum	m_d	2371	2052	kg	Spec Sheet
Mass of Frame	m_f	4225	3098	kg	Spec Sheet
Eccentric Moment	$m_{ec}r_{ec}$	1.45	1.02	kg.m	Spec Sheet
Rotational Frequency	ω_{ec}	314	314	rad/s	Measured
Drum Width	w	2	1.68	m	Spec Sheet
Drum-Frame Stiffness Coefficient	k_{df}	3400	3250	kNs/m	Manufacturer
Drum-Frame Damping Coefficient	η_{df}	544	530	kN/m	Manufacturer
Drum-Asphalt Contact Area	A_c	0.078	0.064	m^2	Estimated

Parameters of Asphalt Model

Two different asphalt mixes were used in the test projects considered in this research. In order to perform simulations for both the projects the asphalt model parameters needed to be obtained so that the model representing asphalt layer can characterize the mechanical behavior of both the asphalt mixes. A methodology described in the previous section (Section 3.2.2) was followed in order to develop empirical

relationships of the model parameters as functions of temperature and air void contents for the frequencies used by the rollers during field compaction. The equations can be expressed as follows.

Equations for parameters of asphalt mix used in Project I.

$$K_{avi}(V_a,T) = 4764 - 443.6V_a - 53.5T + 14.4V_a^2 + 3.3V_aT + 0.26T^2 + 0V_a^3 - 0.0059V_aT^2 - 0.00049T^3 \quad (3.7)$$

$$\eta_{avi}(V_a,T) = 387.7 - 96V_a - 1.3T + 8.7V_a^2 + 0.11V_aT + 0.0049T^2 - 0.26V_a^3 - 0.0043V_a^2T - 0.000096T^2 - 0.0000096T^3 \quad (3.8)$$

$$K_{aei}(V_a,T) = 5340 + 84V_a - 54T - 28.5V_a^2 + 0.23V_aT + 0.31T^2 + 0.15V_a^2T - 0.0085V_aT^2 - 0.00054T^3 \quad (3.9)$$

$$\eta_{api}(V_a,T) = 7799 + 1656V_a - 144.4T - 138.4V_a^2 - 6.8V_aT + 1.1T^2 + 0V_a^3 + 0.82V_a^2T - 0.0025V_aT^2 - 0.0019T^3 \quad (3.10)$$

Equations for parameters of asphalt mix used in Project II.

$$K_{avi}(V_a,T) = 3764 + 1198V_a - 92.56T - 119.3V_a^2 - 2.532V_aT + 0.657T^2 + 0.4363V_a^3 - 0.009531V_aT^2 - 0.001458T^3 \quad (3.11)$$

$$\eta_{avi}(V_a, T) = 36.58 + 8.904V_a - 0.7876T - 0.9235V_a^2 - 0.01229V_aT + 0.005355T^2 - 0.001566V_a^3 + 0.00281V_a^2T - 0.00007T^2 - 0.0000119T^3 \quad (3.12)$$

$$K_{aei}(V_a, T) = 8728 - 64.68V_a - 107.9T - 33.89V_a^2 + 5.274V_aT + 0.5729T^2 - 0.0667V_a^2T - 0.01402V_aT^2 - 0.001153T^3 \quad (3.13)$$

$$\eta_{api}(V_a, T) = 13380 + 865.2V_a - 231T - 128V_a^2 + 0.7825V_aT + 1.522T^2 + 0V_a^3 + 0.6002V_a^2T - 0.028V_aT^2 - 0.003304T^3 \quad (3.14)$$

Graphical representations of the four parameters $K_{ae}, \eta_{ap}, K_{av}$, and η_{av} are shown in Figure 3.2-3.5.

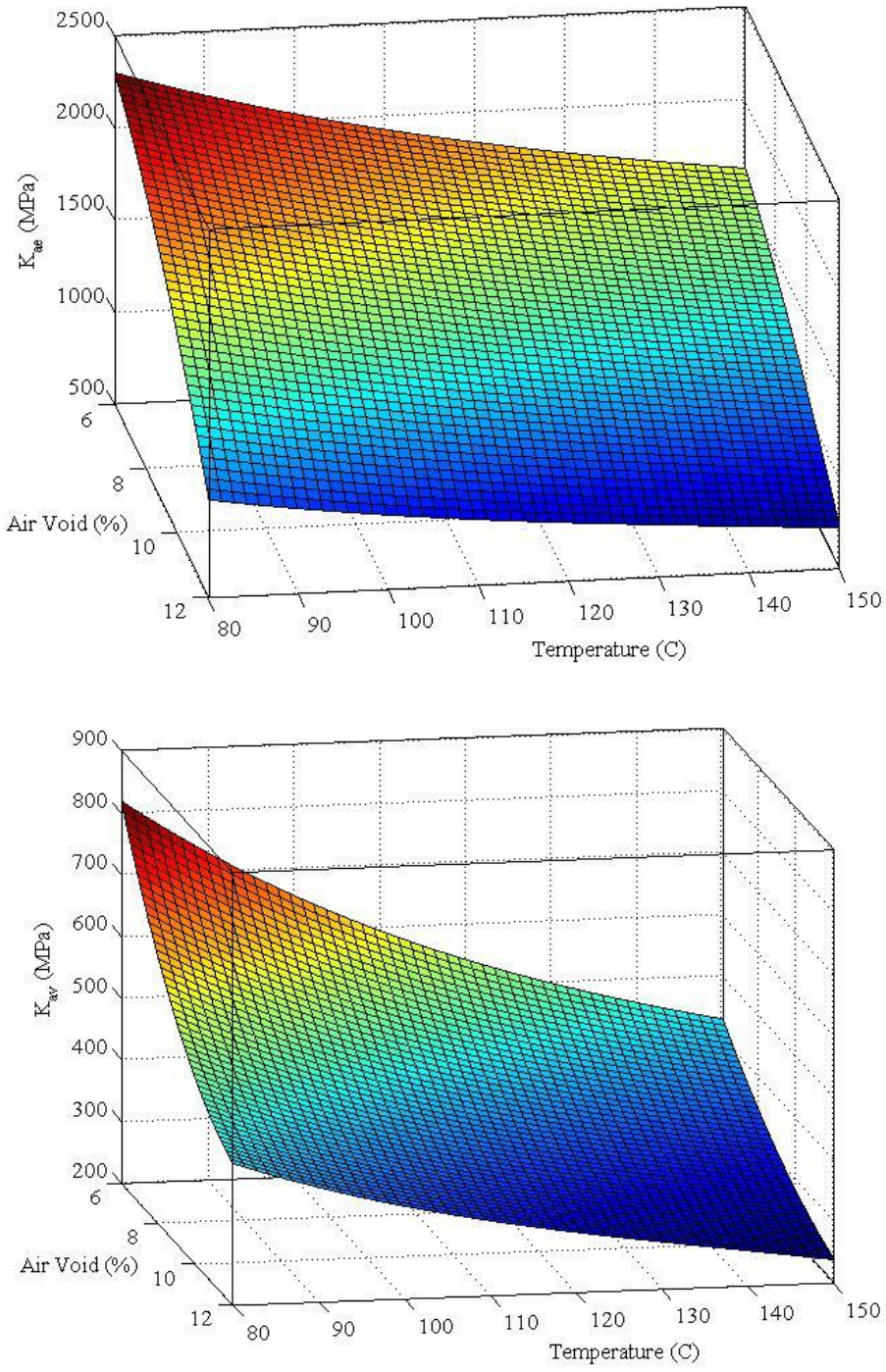

Figure 3.2 Three dimensional plots of parameters K_{ae} and K_{av} as a function of Temperature and Air void contents for asphalt mix used in Test Project I.

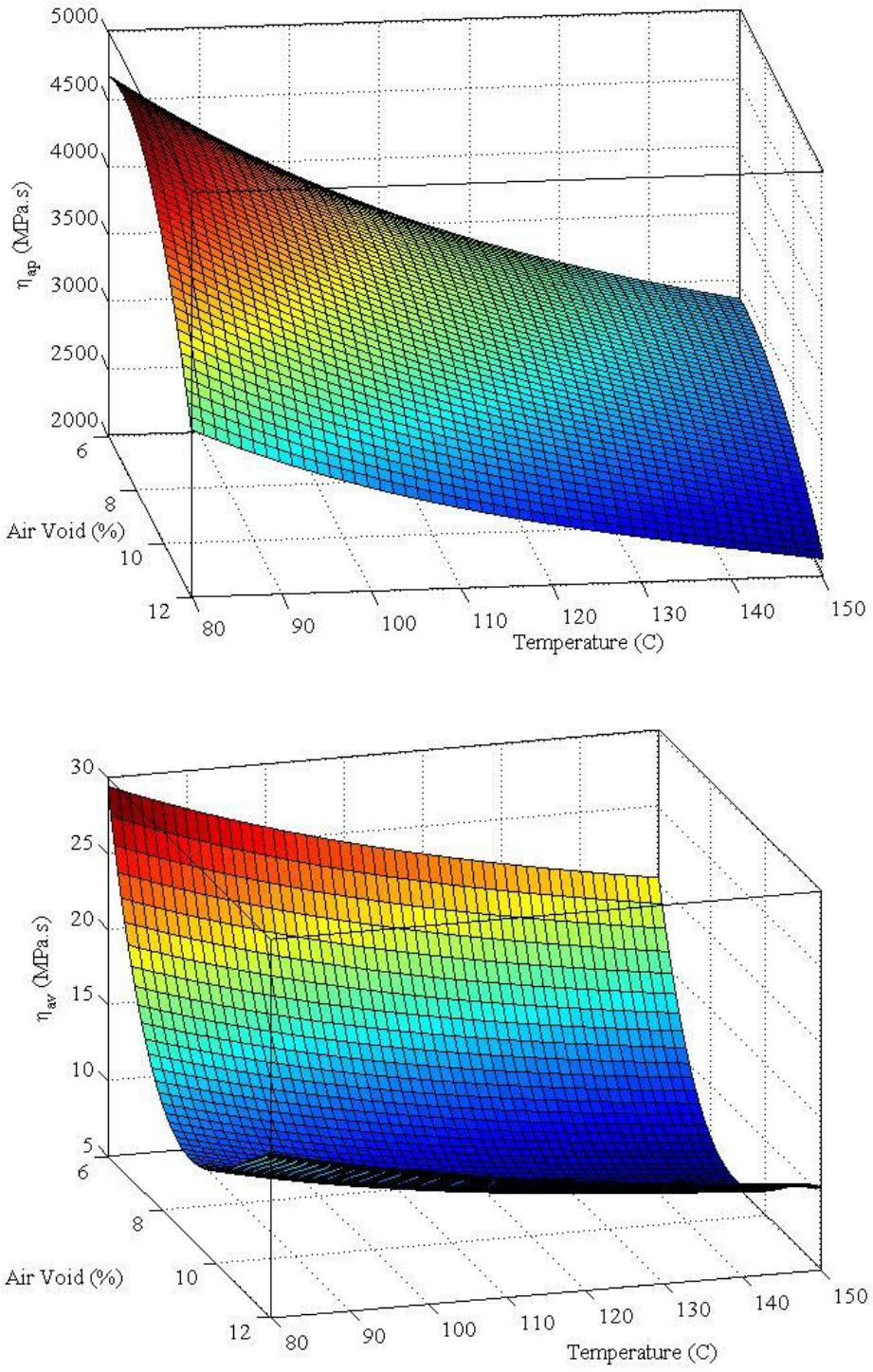

Figure 3.3 Three dimensional plots of parameters η_{ap} and η_{av} as a function of Temperature and Air void contents for asphalt mix used in Test Project I.

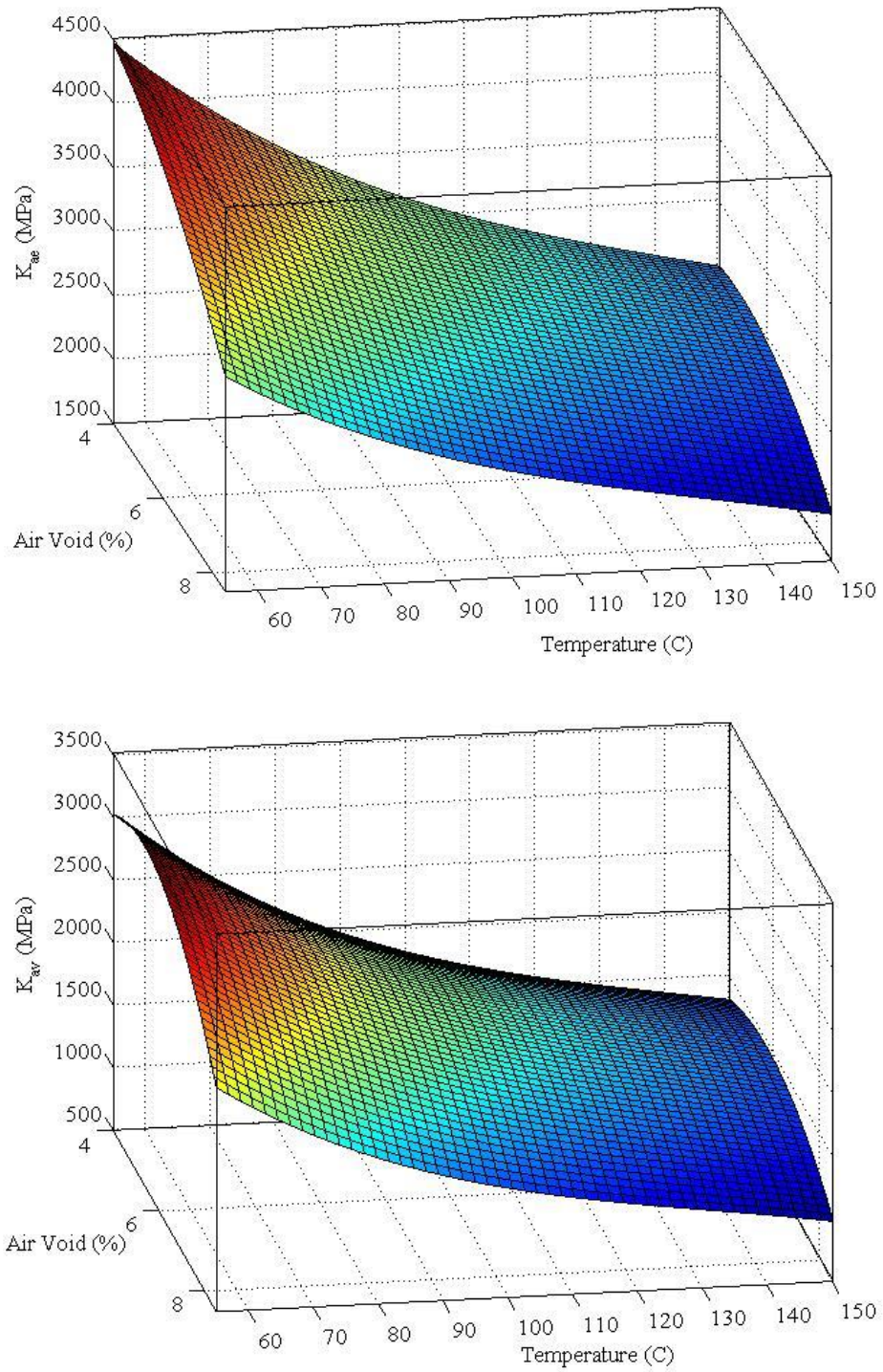

Figure 3.4 Three dimensional plots of parameters K_{ae} and K_{av} as a function of Temperature and Air void contents for asphalt mix used in Test Project II.

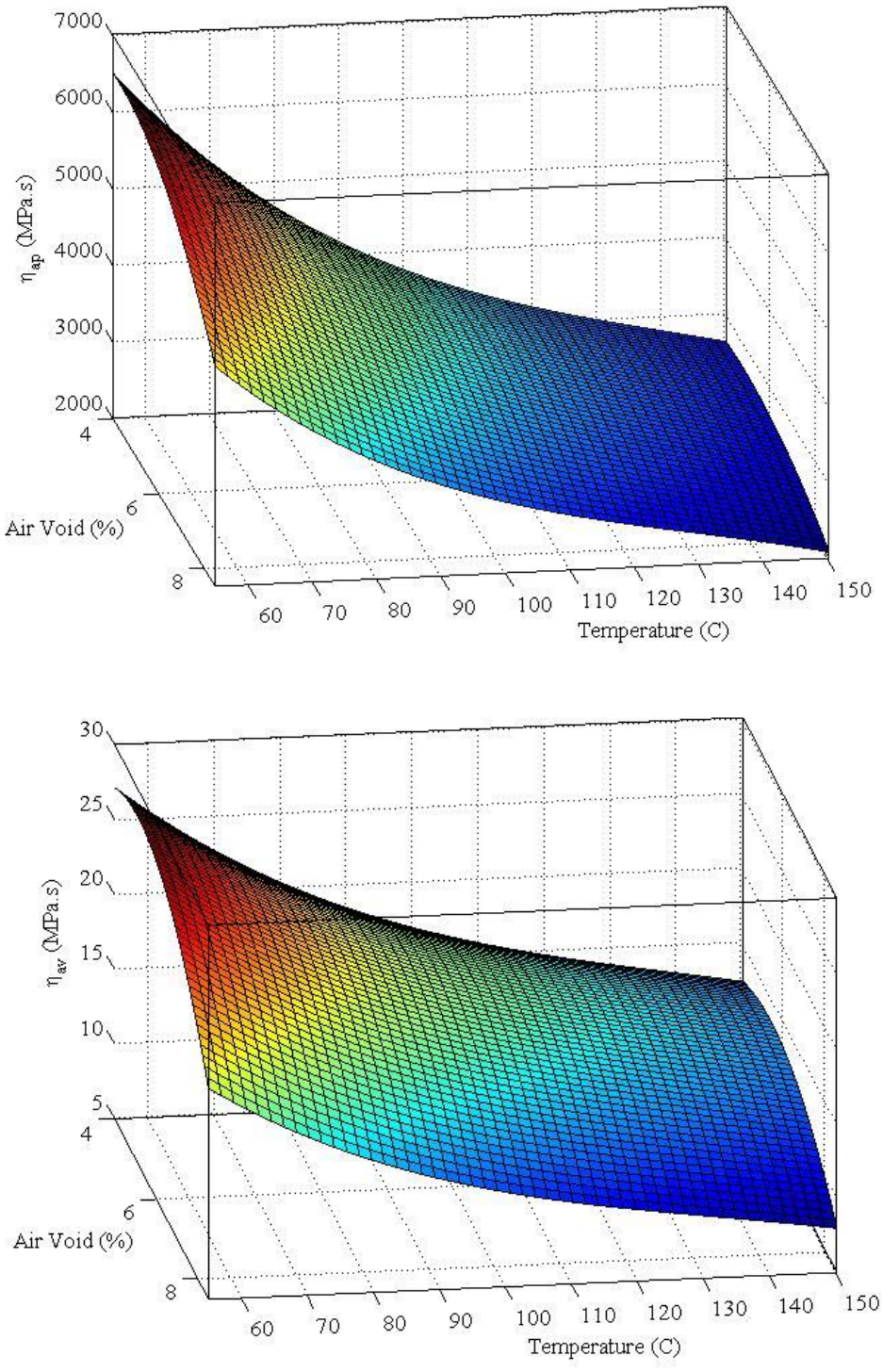

Figure 3.5 Three dimensional plots of parameters η_{ap} and η_{av} as a function of Temperature and Air void contents for asphalt mix used in Test Project II.

3.4 Analysis and Verification of Simulation Results

3.4.1 Effect of Mixture Temperature on Compaction

First set of simulations were performed to study the ability of the model in incorporating the effect of mix temperature during compaction. A 10-meter long single lane stretch of asphalt pavement was considered for simulation of compaction. Two different laydown mix temperatures of 80^{o}C and 150^{o}C were considered. Simulations were performed for five consecutive passes of vibratory compaction on this stretch. The reduction of air void percentages after each pass of the roller for the two models corresponding to Test Project I and Test Project II are shown in Figure 3.6 and 3.7. Simulation results show that the temperature of the asphalt mix has a significant influence on it's stiffness. With the reduction of temperature the stiffness of asphalt increases and makes it difficult to compact the mix. Therefore, same amount of compaction effort will result in less reduction of air void for an asphalt mix with temperature of 80^{o}C than the mix with 150^{o}C temperature. This is observed in the numerical simulation results for both the test projects.

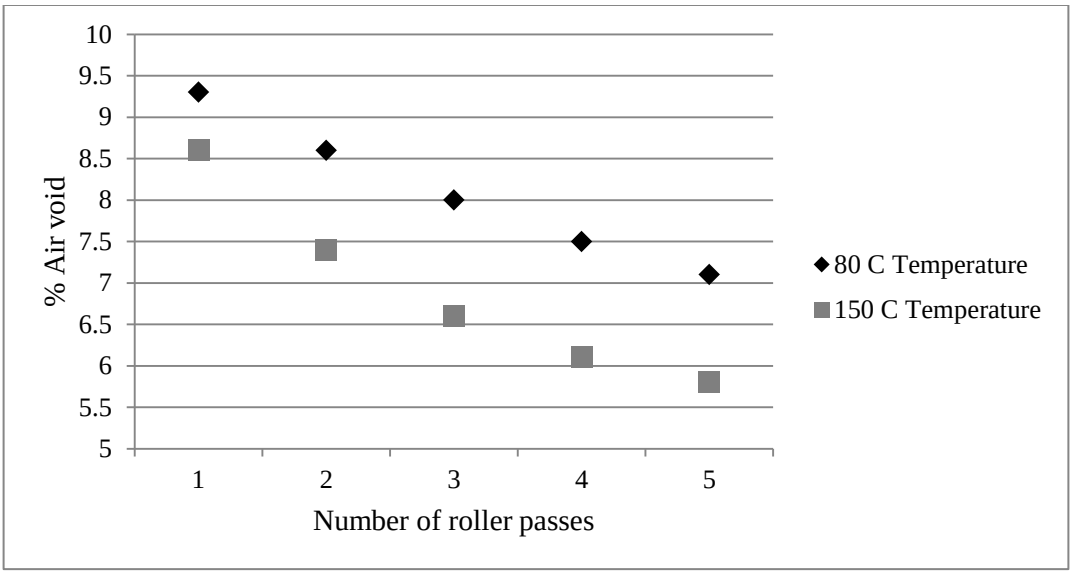

Figure 3.6 Simulated pass by pass air void percentages at 80°C and 150°C for Test Project I.

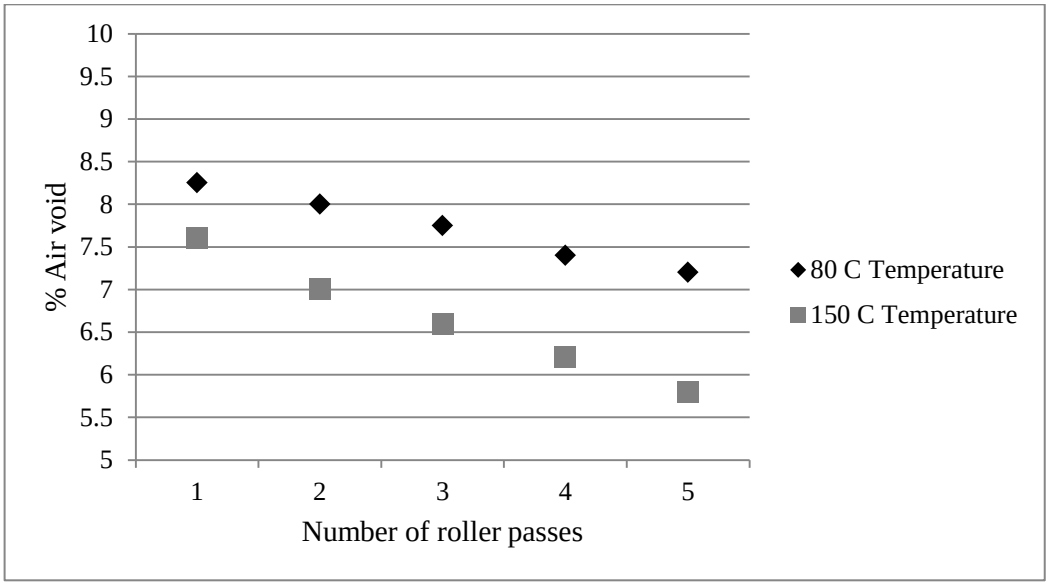

Figure 3.7 Simulated pass by pass air void contents at 80°C and 150°C for Test Project II.

3.4.2 Analysis of Drum Vibrational Characteristics

The ability of the model in capturing the drum vibratory response is studied in this section. To accomplish this, at each test project during field construction, a 10 meter long single lane stretch was selected and the roller vibration data were extracted for 5 consecutive passes on this stretch. Spectral analysis was performed on the vibration data to obtain the power spectral density (PSD) for each of the passes. The models developed for each test project were simulated and the drum vibration response for each pass was also collected and corresponding PSD values were estimated. The PSD values at the dominant harmonics of field vibration data were then compared with the simulated pass by pass PSD data of the corresponding experimental model. Figure 3.8-3.11 show a comparison of the power spectral density values of simulated experimental results and the corresponding field compaction results. The complex mechanical behavior of the asphalt mix and spatial variations in properties of the mix introduces nonlinearity in the contact vibratory response of the drum. This is manifested in the spectral response of vibration signal. The density and stiffness of asphalt pavement increases after each rolling pass. This increases the reaction force of the pavement on the roller causing the amplitude of the drum to increase. As a result, the power contents at the harmonics of the drum vibration are also increased. This is observed in the field vibration spectra for both the test projects. The increase of power content at different harmonics is also observed in the simulation results. Comparison between the simulated and the corresponding field measured vibration spectrum shows that the model is able to capture the dynamical response of the drum at not only the fundamental frequency, but also at the higher harmonics.

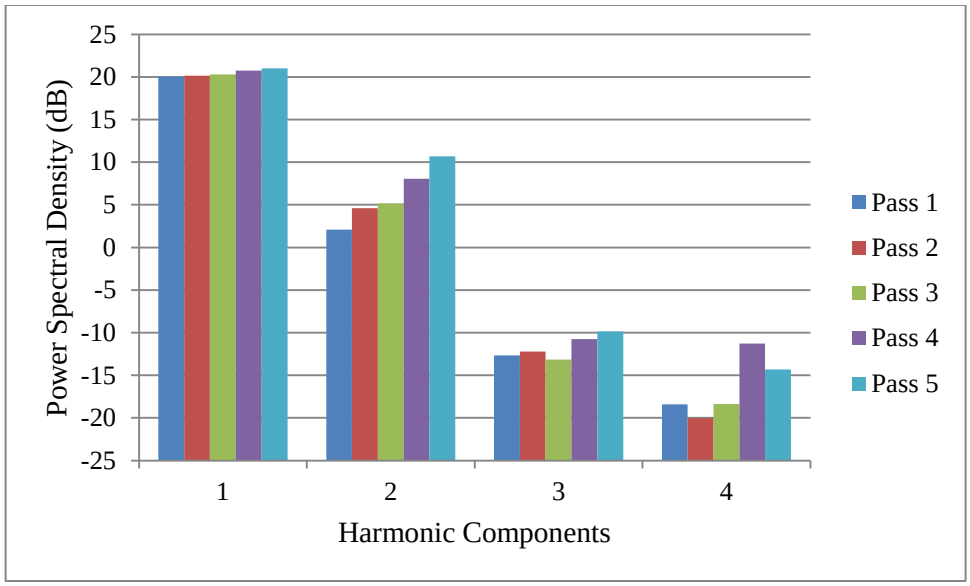

Figure 3.8 Power content at different harmonics of field measured drum vibration for Test Project I.

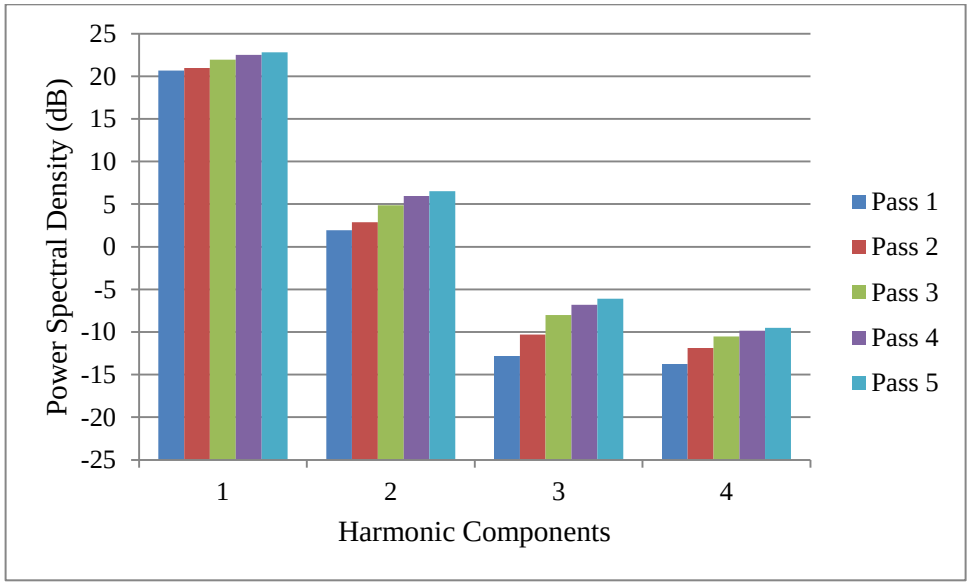

Figure 3.9 Power content at different harmonics of simulated drum vibration for Test Project I.

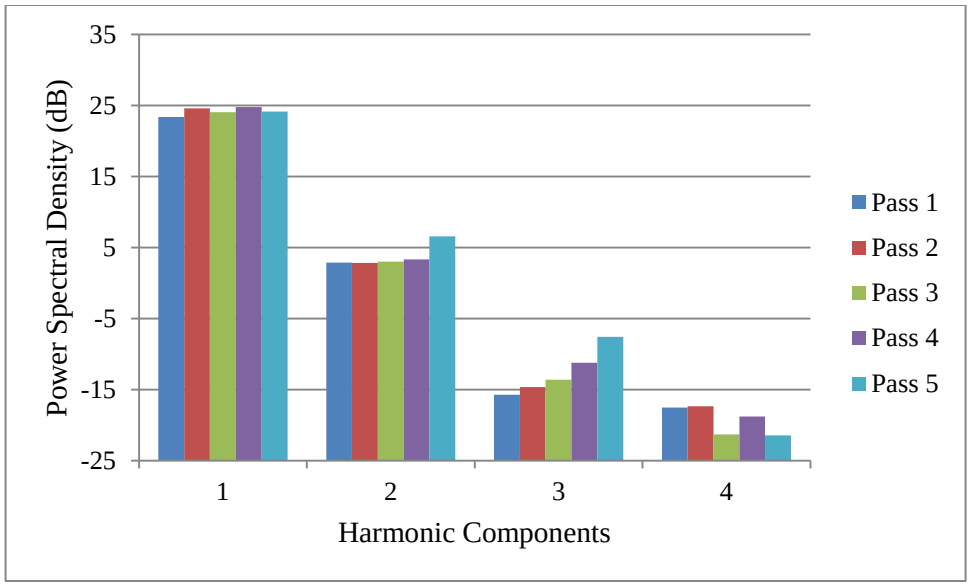

Figure 3.10 Power content at different harmonics of field measured drum vibration for Test Project II.

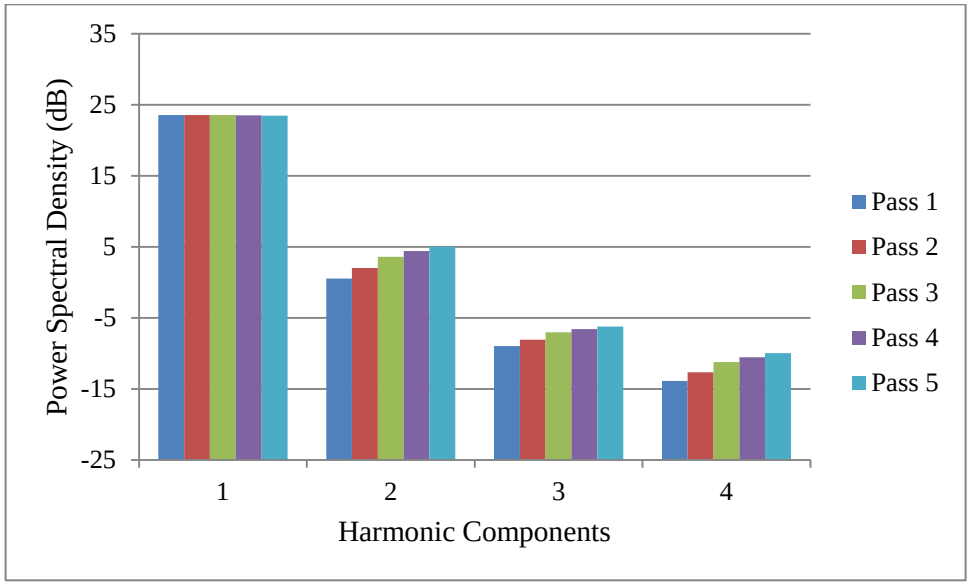

Figure 3.11 Power content at different harmonics of simulated drum vibration for Test Project II.

3.4.3 Asphalt Pavement Densification Process

The ability of the model in replicating the pass by pass densification process was also studied in this research. The pass by pass density of a 10 meter long stretch was recorded during simulation. The average density of each pass for the simulated models was then compared with the corresponding field compaction density results. In the field investigations, the IACA was used to estimate the density in real time. IACA had been used extensively in a number of field investigations and it's applicability in estimation of pavement density during compaction had been studied over the past several years (Commuri and Zaman, 2008; Beainy et al., 2011; Commuri et al. 2014). In this study also it's accuracy was verified with lab measured density results. In order to accomplish this, 8 random locations were marked on the pavement in each test project. During compaction, the IACA recorded its estimated density for each marked location. After completion of compaction, cores were extracted from each location to measure their densities in the laboratory. The IACA estimated results were then compared with the lab measured densities. Table 3.2 shows a comparison of the IACA estimated densities and the corresponding lab densities for both the projects. It is found in both the test projects that the IACA estimated densities are within 1% of the lab measured densities for more than 80% of the locations. The error is within 0.5% on more than 68% of the locations.

Table 3.2 Validation of IACA results on the two project locations.

Test Location 1	Core Name	C1	C2	C3	C4	C5	C6	C7	C8
	IACA Est. Density	93.7	93.3	93.7	95.7	95.8	94	94.1	94.2
	Lab Measured Density	93.6	93.5	93.6	92.4	93.3	92.6	94.5	93.9
	Error (Lab-IACA)	-0.1	0.2	-0.1	-3.3	-2.5	-1.4	0.4	-0.3
Test Location 2	Core Name	M1	M2	M3	M4	M5	M6	M7	M8
	IACA Est. Density	94.5	93.7	94.9	94.2	94.8	94	95.8	94.8
	Lab Measured Density	94.1	94.1	94.5	94.2	94.7	94.6	95.1	95.3
	Error (Lab-IACA)	-0.4	0.4	-0.4	0	-0.1	0.6	-0.7	0.5

During compaction, the IACA was used to estimate the pass by pass densities of a given 10 meter stretch. The estimated densities were recorded and the average densities at each pass were obtained from them. These field estimation results were then compared with the simulated density results. A comparison between the simulated pass by pass average density and the corresponding IACA estimated field densities for both the test projects are shown in Figure 3.12 and 3.13. It is evident from the results that, the model can represent the pass by pass densification process with a reasonably good accuracy (error less than 1%).

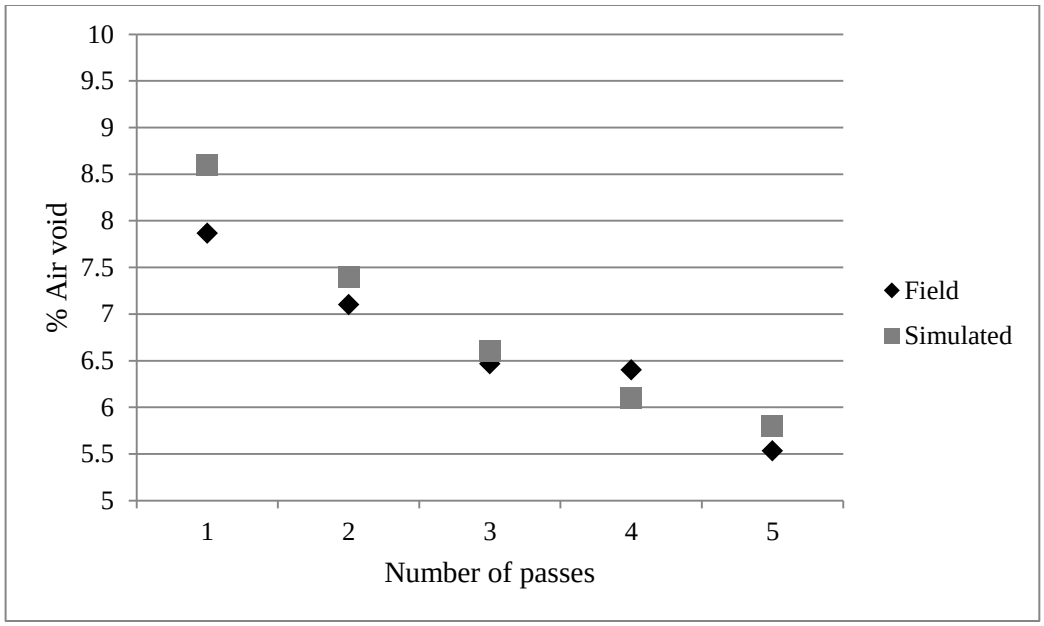

Figure 3.12 Comparison of pass by pass average air void contents of a stretch between model simulation results and IACA estimated field results for Test Project I.

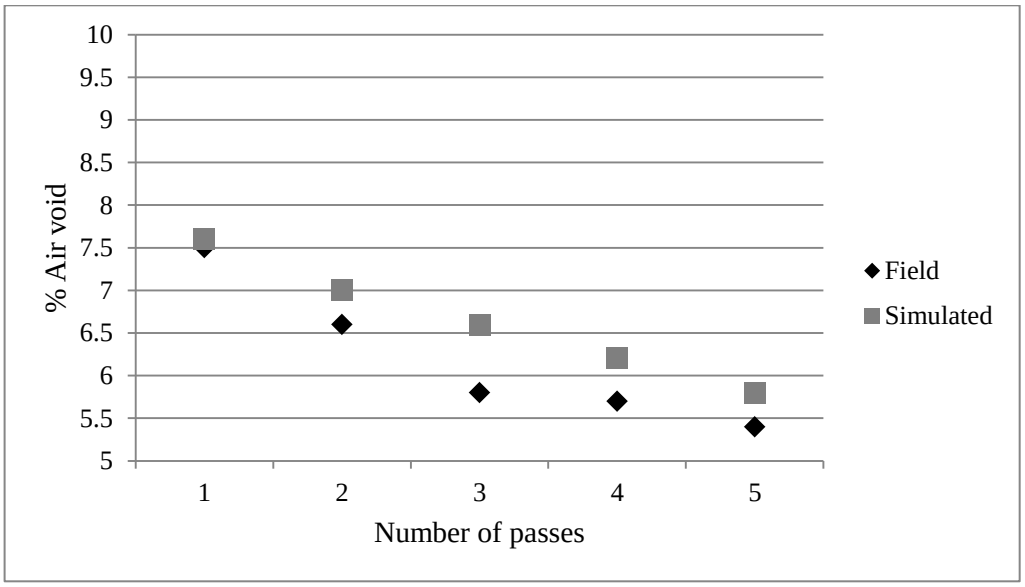

Figure 3.13 Comparison of pass by pass average air void contents of a stretch between model simulation results and IACA estimated field results for Test Project II.

3.4.4 Effect of Flexible Base on Compaction

One of the assumptions made during the development of the Interaction model in Chapter 2 is that the asphalt layer is placed on top of a rigid base. However, in real world the asphalt layers are usually placed on top flexible base layers such as asphalt pavement, cement concrete, stabilized soil, aggregate base etc. Therefore, assumption of a rigid base introduces some error during simulation of field compaction process. In order to examine the effect of the base layer, the model was integrated with three different flexible base layers including lean concrete, cement stabilized aggregate and cement stabilized soil. The typical stiffness values of these bases are found in MEPDG guideline and used in this analysis (ARA, 2004). Table 3.3 shows the typical values of stiffness for different types of base materials.

Figure 3.14 shows the pass by pass progression of densification of an asphalt pavement with different underlying base layers. It is observed from the figure that the densification process is faster when the stiffness of underlying base is higher. This is due to the fact that if the stiffness of the base layer is low, part of the compaction energy is absorbed by this base during compaction. This results in a slower densification of the asphalt layer.

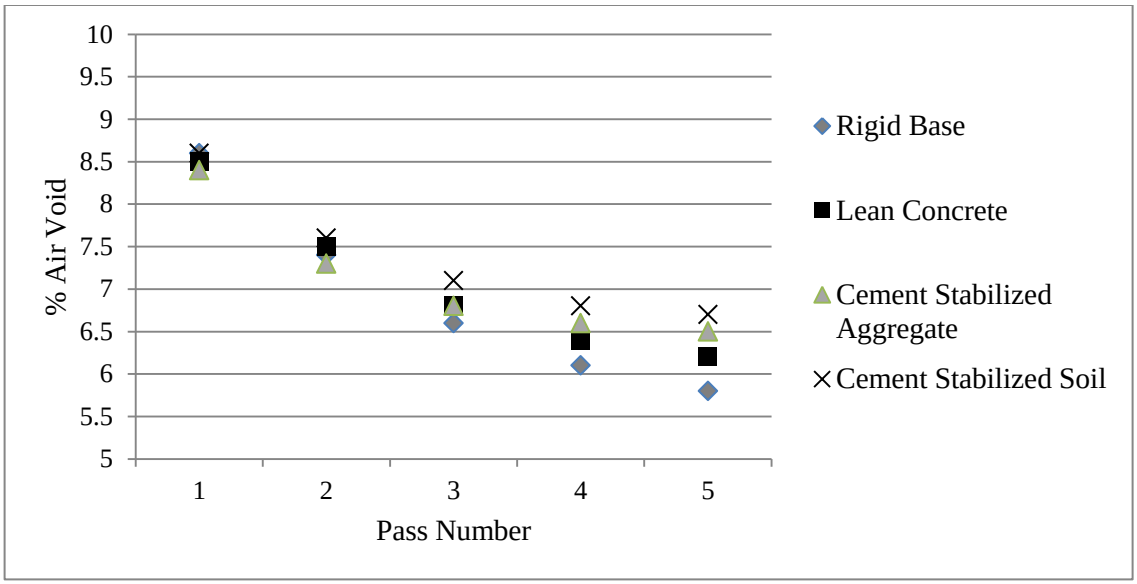

Figure 3.14 Effect of base layers on the progression of compaction of asphalt pavement

Table 3.3 Typical Stiffness values of different base layer (ARA, 2004).

Material Type	**Typical Mr (MPa)**
Rigid Base	N/A
Lean Concrete	13790
Cement Stabilized Aggregate	6895
Cement Stabilized Soil	3447

3.5 Validation of Two Dimensional Model of Asphalt-Roller Interaction

The aim regarding the development of a two dimensional extension of the interaction model was to study its ability to incorporate the effect of shear force in the vibration dynamics of the drum. In order to accomplish this, the vibrational characteristics of the roller drum were examined through Matlab simulations. Figure 3.16 shows a simulated

drum acceleration signals for both the vertical and horizontal directions. The simulated results were compared with filed compaction data to verify its effectiveness. The field compaction data were obtained during the construction of US 77 in Noble, Oklahoma. A IR DD 118 HF vibratory roller is used for compaction of asphalt pavement. A Crossbow CXL10HF3 triaxial accelerometer was used to measure the vibration of the drum in both horizontal and vertical direction. The vibration data were recorded by a data acquisition system and a rugged tablet pc. Figure 3.15 shows the drum acceleration signals recorded during field compaction (Imran et al., 2015). The field data is filtered to reduce the high frequency noise. Comparison between the model and the field acceleration data shows that the model is able to capture the response of the roller drum in both the vertical and horizontal directions. It is observed from the field data in Figure 3.15 that, the amplitude of the horizontal acceleration is less than that of the vertical acceleration. Besides, there is a phase lag between the horizontal acceleration and its vertical counterpart. This is because of the fact that the applied eccentric force acts radially towards all direction in a rotating manner due to the rotation of the unbalanced eccentric mass around the shaft of the drum. It can be noted that the phase difference between the vibrations is higher in the model simulation data than in the field data. One possible explanation of this is only the shear stiffness of the asphalt pavement is considered in the model and was expressed by a spring. The shear viscosity of asphalt was not taken into account. This results in variation in the delayed response from the actual field data.

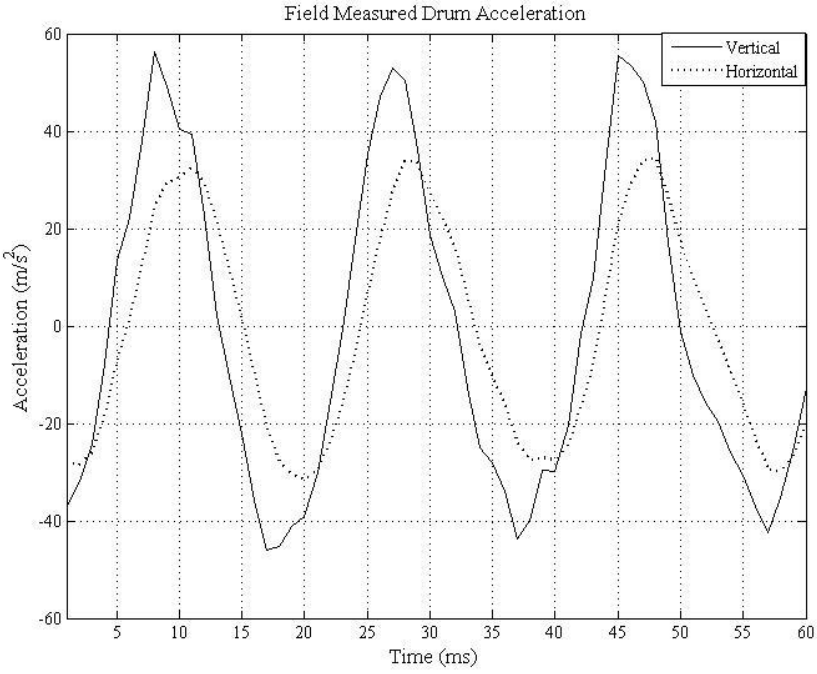

Figure 3.15 Drum Acceleration signal captured during field compaction.

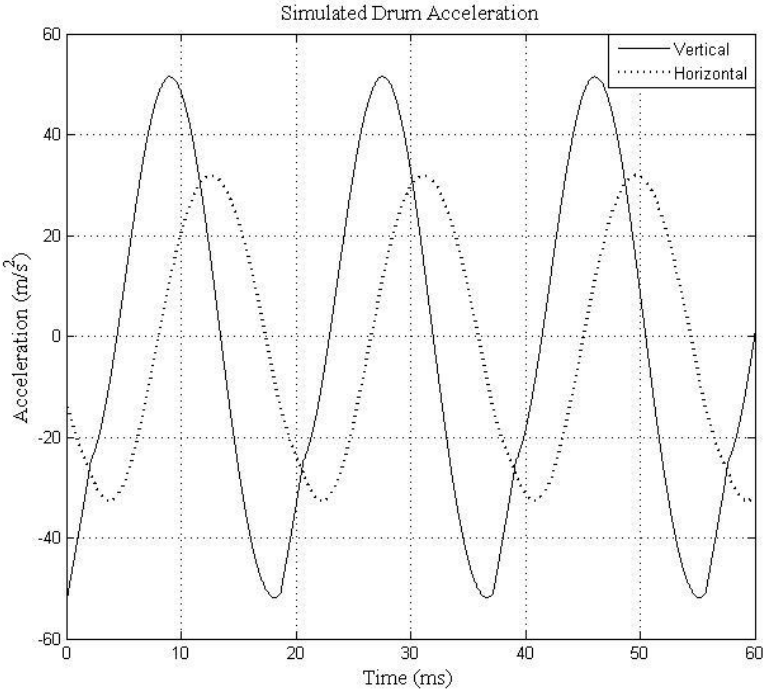

Figure 3.16 Drum Acceleration signal from model simulation.

The effect of asphalt density on the drum vibration during compaction was also studied in this research. Numerical simulations were performed to obtain drum acceleration for 9%, 7% and 6% air void contents of asphalt mix. Figures 3.17 and 3.18 show the comparison between field measurements and simulated vertical and horizontal drum acceleration for different air void contents. It is observed from the figures that the model was able to capture both the vertical and horizontal vibration of the roller during compaction on different level of air void contents. It is also observed that the model was capable of predicting the increase in the magnitude of the drum acceleration as the stiffness of the pavement increases. This is also in accordance with the field vibration results. Intelligent Compaction devices are mostly based on the hypothesis that the vibratory roller and the underlying pavement constitute a coupled system during compaction. As a result, the stiffness of the asphalt has an influence on the vibration of the drum. As the compaction density and stiffness of the asphalt pavement increases the reaction force of the pavement against the compacting force also increases. This results in higher magnitude in the drum acceleration particularly in the higher frequency components. The spectral characteristics of the model response are compared with those of field vibration response. Figure 3.19-3.22 show the spectral density of field as well as simulated vibratory response. It is observed from the figures that the model is capable of capturing the spectral response of drum in both vertical and horizontal direction.

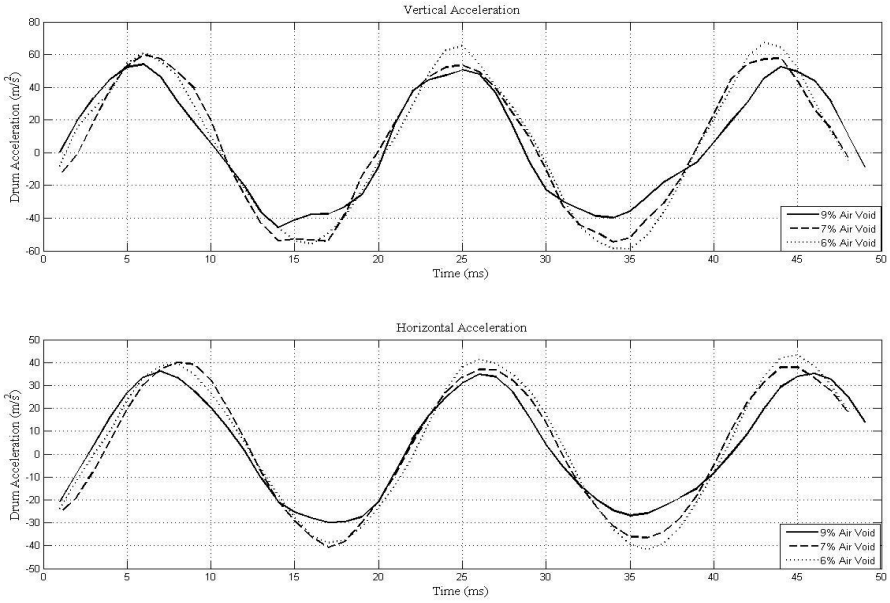

Figure 3.17 Field measured acceleration of drum during compaction of asphalt pavements of different air voids in vertical and horizontal direction.

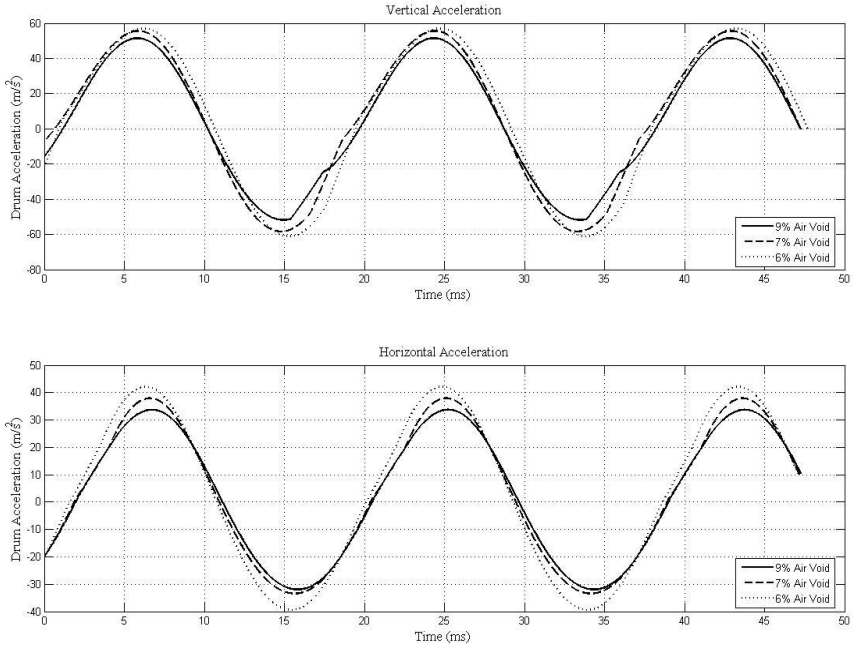

Figure 3.18 Simulated acceleration of drum during compaction of asphalt pavements of different air voids in vertical and horizontal direction.

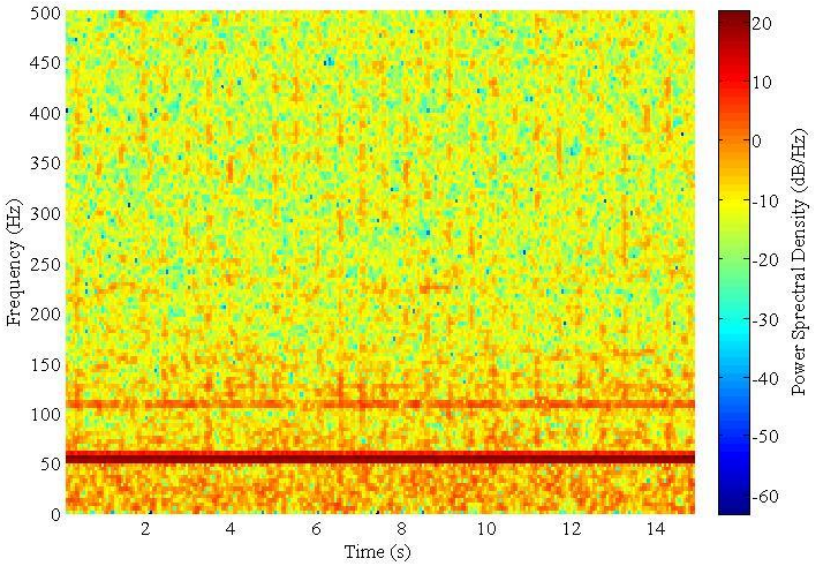

Figure 3.19 Power spectral representation of horizontal drum acceleration during field compaction.

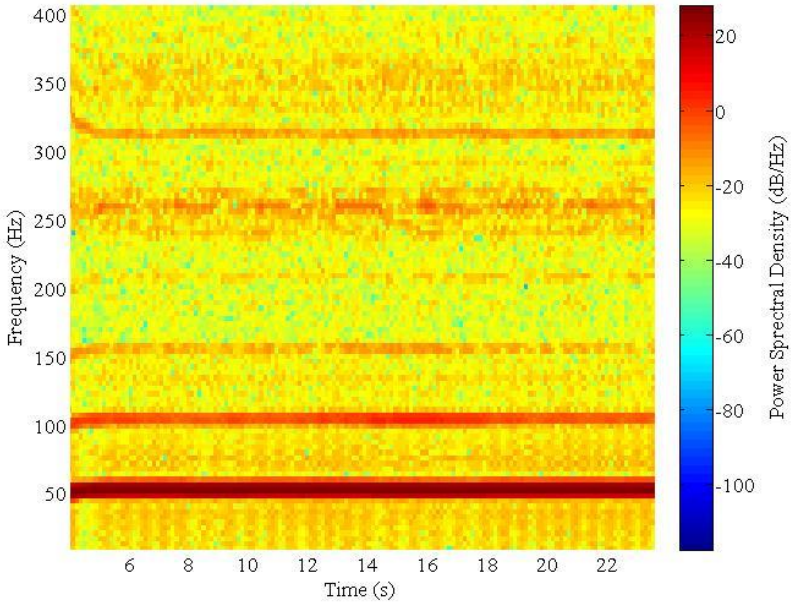

Figure 3.20 Power spectral representation of vertical drum acceleration during field compaction.

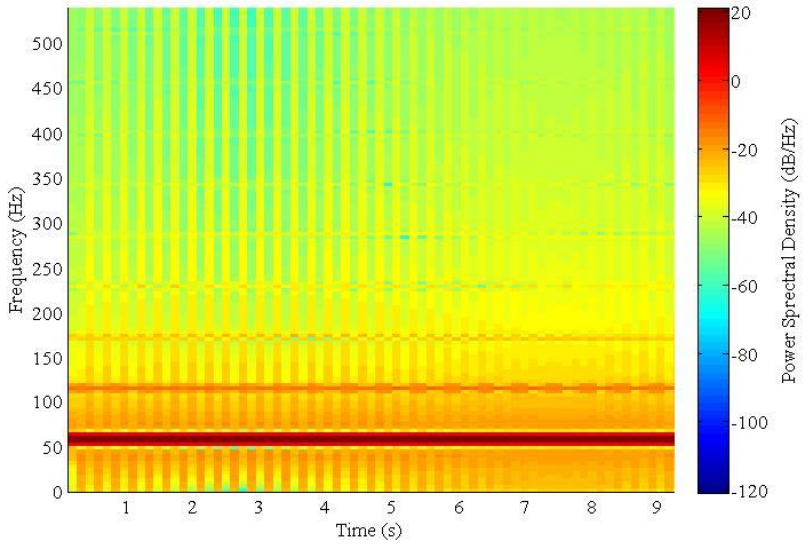

Figure 3.21 Power spectral representation of horizontal drum acceleration from model simulation.

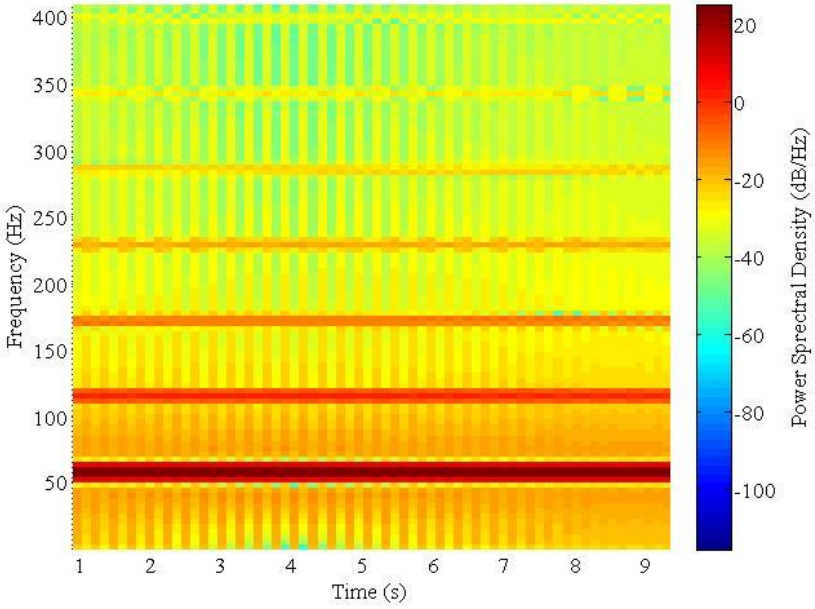

Figure 3.22 Power spectral representation of vertical drum acceleration from model simulation.

The final set of simulations was performed to investigate the ability of the roller in replicating the field compaction using a conventional rolling pattern. A rolling pattern of 5 passes on the 10 meter stretch is considered and shown in Figure 3.23(a). The width of the stretch is 3.6 meter. The drum width is 2 meter which means there is some overlap between adjacent passes as the roller moving forward and backward to execute the rolling pattern. In the simulation, the mix temperature is set constant at 150^0 C and the initial density is assumed to be at 90%. Figure 3.23 (b) to (f) has shown the density profile of the stretch after each pass. It is shown from figure that after the final pass there is approximately 2% variability in the density at different regions of the stretch due to the selection of rolling pattern. Previous field investigations performed by researchers at the University of Oklahoma (Beainy et al., 2011) on interstate I86 near Hornell, New York showed that there can be a variation in density for up to 1.8% between cores with spatial distance of just a few inches.

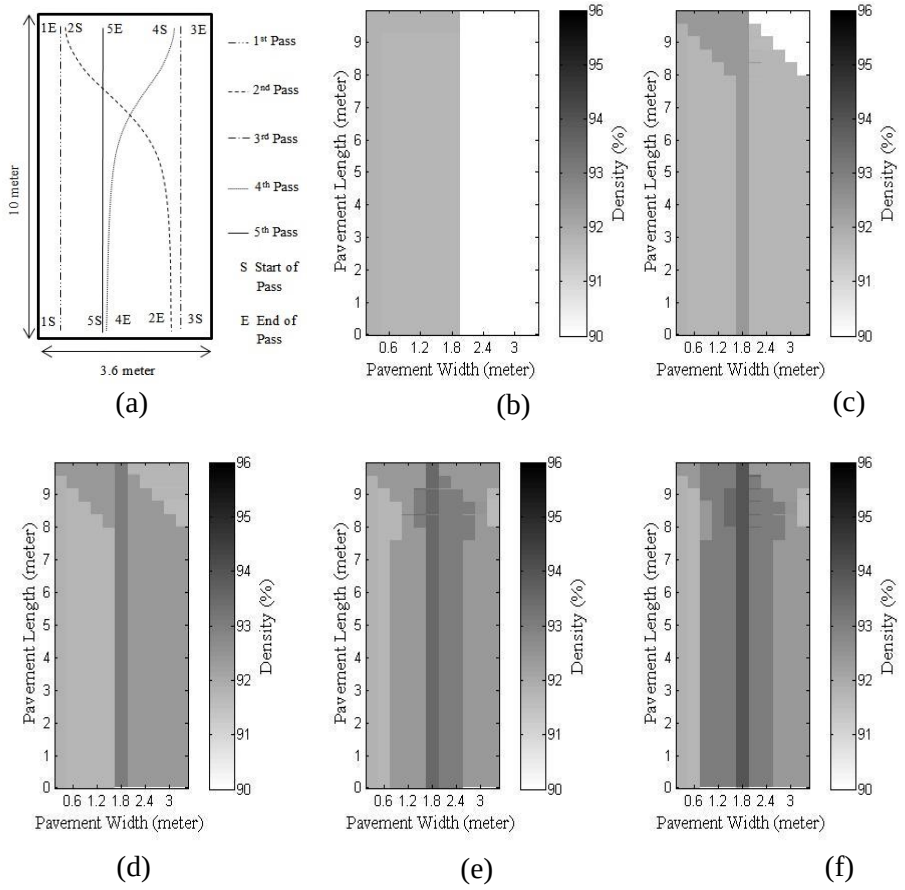

Figure 3.23 Simulation of compaction on an asphalt pavement using conventional rolling pattern (a) Rolling Pattern, Density profile of pavement after (b) 1st pass, (c) 2nd pass, (d) 3rd pass, (e) 4th pass and (f) Final pass.

3.6 Conclusions of the Chapter

The interaction model developed in Chapter 2 is tested in this chapter through numerical simulations. The determination of model parameters from roller specifications and asphalt mix properties is discussed. The simulation results and verification of the model with different field compaction data show that the model

(i) can address the effect of mix temperature during compaction,

(ii) is capable of representing the vibrational response characteristics of the drum during rolling passes, and

(iii) and can be used to study the pass by pass densification of asphalt mix.

The extension of the interaction model to two dimensional case is also studied and tested through numerical simulations. It is found that

(i) the model can capture the vibratory responses of drum in both vertical and longitudinal direction, and

(ii) can be used to study compaction achieved when conventional rolling pattern is employed.

The results and findings from this chapter indicate that the interaction model can become an effective tool for developing and studying next generation of Intelligent Compaction technologies.

CHAPTER 4 An Artificial Neural Network Based Intelligent Compaction Analyzer for Real Time Estimation of Subgrade Quality

4.1 Introduction

Subgrade plays an influential role in the long-term performance of pavement structure. Subgrade provides support for the upper layers of pavement and carries traffic loads that are transferred through the upper layers. A well compacted and good quality subgrade increases the load bearing capacity of pavement and reduces susceptibility to moisture and other weather condition-related distresses. Therefore, it is important to determine and maintain quality of compaction for the entire pavement. In this chapter the problems of traditional quality control methods of subgrade compaction is addressed and a novel artificial neural network based Intelligent Compaction system named Intelligent Compaction Analyzer (ICA) is proposed to overcome such limitations. The ICA provides continuous quality estimation of subgrade in real time. It is based on the idea that the vibrating drum of a moving roller and the underlying subgrade form a coupled system and exhibit characteristic vibrations according to the stiffness of the subgrade. It is an extension of the research conducted by Commuri and Zaman (2008 and 2010) that was focused on real time quality estimation of asphalt pavement. The ICA analyses vibrations of the drum in real time, identifies the vibration pattern and classifies them into different levels. These levels are representatives of different stiffness levels of the subgrade. An artificial neural network (ANN) based classifier is used in the ICA for this purpose. A training method is developed to train the ANN using

field vibration data. A calibration method is introduced to obtain the ICA estimated moduli from the ANN output using laboratory resilient modulus test results and in situ density and moisture content data collected from field.

4.2 Background on the Quality Control of Subgrade

The traditional quality control (QC) methods in subgrade compaction are usually limited to in-situ testing of density and moisture content, preferably using a Nuclear Density Gauge (NDG) (Rahman et al. 2008). Several other testing, such as Dynamic Cone Penetration (DCP) (Davisch et al. 2006; Siekmeier et al. 2000; Burnham 1997), Falling Weight Deflectometer (FWD) (Nazzal and Mohammad 2010; Russell and Hossain 2000) are also used to determine the strength and stability of the subgrade. One of the major limitations of these QC methods is that they are spot testing methods that generally cover less than 1% of the entire subgrade area and do not evaluate the entire subgrade. The tests are also time consuming and can be conducted only post compaction.

One approach to address the limitations of spot testing methods that has garnered lots of attention in recent years is Intelligent Compaction. Intelligent Compaction is a means of ensuring continuous control of subgrade quality during compaction(Camargo et al. 2006; Rinechart and Mooney 2008; Von et al., 2010; Chang et al. 2011). Intelligent Compaction (IC) techniques are generally based on the hypothesis that the roller and the pavement form a coupled system. Hence, the response of the system to vibratory compaction is influenced by the properties of the layers being compacted. During the compaction process, the stiffness of the underlying layer(s) increases and as a

consequence, the vibration patterns experienced by the roller change. The amplitude and frequency of these vibrations, therefore, can be used to estimate the properties of the layer (asphalt, soil, aggregate, etc.) being compacted. Sandstrom (1998) utilized the frequency and amplitude of vibration of the roller to compute the shear modulus and a "plastic" parameter of subgrade. These values were then used to adjust the velocity, frequency and amplitude of the roller for optimal compaction of the subgrade. Mooney and Adam (2007) expressed the ratio of the amplitude of the first harmonic of drum vibration to the amplitude of the fundamental frequency as a measure of nonlinearity of the soil-drum interaction which is used as an indicator of the stiffness level of the soil. Anderegg and Kaufmann (2004) used lumped parameter model to develop an analytical solution of roller subgrade interaction. The nonlinearity in the drum vibrations were postulated as a result of periodic loss of contact between the roller and the drum. The soil stiffness was extracted from the drum acceleration and phase difference between the eccentric force and drum response. White et al. (2005) utilized the concept of vehicle terrain interaction and evaluates the rolling resistance during compaction as an indicator of soil stiffness (White and Vennapusa 2009; Vennapusa et al., 2010).

Based on some of the above mentioned concepts, several IC solutions are available in the industry. Some of the notable ones include Compaction Information System (Sakai 2016), Bomag Variocontrol (Bomag 2016), Ammann Compaction Expert (Ammann 2016), AccuGrade (Young and Oetken 2016), and Dynapac Compaction Analyzer (Dynapac 2016). They provide assessment of the subgrade quality using the product specific Intelligent Compaction Measurement Value (ICMV). A brief description of some IC solutions available in the industry is given below.

Roller- Integrated Stiffness (k_b)

The Roller-Integrated Stiffness (k_b) is developed and used by the Ammann/Case (2016). In this technology, the soil is considered to be a linear elastic material in order to estimate the stiffness k_b. k_b in this approach is calculated as a ratio of the roller-soil interaction force and the amplitude of measured vibration, and is expressed as follows.

$$k_b = 4\pi^2 f^2 \left[\frac{m_d + m_e r_e \cos\varphi}{a}\right] \quad (4.1)$$

where, f is the excitation frequency, m_d is the mass of the drum, $m_e r_e$ is the eccentric moment of the unbalanced mass, φ is the phase angle, and a is amplitude of vibration.

Vibratory Modulus (E_{vib})

BOMAG developed an IC system that is designed to measure the dynamic stiffness (E_{VIB} in MN/m^2) of the compacted pavement (Bomag 2016). The relationship between drum force F_s, displacement z_d and the E_{VIB} value is expressed by the following equation.

$$z_d = \frac{1-\eta^2}{E_{VIB}} \frac{F_s}{L} \frac{2}{\pi} \left(1.8864 + ln\frac{L}{B}\right) \quad (4.2)$$

where

$$B = \sqrt{\frac{16}{\pi} \frac{R'(1-\eta^2)}{E_{VIB}} \frac{F_s}{L}} \quad (4.3)$$

η is the Poisson's ratio of the material, L is the length of the drum, B is the contact width of the drum, and R' is the radius of the drum.

Machine Drive Power (MDP)

The IC system manufactured by Caterpillar use a parameter named Machine Drive Power (MDP) to evaluate the rolling resistance during compaction as an indicator of soil stiffness (White et al. 2005). Machine Drive Power is defined as the amount of additional power required (in kJ/s) by the roller to compact a given soil (or subbase) layer over the power level required to compact the calibration layer. A positive value of MDP indicates that the layer being compacted has not yet reached the level of compaction associated with the calibration layer. Similarly, a negative value of MDP suggests that the layer is more compacted than the calibration layer because it requires less power to propel the roller. MDP is calculated using the following equation.

$$MDP = P_g - Wv\left(\sin\alpha + \frac{A'}{g}\right) - (mv + b) \tag{4.4}$$

where MDP is machine drive power (kJ/s), P_g is the gross power needed to move the machine (kJ/s), W is the roller weight (kN), A' is the machine acceleration (m/s^2), g is the acceleration of gravity (m/s^2), α is the slope angle (roller pitch from a sensor), v is the roller velocity (m/s), and, m (kJ/m) and b (kJ/s) are machine internal loss coefficients specific to a particular machine.

Compaction Meter Value (CMV)

Compaction Meter Value is a dimensionless indicator of compaction quality developed by Geodynamic in cooperation with the Dynapac Research Department (Dynapac 2016). The main hypothesis of this system is the ratio of the amplitude of first harmonic of the roller vibration and the amplitude of its fundamental frequency is significantly

influenced by the compaction level achieved in the underlying pavement (Sandström and Pettersson 2004). The value of CMV is also dependent on the dimension of the roller and operational parameters such as frequency, amplitude, and speed of the roller. CMV is calculated using the following equation.

$$CMV = C\frac{A_{2\Omega}}{A_{\Omega}} \tag{4.5}$$

where C is a constant, $A_{2\Omega}$ is the amplitude of the first harmonic component of the drum vibration and A_{Ω} is the amplitude of the fundamental component of vibration.

Compaction Control Value (CCV)

Sakai introduced an IC system named Compaction Information System (CIS). In this system, a Compaction Control Value (CCV) is used as an indicator of the stiffness of the pavement. The main idea of the CCV is that as the stiffness of ground increases, the roller drum bounces on impact and loses contact with ground (Chang et al., 2011). As a result, variations in the drum acceleration are encountered. The measure of stiffness, CCV used in this system is a unit-less quantity and is expressed using the following equation,

$$CCV = \left[\frac{A_{0.5\Omega} + A_{1.5\Omega} + A_{2\Omega} + A_{2.5\Omega} + A_{3\Omega}}{A_{0.5\Omega} + A_{\Omega}}\right] * 100 \tag{4.6}$$

where A_{Ω} is the value of amplitude spectrum of the fundamental frequency of vibration; and $A_{N\Omega}$ is the value of amplitude spectrum of the N^{th} harmonic/sub harmonic of vibration.

Although these ICMV values are useful as indicators of the quality of the subgrade, their relationship with the mechanistic design parameters such as resilient modulus or subgrade modulus (ARA, 2004) are yet to be established. The relationship of these product specific values and the in-situ testing results are also under investigation (Chang et al., 2014).

4.3 Analysis of Drum Vibration

The ICA is based on the hypothesis that the roller and the underlying subgrade form a coupled system. Therefore, any variation in the stiffness of the soil subgrade will be manifested as a variation in the vibration pattern. In order to validate this hypothesis, investigations were performed in the field during compaction of subgrade. The response of the smooth drum vibratory roller during compaction of subgrade pavement was studied at first. The investigation was performed during a full-depth asphalt pavement construction on 60th St. in Norman, OK. The stretch was 3.4 km long and located between Tecumseh road and Franklin road. A brief description of the project is provided in Chapter 5 of this dissertation. A smooth drum vibratory roller was used here for proof rolling as the final step of compaction process. The roller was instrumented with an accelerometer, a GPS receiver and a data acquisition system to measure and store the drum vibration signal and corresponding location of the roller during compaction. In order to understand the vibration pattern, the vibration signals generated by the roller were analyzed. The spectrogram analysis of the typical vibration can be seen in Figure 4.1 (Mitra, 2006).

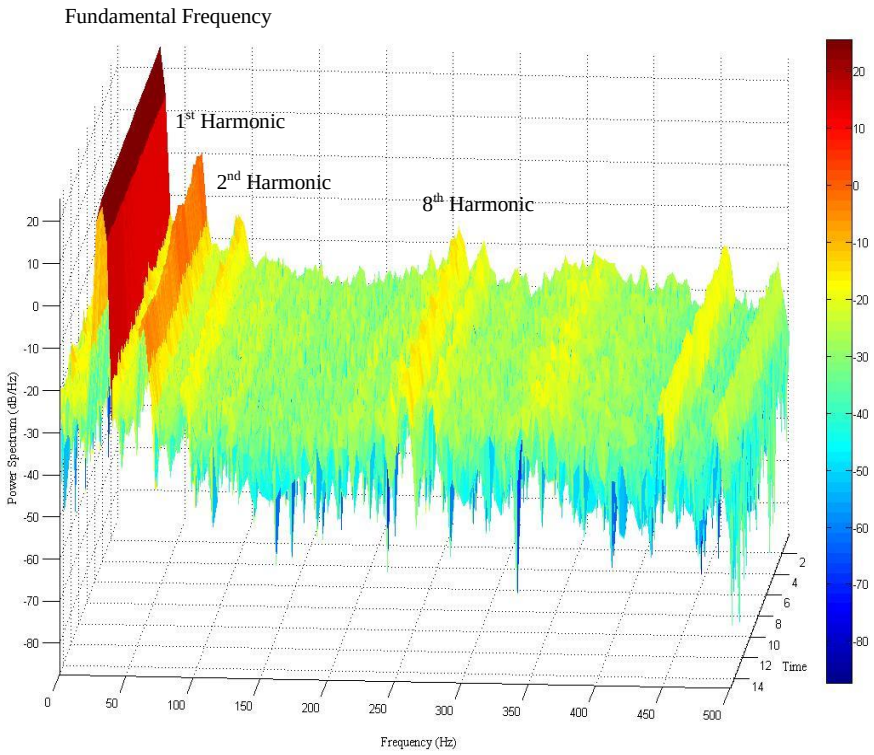

Figure 4.1 Spectral Representation of a typical drum vibration during compaction of soil subgrade.

It is observed from the spectrogram that the response of the drum to an eccentric vibratory force is a nonlinear one and spread over a range of frequencies. The spectral distribution also suggests that the response is dominated in certain harmonic frequencies.

The variations in drum vibration responses in accordance with the stiffness of the underlying subgrade were studied next. In order to accomplish this, nine different test locations on the subgrade were selected and Falling Weight Deflectometer (FWD) test was performed to obtain subgrade resilient moduli (M_{FWD}) in these locations. The power spectral density of the vibrations around the vicinity of each location was

analyzed and compared to one another. Three types of comparisons were performed. First comparison was performed between the vibration spectra corresponding to two locations with high range of modulus values (556 MPa and 519 MPa). The comparison of spectrum is shown in Figure 4.2. It is found that the power content at different harmonics of 31 Hz, 62 Hz, 93 Hz and 124 Hz in the location with FWD modulus value of 556 MPa were found to be 25.04 dB/Hz, -1.61 dB/Hz, -16.54 dB/Hz and -25.9 dB/Hz respectively. Whereas, the power spectral values for the same harmonics in the location with modulus value of 519MPa were found to be 25.04 dB/Hz, -3.4 dB/Hz, -18.8 dB/Hz and -25.9 dB/Hz respectively. Similar comparison was performed for two other locations with low range of modulus (244 MPa and 247 MPa), shown in Figure 4.3. In this case, the power content at four dominant harmonics are found to be 24.55 dB/Hz, -2.7 dB/Hz, -13.55 dB/Hz and -23.17 dB/Hz for location of with stiffness value of 244 MPa and 24.55 dB/Hz, -2.17 dB/Hz, -13.55 dB/Hz and -23.17 dB/Hz for location with stiffness value of 247 MPa. Finally, the third comparison intended to analyze the difference between power spectrum around locations with high (939 MPa) and low (174 MPa) modulus values. This is depicted in Figure 4.4. In the location with high stiffness (939 MPa), the power contents at the first four harmonics are 24.78 dB/Hz, -1.42 dB/Hz, -16.04 dB/Hz and -25.05 dB/Hz. In the location with low stiffness (174 MPa), the power content at first four harmonics are 24.74 dB/Hz, -6.9 dB/Hz, -22.5 dB/Hz and -27.25 dB/Hz. It can be seen in these figures that the locations with similar range of modulus values exhibit similar power spectral density pattern. On the other hand, a significant increase in the power spectral density was found as the stiffness of the pavement increases.

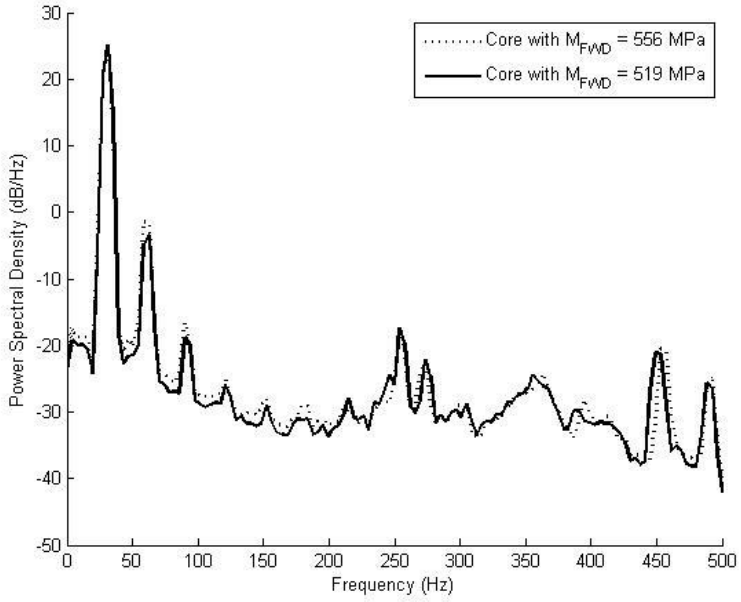

Figure 4.2 Power spectrum of drum vibrations on locations with high stiffness (M_{FWD} = 556 and 519 MPa).

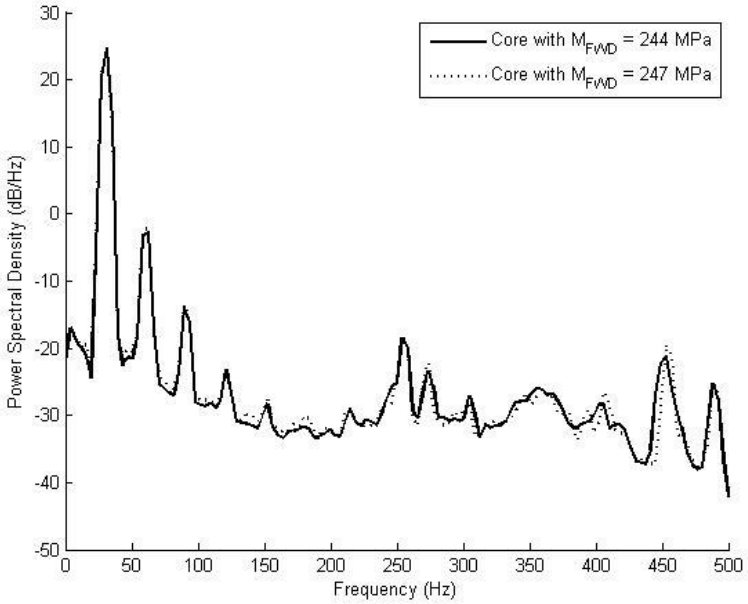

Figure 4.3 Power spectrum of drum vibrations on locations with low stiffness (M_{FWD} = 244 and 247 MPa).

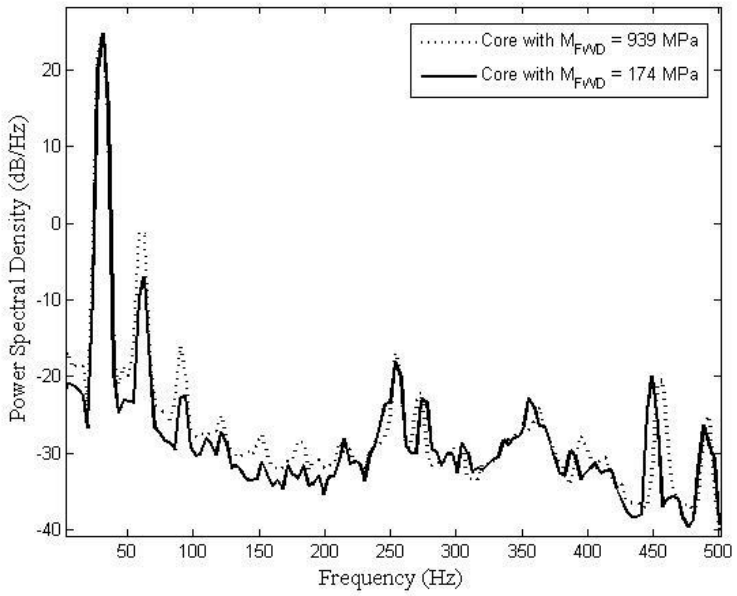

Figure 4.4 Comparison of Power spectrum of drum vibrations on locations with lowest and highest stiffness values (M_{FWD} = 174 and 939 MPa).

4.4 Development of ICA

It was observed from the analysis in previous section that the stiffness of the pavement can be inferred from the vibration of the drum during compaction. Different levels of spectral density are found during compaction of soil with different range of stiffness values. However, similarity in the spectral response was also observed in locations with equal level of stiffness. Therefore, identification of these spectral patterns and classification of them according to different level of stiffness values can be useful to indicate the quality of the soil subgrade. In this section, a model is developed that uses the drum vibration signal and classifies them into different levels in accordance with the different level of compactions. The vibration signal is processed and power spectral features are obtained from the signal. An artificial neural network based classifier is

then used to classify the vibration according to its feature values. A method is developed to train the ANN using the vibration of the drum during compaction of a control stretch.

4.4.1 Signal Processing and Estimation of Power Spectrum

The vibration of the drum of a moving smooth drum vibratory roller is influenced by its interaction with the underlying subgrade. Therefore, any variation in the mechanical properties of the subgrade will affect the response of the drum. The stiffness could also vary from location to location due to non-homogeneous properties of the soil. The stiffness of subgrade increases from one roller pass to the next. This variation in soil stiffness causes variations in the vibration of the drum. To study the changes in the vibration, the accelerometer data is processed using a 'Short Time Fourier Transform' signal processing method with a moving window function to estimate the power spectrum. The window contains 256 contiguous sampled data with an overlap of 128 previous values. The signal of each windowed segment is then converted to frequency domain representation using FFT. The FFT is a tool that uses window of sampled signal and calculates the frequency spectrum of the vibration signal. Since the vibration is sampled at 1 kHz, the Nyquist frequency is 500Hz. The output of a single sided FFT is, therefore, a frequency spectrum distributed between 0Hz and 500Hz. The power content at different frequencies for each segmented signal is then used as an input to the Artificial Neural Network Classifier.

4.4.2 Artificial Neural Network Classifier

Estimating the stiffness of the subgrade from the drum vibration is not a trivial problem. An artificial neural network (ANN) based classifier is developed to recognize the pattern of vibration and classify them to different levels according to some pre-specified patterns. A detailed description of the ANN and its training method is given below.

Development of ANN Model

The ANN developed in this research is a multilayer perceptron (MLP) neural network with 74 inputs. The power content obtained from the frequency spectrum of each segmented signal is expressed as a 74 element vector. Each element of the vector represents the signal power of a particular frequency band. The signal power of frequencies ranging from below the excitation frequency to above the fifth harmonics of the excitation frequency is selected to be used as the input. The network has an input layer, two hidden layers and an output layer. The input layer contains 74 nodes. There are 15 and 7 nodes in the first and second hidden layers and one node in the output layer (Figure 4.5). The governing equation of each node of a given layer can be expressed as,

$$y_i\left(x^{(k)}\right) = f(z_i) = f\left(w_i' x^{(k)} + b_i\right) = f\left(\sum_{j=1}^{n} w_{ij} x_j^{(k)} + b_i\right) \tag{4.7}$$

where, $x_j^{(k)}$ is the jth input of layer k. $y_i\left(x^{(k)}\right)$ is the ith ouput. w_{ij} is the weight value from the jth input to the ith output. $f()$ is the activation function (Figure 4.6). In the output layer, a linear function is used as the activation function, whereas in other layers, a tan sigmoidal function is used.

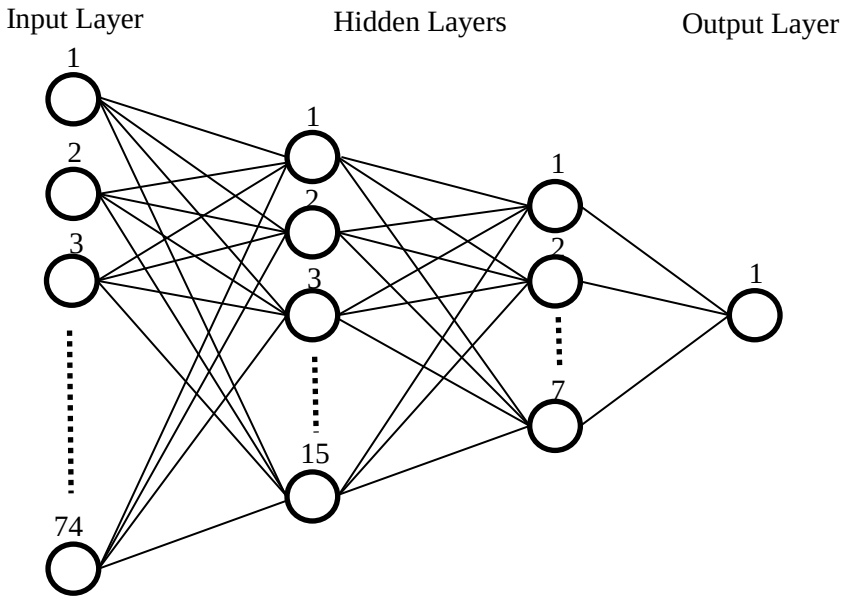

Figure 4.5 A general structure of the MLP feed forward neural network.

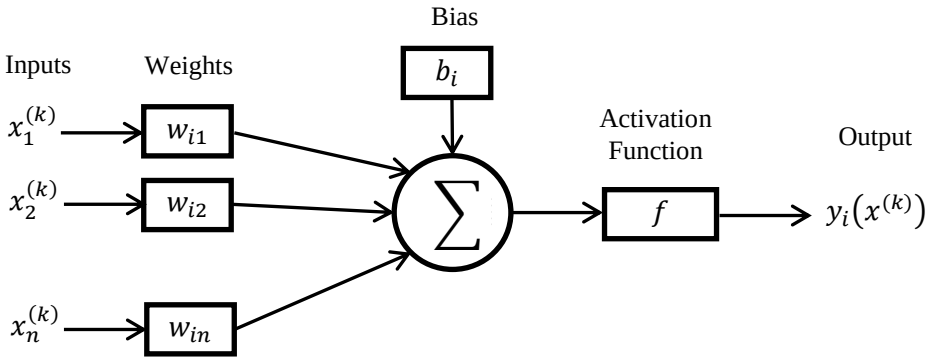

Figure 4.6 Diagram of a single neuron.

Learning Algorithm

The ANN undergoes a supervised learning method to be able to classify the vibration patterns. A backpropagation learning algorithm based on Levenberg Marquardt (LM)

algorithm is used to train the network. LM algorithm can be considered as an interpolation between the Gauss-Newton method and Gradient Descent method, and provides an iterative procedure to locate the minimum of a multivariate function. LM is designed to minimize the functions that are expressed as sum of squares and of the form,

$$E = \frac{1}{2}\|e\|^2 = \frac{1}{2}\sum_k (e_k)^2 \tag{4.8}$$

where e_k is the training error in the kth output. E is the vector of element e_k.

The LM algorithm is designed to approach second-order training speed without having to compute the Hessian matrix. When the performance function has the form of a sum of squares, then the Hessian matrix can be approximated as

$$H = J^T J \tag{4.9}$$

The gradient can be computed as

$$g = J^T e \tag{4.10}$$

Where, J is the Jacobian matrix that consists of the first derivatives of the network training errors with respect to the network weights.

The Levenberg-Marquardt algorithm uses a modified approximation of the Hessian matrix shown as

$$w_{l+1} = w_l - [J^T J + \mu I]^{-1} J^T e \tag{4.11}$$

For very large values of λ, the LM algorithm turns to standard gradient descent, whereas for very small values of λ, it becomes the Newton method.

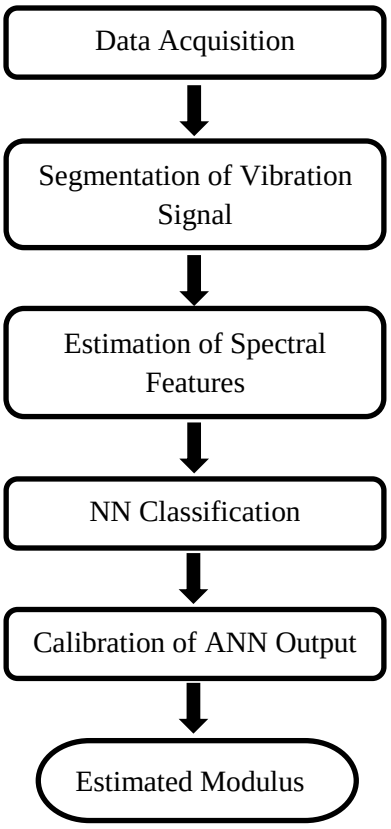

Figure 4.7 Functional schematic of artificial neural network based Intelligent Compaction Analyzer.

4.4.3 Training of ANN Model

The developed ANN model is trained using field compaction data before it is used for estimation of stiffness. In order to train the ANN, a control strip of at least 10 meter long in the subgrade pavement is selected before compaction. A vibratory roller

equipped with ICA is allowed to perform regular compaction on that control strip. Vibration data of the drum along with corresponding GPS locations are recorded continuously by the ICA during compaction. It is assumed that this control strip is a representative of the entire subgrade and encompasses all the variability that possibly can exist within the subgrade material. Therefore, it can be assumed that the vibration data includes all the vibration patterns starting from the initial pass when the subgrade is not compacted and the stiffness is low to the final pass when the subgrade is well compacted and the stiffness is high. The vibration data is then segmented using the Short Time Fourier Transform method described in the previous section and power spectrum of each segment is obtained. Since the power contents in the vibration of the drum increase as the stiffness of subgrade increases, the power content of each segment can be used as a primary indicator of the level of stiffness of the location corresponding to that particular segment. A power feature value represented as the second order spectral moment of each segment for the selected range of frequencies is calculated. These power feature values are then used to determine four characteristic vibration patterns. The first one is the minimum of the power feature values and can be attributed to the vibration corresponding to the location where the stiffness is the lowest. This vibration pattern is considered as level 1. The next one is the maximum of power feature values and attributed to the vibration pattern corresponding to the location with highest stiffness. This vibration pattern is labeled as level 4. The intermediate vibration levels 2 and 3 are obtained by linear interpolation of the maximum and minimum power feature values. The signal where the vibration is not employed is marked as ‘no vibration’ and labeled as level 0. Figure 4.8 shows different spectral levels obtained

from the field vibration data. The power spectral values corresponding to all four levels of vibrations along with the values from no vibration spectrum are then used as input data to train the network. The target data are the corresponding level numbers. Table 4.1 depicts the performance of the ANN for training data of four different test locations.

Table 4.1 Evaluation of the accuracy of the artificial neural network model

Test Locations	**MSE**		
	Training	**Test**	**Validation**
Loc. 1	0.2687	0.2914	0.2801
Loc. 2	0.2435	0.4630	0.0975
Loc. 3	0.0387	0.2976	0.4312
Loc. 4	0.0033	0.4162	0.3480

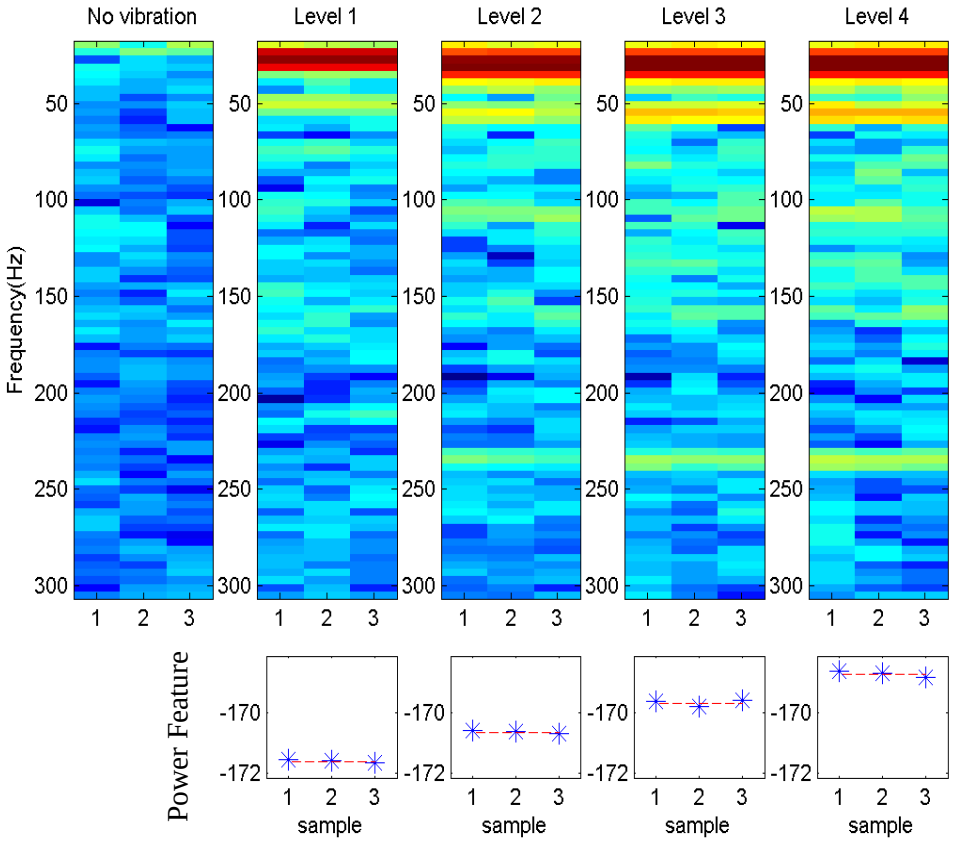

Figure 4.8 Spectral features corresponding to five levels of compaction.

4.5 Field Investigation Procedure

A general procedure is implemented in all construction projects for demonstrating the applicability of ICA. The steps in the procedure are given below.

4.5.1 Characterization of Natural and Stabilized Soils

Virgin soil samples from the project site and additives used for stabilization are collected prior to the construction of subgrade (Figure 4.9). Properties of the raw and stabilized soil are studied in the laboratory. The particle size distribution (ASTM D2487

2011) and Atterberg's limit (AASHTO T090 2014, AASHTO T089 2013) tests are performed to determine the classification of the soil. The moisture-density relationship of stabilized soils (soil-additive mixes) were then determined using Proctor Test (ASTM D698).

Figure 4.9 Collection of natural soil and CKD from field location.

4.5.2 Resilient Modulus Testing and Development of Regression Model

Resilient modulus (M_r) is used for characterizing the non-linear stress-strain behavior of subgrade soils subjected to traffic loadings. In the mechanistic pavement design, the unbound materials are characterized in terms of resilient nodulus. The resilient modulus is obtained through a repeated tri-axial test, and the test is performed as according to AASHTO T307-99 (AASHTO, 2012; AASHTO, 2010). Specimens for the resilient modulus test are prepared by mixing the soil with corresponding additive that is used to stabilize the subgrade in the field. The stabilized soil mixture is compacted in a

cylindrical mold with diameter of 101.6 mm (4 inches) and height of 203.2 mm (8 inches). Resilient modulus tests are conducted for different dry density and moisture content values and 15 different combinations of deviatoric stress (σ_d) (14, 28, 41, 55 and 70 kPa) and confining pressure (σ_3) (14, 28 and 41 kPa). The tests are performed using a Material Testing System machine (Figure 4.10).

Figure 4.10 Resilient Modulus Testing in Laboratory

Based on the test results, regression relationship can be developed to estimate the M_r as a function of moisture content, dry density and stress state. A number of constitutive models are available in literature for prediction of resilient modulus (ARA, 2004;

Andrei et al. 2004; AASHTO, 1993). The model that is used in this research is given below.

$$M_r = k_1 p_a \left(\frac{\theta}{p_a}\right)^{k_2} \left(\frac{\sigma_d}{p_a}\right)^{k_3} \quad (4.12)$$

where M_r is the resilient modulus; k_1, k_2 and k_3 are the regression coefficients in the constitutive model; p_a is the atmospheric pressure; θ is the bulk stress and σ_d is the deviatoric stress.

The M_r values obtained from resilient modulus test results for different combination of moisture contents and dry densities along with the applied stress state are used to backcalculate the k_1, k_2 and k_3 coefficients. Since the resilient modulus is a stress dependent parameter, development of regression models requires determination of the stress state that is representative of the field condition. In this regard, Mooney and Rinehart (2009) performed a study where the in-situ stress state (at 140 mm depth) was measured during compaction of a subgrade consisting of clayey sand using a vibratory roller. The static mass (11,500 Kg) and the operating frequency (~34 Hz) of the roller used in that study were similar to the vibratory rollers used in this dissertation. The magnitude of the vertical normal stress was measured as approximately 100 kPa, while the stresses in the transverse and longitudinal directions were approximately 25 to 40 kPa. These stress levels result in deviatoric stresses between 60 and 75 kPa. Therefore, for the estimation of ICA modulus (M_{ICA}) in this research, the deviatoric stress, confining pressure and bulk stress are assumed as 69, 41 and 192 kPa, respectively. This stress state is also similar to that used in the last sequence of the resilient modulus test conducted in the laboratory, as per AASHTO T307. 80% of the laboratory test data

are generally used for determining these coefficients. The remaining 20% data are used to validate the accuracy of the developed models. Equations 4.13 – 4.15 present the general form of the regression models for k_1, k_2 and k_3.

$$k_1 = a_1 + b_1(M_c) + c_1(\gamma_d) \tag{4.13}$$

$$k_2 = a_2 + b_2(M_c) + c_2(\gamma_d) \tag{4.14}$$

$$k_3 = a_3 + b_3(M_c) + c_3(\gamma_d) \tag{4.15}$$

4.5.3 Instrumentation of Vibratory Roller

The vibratory roller is equipped with ICA before the start of compaction. The ICA consists of an accelerometer, a GPS receiver, and an on board data acquisition, analysis and display system. A 13,200C uniaxial accelerometer from Summit Instruments is mounted on the axle of the drum in order to capture the vibration of the drum. A Trimble ProXT series Global Positioning System (GPS) receiver was used to record the spatial location of the roller. A rugged tablet PC from MobilDemand (xTablet T8700) was used for real time data acquisition and display. A Simulink model is developed for filtering the vibration signal, extracting features from the signal and run the artificial neural network classifier in order to obtain ICA modulus values. The Matlab Real Time Windows Target is used to run the Simulink model in real time on the tablet PC. An ICA instrumented vibratory roller during subgrade compaction is shown in Figure 4.11.

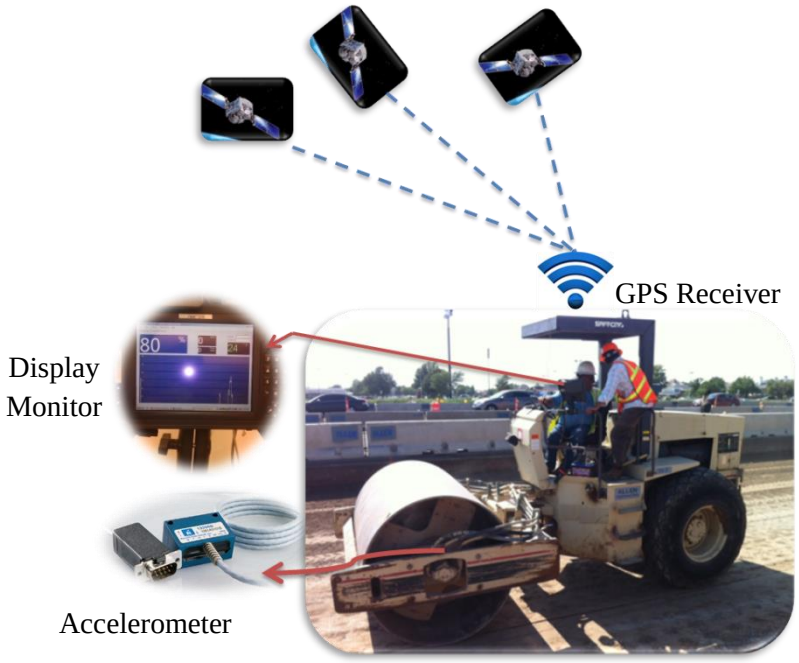

Figure 4.11 ICA installed vibratory roller.

4.5.4 Calibration of ICA in Field

At the beginning of testing, the artificial neural network in the ICA is trained on a control strip of at least 10 meter long using the method described in the previous section. After the training of the ANN, the ICA is calibrated to map the output of the ANN to the corresponding resilient modulus values. Before the beginning of the compaction of control strip the density and moisture values at random locations on the uncompacted subgrade are measured using a Nuclear Density Gauge. These density and moisture values are used to estimate the M_r values of the uncompacted subgrade using Equations 4.13 - 4.15. After the compaction is performed by the roller, three random locations usually 3 meters apart from one another are selected and corresponding nuclear gauge readings are taken from these points which are then used to obtain

corresponding resilient modulus values. From these M_r values, a range is assumed where the minimum value of the range corresponds to the stiffness of the uncompacted subgrade and the maximum value corresponds to the maximum stiffness of the compacted subgrade. Initial calibration is then performed by linear mapping of the ANN output range to the assumed range of M_r values. These initial calibration parameters are then used to estimate the ICA modulus values for the three selected locations. These initial ICA estimates are compared with the laboratory resilient modulus values of the selected locations. Finally, the calibration parameters are adjusted in a way that can minimize the square of the estimation error.

4.5.5 Field Validation of ICA Estimated Modulus

The calibrated ICA is used to estimate and record the stiffness of the entire subgrade during proof rolling. It also stores several related information such as GPS locations and speed of the roller, and vibrations of the drum etc. After the completion of proof rolling several test locations are marked in the subgrade. Moisture content and dry density values of each location is measured using Nuclear Density Gauge (Barman et al.; 2015). These values are then used to obtain the laboratory M_r for each test location. The GPS coordinates of the test locations are also recorded which is then used by the ICA to estimate the modulus values. The ICA moduli values are then compared with corresponding laboratory M_r values in order to validate the accuracy of estimation.

Figure 4.12 Moisture content and dry density measurements with NDG.

4.6 Chapter Conclusions

An artificial neural network based intelligent compaction system is introduced in this chapter for real time estimation of subgrade stiffness during compaction. The working principle of the ICA is described and the procedure to use it during field compaction is presented. In the following chapter, the ability of the ICA as a real time quality control tool is discussed.

CHAPTER 5 Validation of Intelligent Compaction Analyzer (ICA) during Field Investigations

5.1 Introduction

Analysis of roller drum vibration at different stiffness levels encouraged the researchers at the University of Oklahoma to use these differences in the vibration patterns to estimate the stiffness of the subgrade. The ICA system described in the previous chapter had been tested and validated during different field investigations in Oklahoma. Investigations were performed at four different construction sites. The field investigation procedure discussed in Chapter 4 was employed in all the projects. In each project, the ICA was trained and calibrated at the beginning of investigation. It was then used to evaluate the subgrade quality and record the estimated modulus along with corresponding GPS location and drum vibration data. The ICA estimated values were validated using spot testing methods that are used in determining subgrade quality. In the first project, a standard FWD test was performed and used for validating the ICA. However, conducting FWD test on the prepared subgrade is a challenging task and was not feasible at all sites due to cost and time considerations. Therefore, an alternate method was developed for validating the accuracy of ICA. This alternate method (discussed in Chapter 4) provides an estimate of the resilient modulus values of the subgrade based on the type of the soil and additive, in-situ density and moisture content readings and an assumed stress state of the subgrade.

During compaction, as-built maps were generated in real time to provide a color coded stiffness profile of the compacted subgrade. These maps can be used to evaluate the

overall compaction achieved and also identify any undercompacted region. In two of the projects the ICA was able to detect undercompacted regions. Results after remedial compaction of these regions showed that the quality of undercompacted regions can be improved with the aid of ICA.

In this chapter, the application of ICA during compaction of subgrade is presented. A brief description of each project along with the results and outcome of field investigation of ICA is discussed. The study and findings of this chapter were part of a project conducted by the researchers at the University of Oklahoma and sponsored by the Oklahoma Department of Transportation (Commuri et al., 2014).

5.2 Project 1 (West 60th Street)

5.2.1 Description of Project

The first field investigation was conducted during the construction of a full-depth asphalt pavement on a 3.4-kilometer (2.13 miles) long stretch at the West 60th street located between Tecumseh Road and Franklin road in Norman, Oklahoma. In this project, the raw subgrade soil was stabilized by mixing 10% Cement Kiln Dust (CKD) up to a depth of 152 mm (6.0 inches) on the day of compaction. A smooth single drum vibratory roller of model Ingersoll-Rand SD-105DX was used for final proof rolling. A schematic of the project location is shown in Figure 5.1.

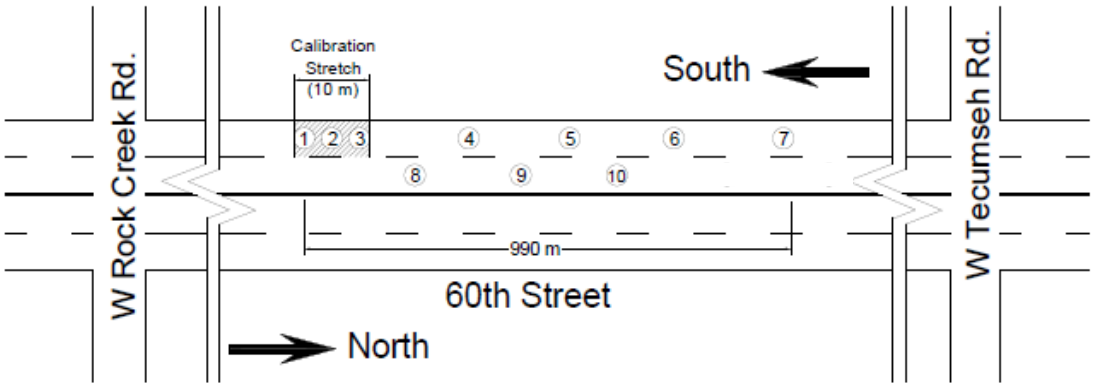

Figure 5.1 Schematic drawing of the different test points in Project 1.

5.2.2 Analysis of Results

The ICA was installed on the vibratory roller prior to compaction operations. A control strip of at least 10 meter length was selected at the beginning of compaction. Training and calibration of the ICA was performed using this control strip according to the procedure described in the previous chapter. The calibrated system was then used over the rest of the pavement and the estimated stiffness was recorded continuously in real time. After the end of compaction, ten test locations were marked and the GPS coordinates of these test locations were recorded. These GPS coordinates were used by the ICA to estimate the stiffness values for each test locations. The FWD tests were also performed on those locations after 28 days of compaction. The FWD modulus values were then used to backcalculate the stiffness values corresponding to 0 days of compaction. Table 5.1 provides the FWD modulus values and corresponding ICA modulus values for the selected ten locations in the subgrade. The correlation between the two sets of data is shown in Figure 5.2. It is observed from the figure that the ICA estimates correlate well with the FWD results (R^2 = 0.67) (Commuri et al., 2014). The

correlation is encouraging considering the fact that the FWD moduli were backcalculated results and taken after 28 days of compaction. These can likely introduce errors in the estimation.

One of the important features in the ICA system is that it can generate as-built map in real time during compaction. This map provides stiffness profile of the compacted subgrade. Figure 5.3 shows an as built map of the subgrade after completion of compaction.

Table 5.1 ICA Estimated Moduli and FWD backcalulated Moduli for selected test locations in Project 1.

Test Locations	ICA Modulus (MPa)	FWD Modulus (MPa)
T1	385	450
T2	397	938
T3	336	519
T4	376	556
T5	351	358
T6	306	174
T7	350	391
T8	344	363
T9	304	244
T10	333	246

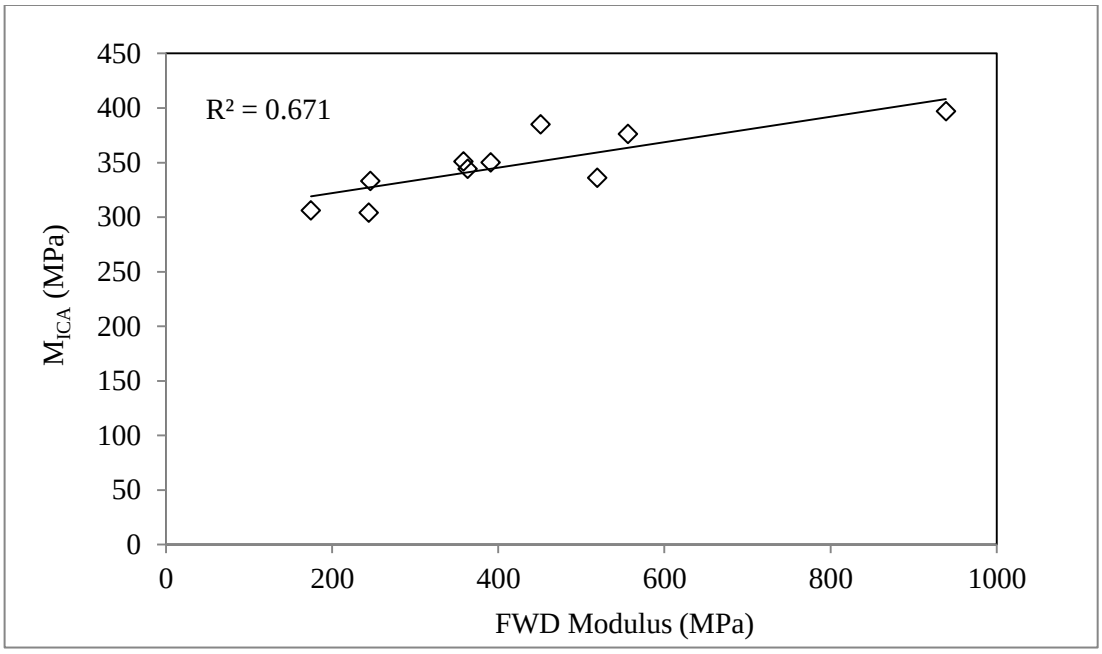

Figure 5.2 Correlation between ICA estimated moduli and FWD moduli for test locations in Project 1.

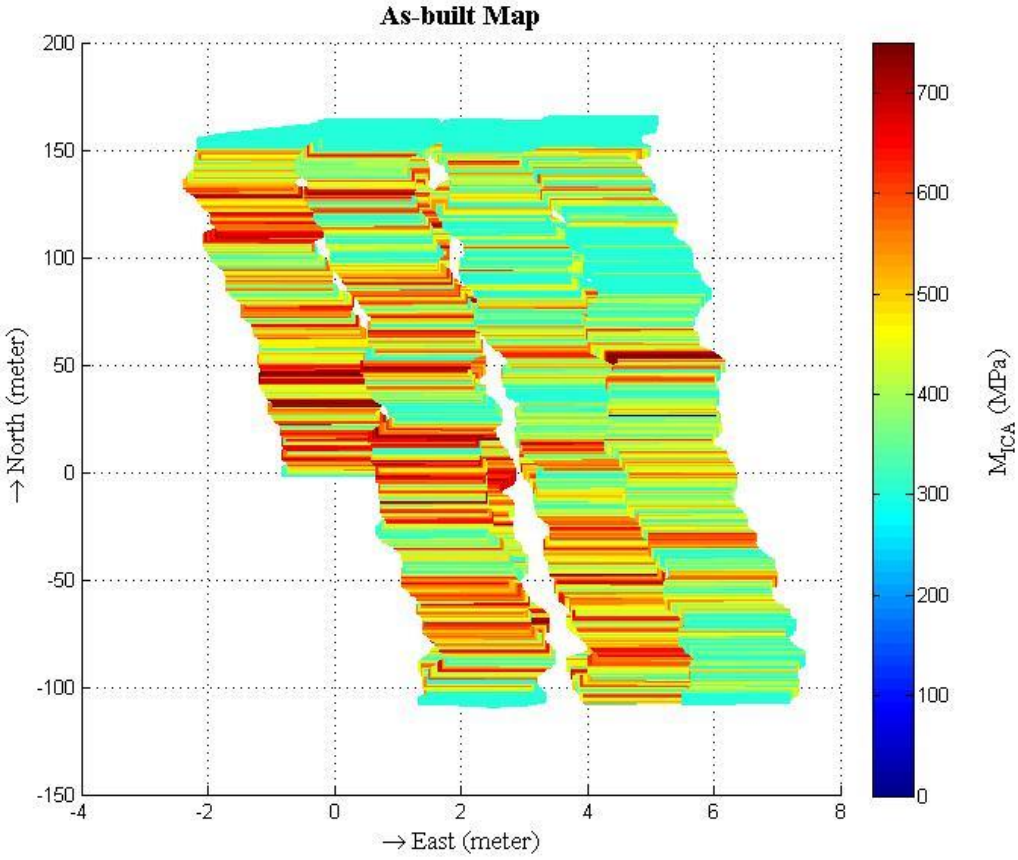

Figure 5.3 ICA generated As-built map showing the stiffness of a compacted subgrade.

5.3 Project 2 (East Hefner Road)

5.3.1 Description of Project

Results from the first field investigation encouraged the advancement of the research of ICA and to study its applicability during field compaction. The second investigation was performed during construction of a full-depth asphalt pavement on a 1.12-kilometer (0.70 miles) stretch in East Hefner Road in Apple Valley, Edmond, Oklahoma. At this location, the subgrade was stabilized by mixing 10% CKD with the existing soil up to a

depth of 304.8mm (12 inches). The proof rolling was performed by an Ingersoll-Rand SD-105DX vibratory roller.

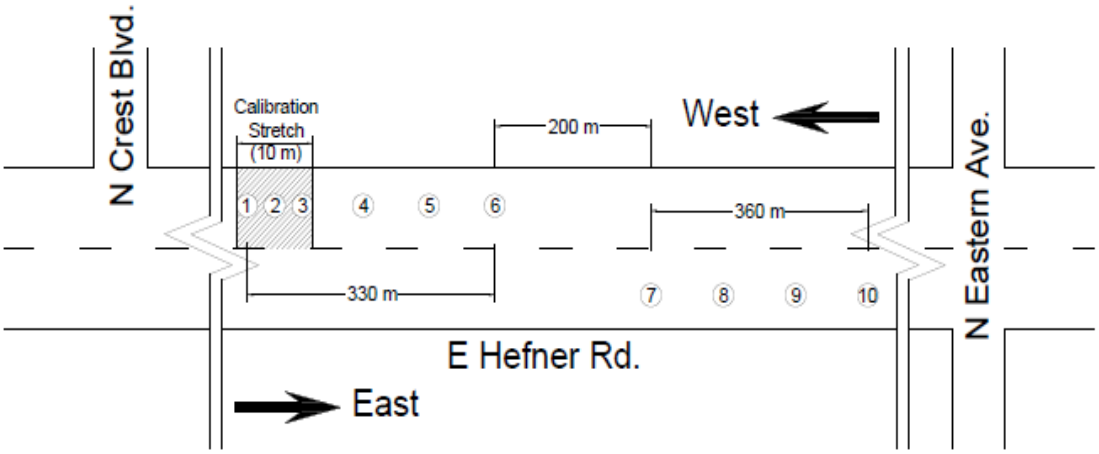

Figure 5.4 Location of different test points in Project 2.

As in the previous validation, the ICA was first mounted on the proof roller. After training and calibration of the ICA on a control strip at the beginning of compaction, it was used to estimate the stiffness during compaction of the rest of the sections. Since it was not feasible to conduct FWD tests in all the test projects, the ICA moduli were validated with laboratory resilient moduli that were obtained from density and moisture content data from field and laboratory testing results. The method for obtaining these resilient moduli values were discussed in Chapter 4 of this dissertation.

5.3.2 Analysis of Results

After compaction of subgrade, ten test locations were marked and the dry density and moisture content data from all the locations were measured using Nuclear Density Gauge. These readings were then used to estimate the resilient moduli (M_r) for each test

location. These moduli were compared with ICA estimated moduli (M_{ICA}). Table 5.2 provides a list of ICA estimated moduli and laboratory resilient moduli for the test locations of this project. Correlation between the ICA moduli and the corresponding laboratory resilient moduli for all the test locations shows that (Figure 5.5) the ICA values can be used as a representative of resilient modulus of the subgrade.

Table 5.2 ICA estimated moduli and Laboratory Resilient moduli for test locations in Project 2.

Test Locations	ICA Modulus (MPa)	Resilient Modulus (MPa)
1	528	794
2	545	580
3	553	658
4	599	700
5	798	967
6	765	851
7	740	995
8	770	871
9	790	795
10	786	870

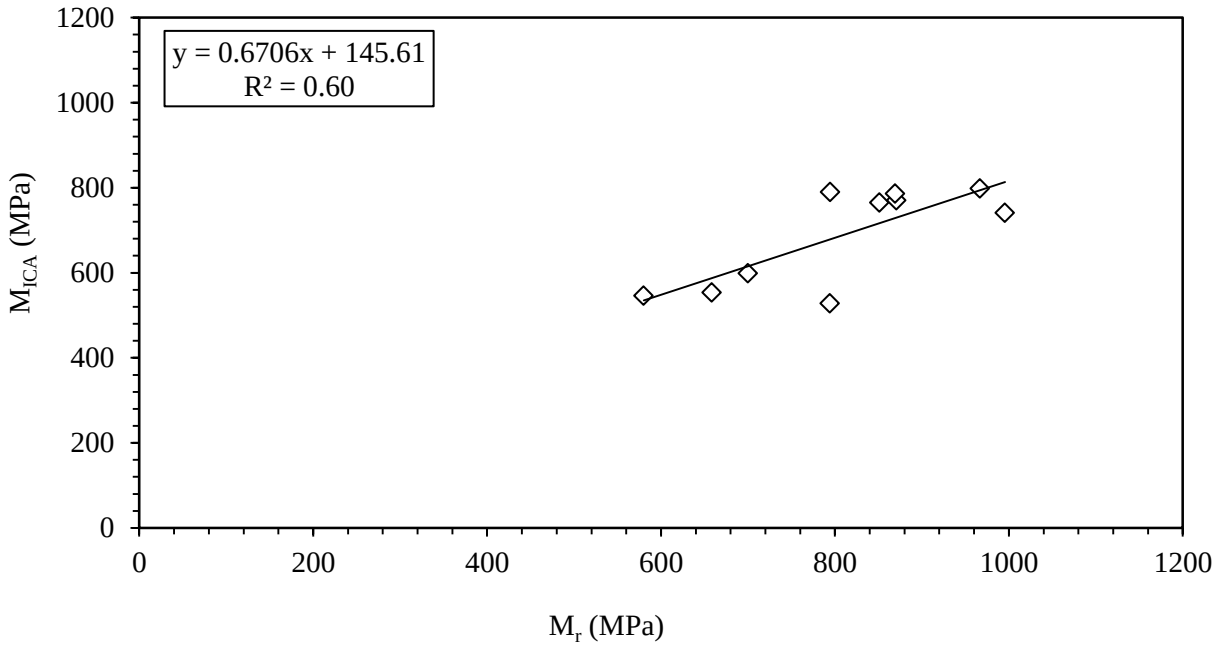

Figure 5.5 Correlation between ICA estimated moduli and laboratory resilient moduli for test locations in Project 2

5.4 Project 3 (I35 Norman, Ok)

5.4.1 Description of Project

The ability of the ICA as a quality control tool was investigated in the third project of this research. The project involved the construction of a 640 meters (2100 ft) long full-depth asphalt pavement on the Northbound section of I35 near Main St., Norman, OK. The subgrade soil was stabilized by mixing 12 % CKD to a depth of 200 mm (8 inches). The subgrade compaction was performed by a pad foot roller (IR SD 100) followed by a steel drum roller (IR SD 100) for proof-rolling.

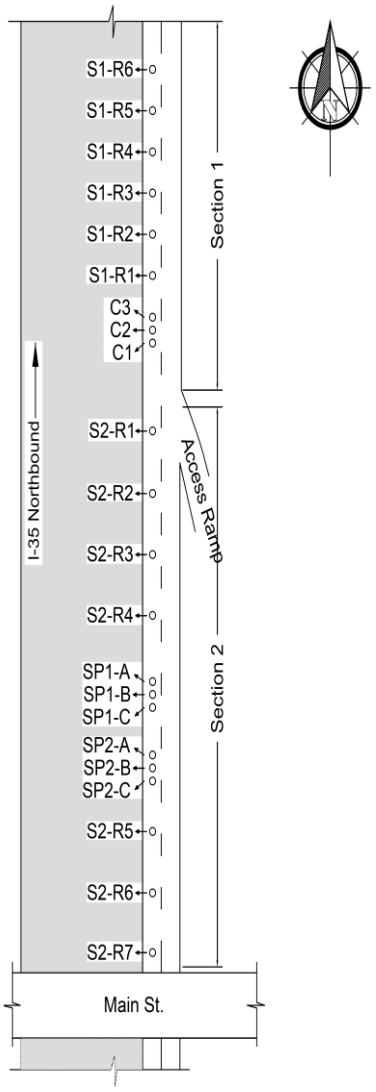

Figure 5.6 Schematic of different test locations in I-35 project.

Figure 5.7 ICA compaction procedure in progress.

The procedure discussed in Chapter 4 was employed for calibration and testing of the project. One important inclusion in this project was the use of ICA as a real time quality control tool during compaction. During compaction, it was used to identify the undercompacted regions so that they can be addressed and remedied. In order to accomplish this, the ICA measurements were recorded and monitored continuously during compaction. The as-built maps exhibiting the the stiffness profile of the subgrade was generated in real time and used to identify undercompacted regions. Once such regions were identified, test locations were marked at random in those regions and the Nuclear Density Gauge measurements were taken. Afterwards, remedial compaction was performed to further increase the stiffnes of these regions. Several test locations were marked across the entire subgrade including 6 locations in the undercompacted

regions (Test Locations SP1A-SP1C, SP2A-SP2C in Figure 5.6). The Nuclear Density Gauge readings were taken from each location and used to estimate Resilient Modulus values for the locations. Figure 5.6 shows a schematic of the construction site and test locations marked on the subgrade.

5.4.2 Analysis of Results

At the end of compaction the dry density and moisture content measurements from the selected test locations were recorded using Nuclear Density Gauge (NDG). Table 5.3 shows the NDG measurement values for this project.

Table 5.3 NDG measurements in 25 selected test locations on Project 3.

Test points	Dry density (kN/m^3)	Moisture content (%)
C1	16.45	17.9
C2	16.40	18.2
C3	16.23	18.2
S1-R1	15.36	16.8
S1-R2	15.68	16.1
S1-R3	16.09	16.3
S1-R4	15.14	17.6
S1-R5	15.85	17.8
S1-R6	16.31	16.8
S2-R1	15.41	15.5
S2-R2	16.37	15.3
S2-R3	16.78	16.4
S2-R4	17.20	15.2
S2-R5	16.68	15.3
S2-R6	15.77	16.8
S2-R7	16.59	15.7
SP1-A	16.07	15.9
SP1-B	16.16	17
SP1-C	16.20	15.8
SP2-A	16.48	17.4
SP2-B	16.40	16
SP3-C	16.32	15.6

These dry density and moisture content measurements were used in the regression model developed for this project (Equations 4.13 – 4.15) to estimate the resilient modulus values. The resilient modulus values were compared with the corresponding ICA estimated modulus at each test location. It is shown in Figure 5.8 that the ICA moduli (M_{ICA}) correlate well with the resilient moduli (M_r) of the subgrade ($R^2 = 0.62$).

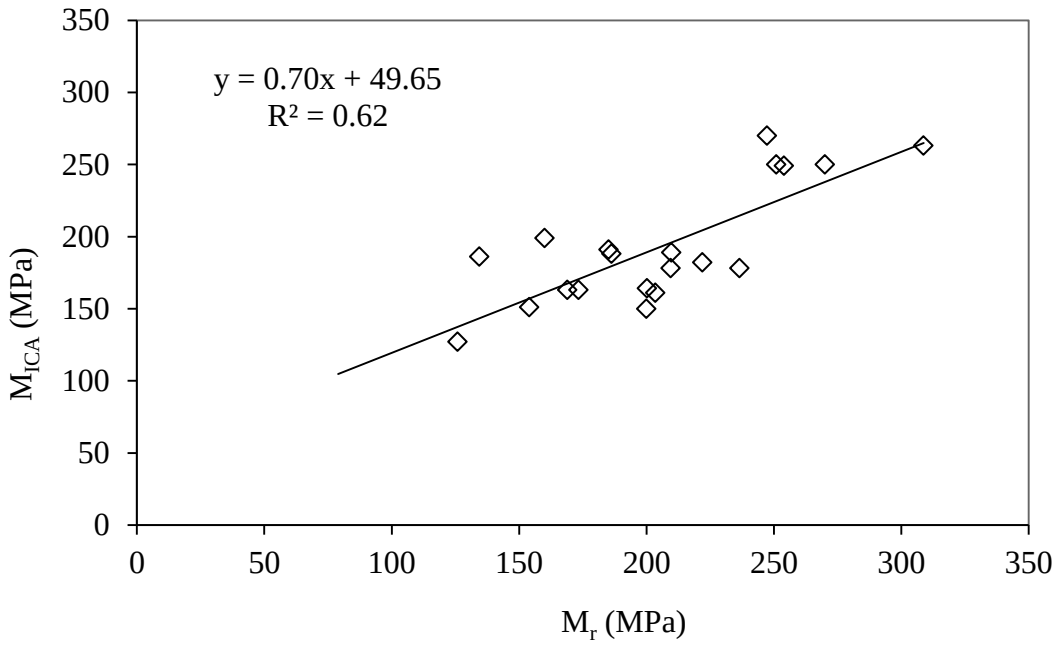

Figure 5.8 Relationship between M_{ICA} and M_r in Project 3.

The improvement in the stiffness of the identified undercompacted region was also studied in this research. Figure 5.9 shows a comparison of the ICA modulus values before and after remedial compaction in the selected test locations of that region. It is observed from the figure that after remedial compaction, the stiffness values of the test locations were improved. In addition to that, the stadndard deviation of stiffness values around a 1 meter vicinity of each test location was seem to decrease. Therefore, it can be said that proper remediation of undercompacted regions not only improved the

quality of subgrade but also increased the uniformity in the compaction of overall subgrade.

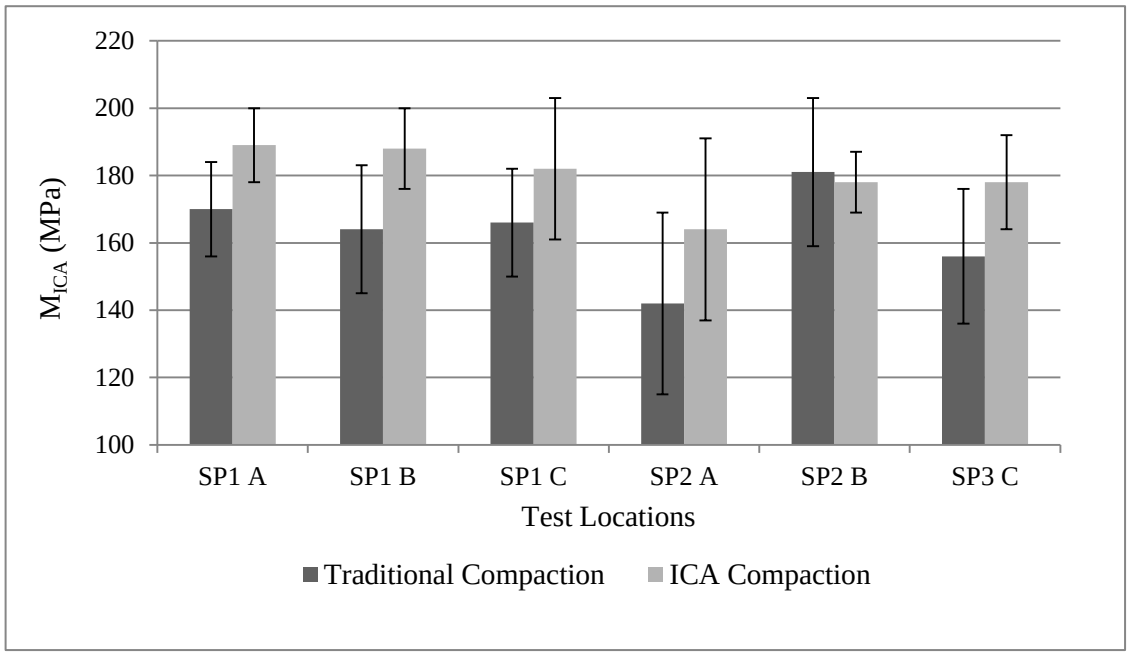

Figure 5.9 Improvement of stiffness after remedial rolling over test locations of the undercompacted regions in Project 3.

5.5 Project 4 (I-35 SERVICE ROAD)

5.5.1 Description of Project

The final ICA demonstration of this research was performed on a 300-m long stretch on the I-35 Service Road. It is located at the University Park area of North-West Norman, Oklahoma. This Service Road is situated on the east side of the I-35 and connects I-35 and NW 24th Avenue. The subgrade was pre-treated by adding 3% quick lime. The average moisture content of the soil during the mixing of quick lime was 22%. The lime-treated soil was subsequently stabilized by mixing 12% CKD to a depth of 202 mm (8 inches) after a 14-day curing period, under ambient conditions.

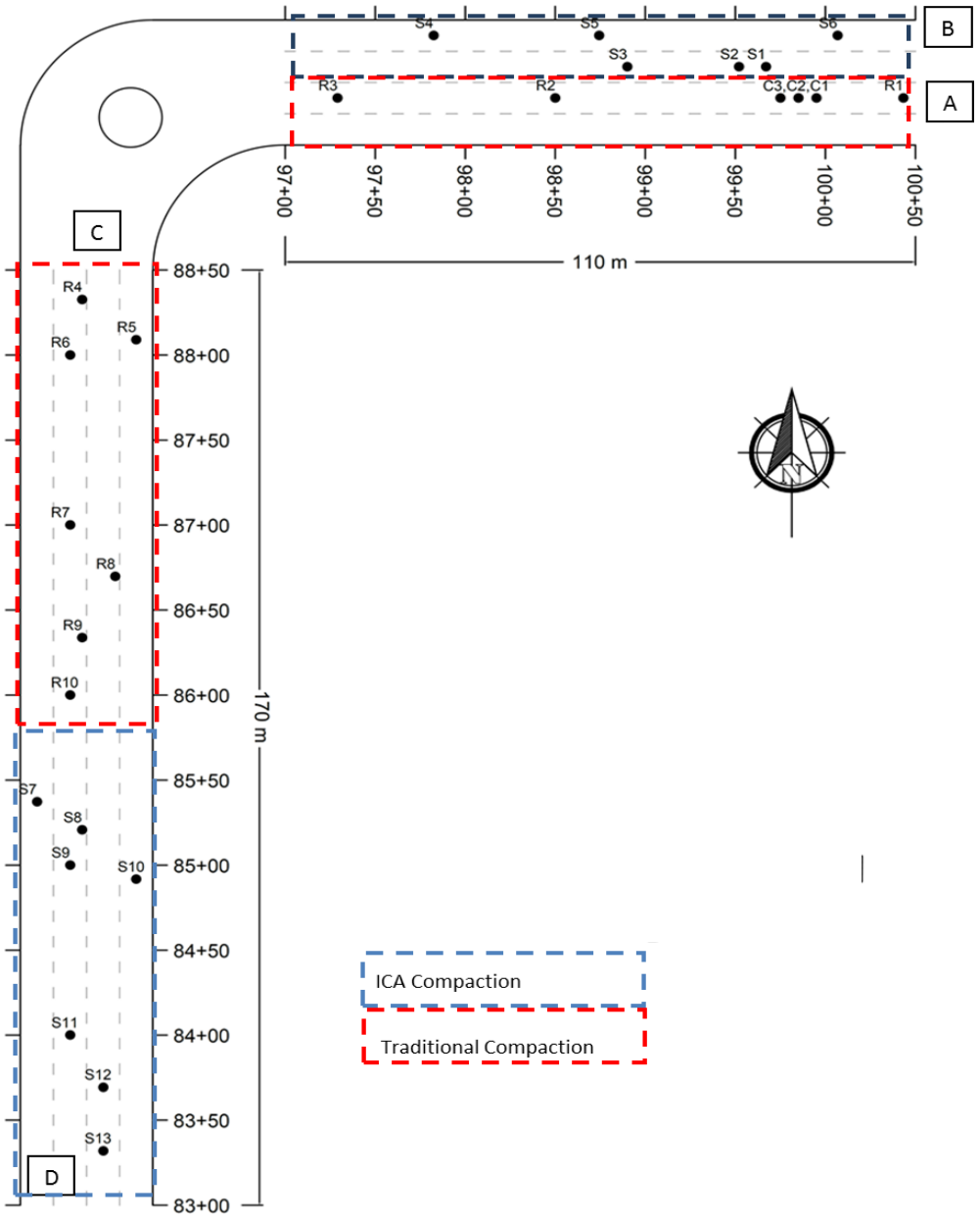

Figure 5.10 Schematic of test locations in Project 4.

5.5.2 Analysis of Results

The ability of ICA in estimating the stiffness of the subgrade was examined in this project. For this, the dry density and moisture content measured at randomly selected test locations were used in the regression model (Equations 4.13 – 4.15) to get the

resilient modulus values. The dry density and moisture content data for the test locations are given in Table 5.4. The resilient modulus values were then compared with the ICA estimated values recorded during compaction process at this project. Figure 5.11 shows that a good correlation is found between the ICA moduli and resilient moduli.

The applicability of the ICA in real time identification of the undercompacted regions during compaction was also examined during investigation in Project 4. Figure 5.10 shows a schematic of the subgrade. In this project the ICA was used to monitor the real time stiffness values during compaction in order to identify the undercompacted areas of the subgrade. In Figure 5.10 the area inside the blue box was identified as regions with low subgrade stiffness according to the estimates provided by the ICA. Seven different test locations were marked in the blue area. The rest of the subgrade was marked red where 19 more test locations were marked. Nuclear density gauge was used to measure the dry density and moisture content in all the test locations (Table 5.4 and 5.5). It is shown in Table 5.4 and 5.5 that the average dry density was significantly lower in the blue region in comparison to the red region (Commuri et al., 2014).

The identification of undercompacted area (blue area) in real time provided the opportunity to perform remedial compaction in order to improve its stiffness. Table 5.5 shows the Nuclear Density Gauge readings of the test locations in blue area before and after the remedial compaction. It is observed that the average density can be improved and nonuniformity in compaction can be decreased by remedial compaction. Figure 5.12 shows the increase in ICA moduli in the seven selected locations of the blue area

after remedial compaction. Figure 5.13 shows the improvement in stiffness profile of a 50 meter stretch in the blue area after remedial compaction.

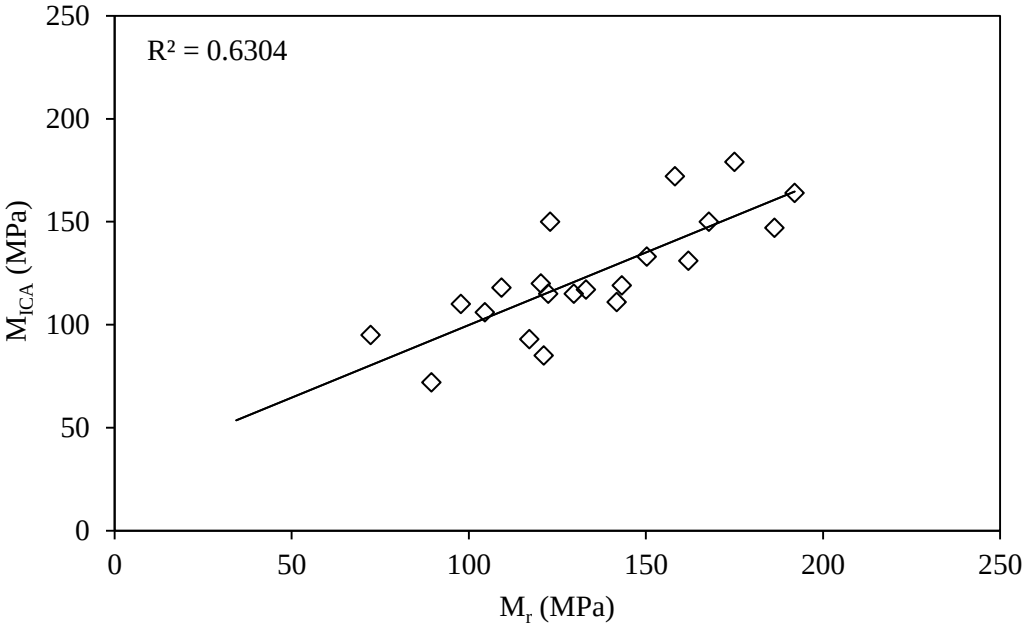

Figure 5.11 Comparison between ICA moduli (M_{ICA}) and laboratory resilient moduli (M_r) for Project 4.

Table 5.4 NDG measurements in 19 test locations on Project 4.

Test Location	Degree of compaction (%)	Moisture content (%)
C1	101.3	19.4
C2	99.9	20.6
C3	95.5	22.4
R1	100.1	21.2
R2	96.4	20.2
R3	97.4	18.4
S1	96.1	24
S2	92.7	25.5
S3	97.1	21.5
S4	93.9	21
S5	96.2	23.7

S6	93.6	23.9
R4	95.9	20.7
R5	91	21.8
R6	94	23
R7	94.7	21.5
R8	97.7	21.6
R9	97	19.8
R10	91.5	21
Average	95.9	21.6
Std. Dev.	2.8	1.8

Table 5.5 Nuclear Density Gauge measurements on selected test locations of undercompacted region in Project 4.

Test Location	**Before remedial passes**		**After remedial passes**	
	Degree of compaction (%)	**Moisture content (%)**	**Degree of compaction (%)**	**Moisture content (%)**
S7	93.4	22.2	87	20.7
S8	89.5	20.7	93.4	21.9
S9	92	21.4	89.8	23.1
S10	93.1	21.9	89.5	20.8
S11	89.8	21.9	89.4	21.4
S12	82.5	20.8	93.1	23
S13	89.4	17	98.1	21.9
Average	90	20.84	91.5	21.8
Std. Dev.	3.42	1.66	3.41	0.89

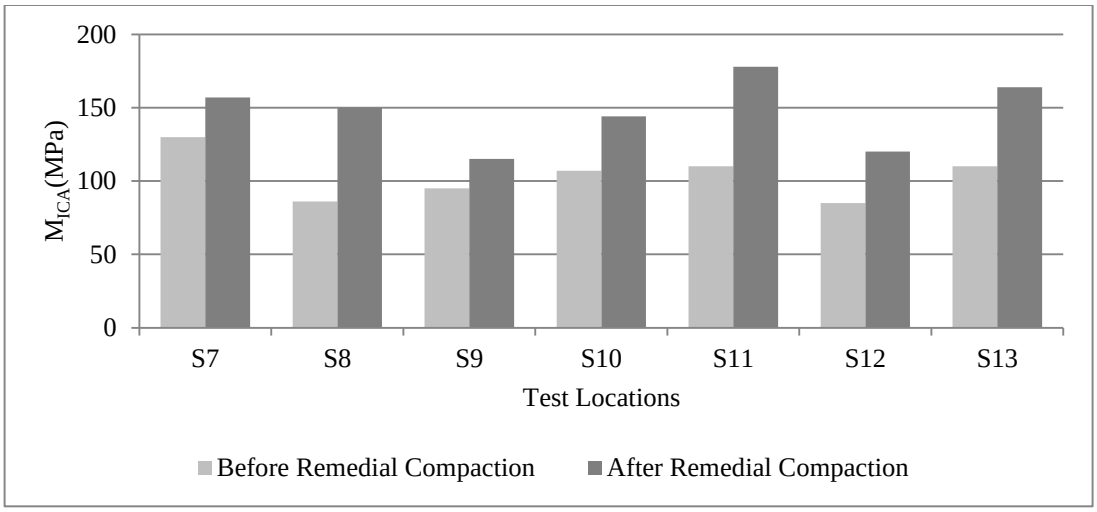

Figure 5.12 Improvement of Stiffness in selected test locations of the identified under compacted region.

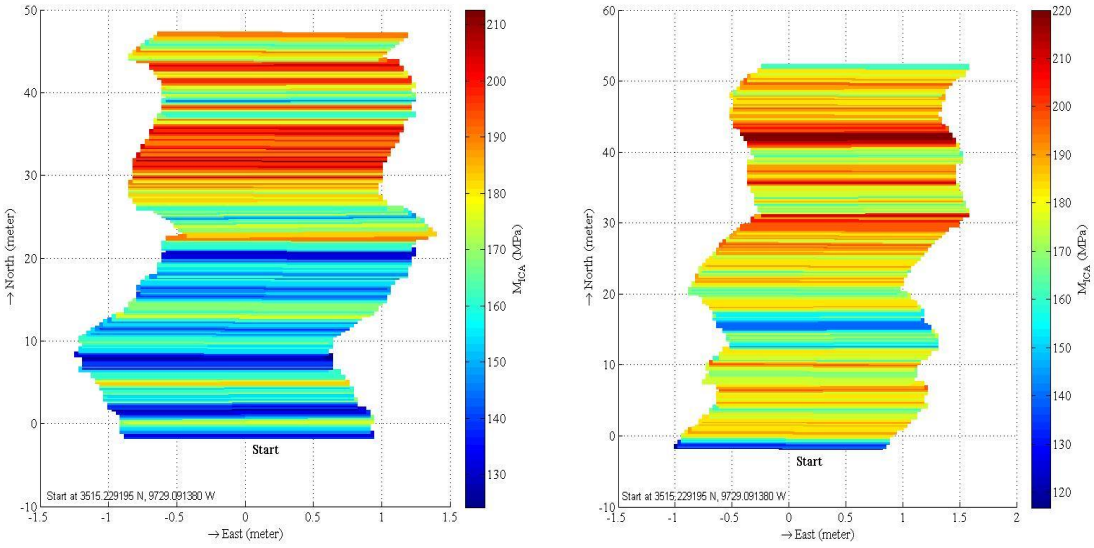

(a) (b)

Figure 5.13 Stiffness profile of a 50 meter stretch in an under compacted region of Project 4 (a) before remedial passes (b) after remedial passes.

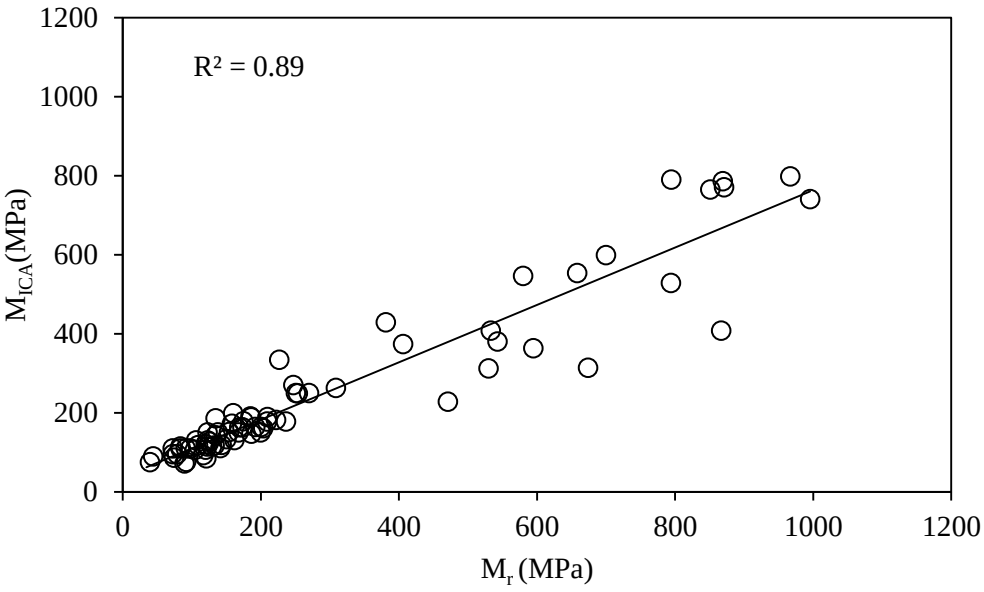

Figure 5.14 Comparison between combined ICA estimated moduli and laboratory resilient moduli for all project locations.

5.6 Conclusions of the Chapter

The application of the Intelligent Compaction Analyzer in estimating the resilient modulus of stabilized subgrade was demonstrated in this chapter. In addition, the feasibility of identification and remediation of under compacted regions in the subgrade was also examined. Four case studies were considered to demonstrate the application of the ICA. In the first project, the ICA was validated with FWD modulus data. In the rest of the projects, the verification was performed with resilient modulus values obtained from field measurements and laboratory test results. It was shown that the ICA estimated values correlates well with both the FWD and resilient modulus values. It is also interesting to note that when the correlations between the ICA modulus and laboratory resilient modulus was studied by combining the data points from for all the

subgrade compaction related projects, the correlation significantly improves as shown in Figure 5.14. The R^2 for the correlation is 0.89.

In the last two projects, the ICA was utilized detect the undercompacted regions so that remedial actions can be taken to improve the quality of these regions. Results showed that the ICA was able to determine such poor quality regions in real time. Remedial rolling in those regions showed that the level of compaction can be improved if they are properly and timely addressed during compaction.

CHAPTER 6 Conclusions and Future Work

Properly compacted subgrade and asphalt pavement layers are necessary in order to ensure well performing and long lasting pavements. Early deterioration of pavements through rutting, potholes, cracking etc. can be minimized through proper quality control during construction of pavements. Current Quality Control methods predominantly focus on assessing quality at a few selected locations after the entire pavement is constructed. Such limited tests often cover less than 1% of the entire pavement surface and do not reveal underlying quality issues that could significantly affect the performance and lifetime of the pavement. These tests are also time consuming, costly, destructive in nature and are not available during the construction process when they could be used to improve the quality.

Intelligent Compaction (IC) has emerged in recent years as a means of assessing the stiffness of the pavement continuously and in real-time during the construction process. However, the commercially available IC systems do not report measurements of any physical quantity associated with the design parameters of pavement and cannot be directly verified through in-situ measurements. Since these technologies are supported by limited theoretical research, very little insight can be gained into the compaction of asphalt pavements. The research on asphalt pavements is mostly geared towards understanding the long term behavior of pavement and not the compaction of asphalt layers using a vibratory roller. Therefore, the systematic development of IC technology requires the modeling of asphalt-roller interaction dynamics during compaction to understand the effect of mix and other process parameters on the compaction that is achieved.

The above mentioned problem in guaranteeing quality during construction and the ability to model and study the effect of different process parameters have been addressed in this dissertation.

6.1 Conclusions of Research

In this dissertation, the problems of overcoming the limitations of IC technologies in both asphalt and subgrade compaction are approached. In case of asphalt compaction, a mathematical model is developed to study the interaction between a moving vibratory roller and the underlying pavement. It is the first time that the development and validation of such a model has been reported in the literature! For subgrade compaction, an Intelligent Compaction method is presented for real time quality estimation of subgrade. This is a first as well! The technique developed in this thesis allows for modulus of subgrade to be estimated and verified using in place tests. The modulus is reported in terms of design modulus (resilient modulus) which also has been accomplished for the first time! The use of the estimated modulus in improving the quality of the compacted subgrade was also verified during field compaction. A brief summary of both the research outcomes and contributions is given below.

6.1.1 Asphalt-Roller Interaction Model

- The dynamical model that was developed to represent the interaction between the roller and the pavement was validated through numerical simulations and comparison with field data. The model is computationally tractable and well suited for numerical simulations.

- The interaction model is capable of taking into account different rheological and volumetric properties of asphalt mix including mix temperature, effective binder content, gradation of aggregates in the asphalt mix, thickness and density of pavement, and roller parameters such as operating frequency, eccentric force, frame-drum coupling, and masses.
- The model parameters can be easily obtained from experimental results and manufacturer's specification.
- Simulation results showed that the model is capable of incorporating the effect of mix temperature on the compaction of pavement.
- Spectral analysis of vibratory response of the drum showed that the model is able to represent the vibratory response characteristics of the drum during compaction in not only the fundamental frequency but also in the harmonics as well.
- The model is also shown to accurately replicate the pass by pass densification process that is observed in the field.
- Comparison with two different field compaction results demonstrated that the model is capable of accommodating different compaction scenarios.
- Although the model is based on the assumption of a rigid base underneath the asphalt layer, the model can easily incorporate the effect of flexible base.
- The model is extended, in a later part of this research, to be able to incorporate the effect of longitudinal shear during compaction. Using field compaction data, it was shown that the model can represent the drum vibratory response observed in the field in both the vertical and longitudinal direction.

- Studies also indicate that the model can reflect the effect of pavement density on the vibration of the drum.
- Simulation results also indicate that the model can be used to demonstrate the compaction of asphalt pavement using a traditional rolling pattern.

6.1.2 Intelligent Compaction Analyzer for Subgrade Quality Estimation

- An artificial neural network based Intelligent Compaction system for real time estimation of subgrade stiffness is developed in this research. It is a continuation of the Intelligent Compaction research conducted by the researchers at the University of Oklahoma.
- The system is able to identify the different vibration patterns that are manifested due to the coupled vibratory interaction between the roller and the subgrade. The difference in stiffness of the subgrade influences the coupled vibratory response and result in different vibration patterns.
- A complete procedure to utilize the system as a real time quality control tool during subgrade compaction is developed. The methods to train and calibrate the system using field compaction results and subgrade properties are also presented.
- Unlike the contemporary Intelligent Compaction systems which indicate the subgrade stiffness in terms of their system specified dimensionless quality indicators, the ICA provides stiffness values in terms of modulus values which can be verified using in situ measurement devices such as Falling Weight Deflectometer, Nuclear Density Gauge etc.
- The ICA moduli can also be validated by comparing them with the laboratory equivalent resilient modulus for the stabilized subgrade.

- The performance and applicability of the system was evaluated in four different field investigations.
- Investigation results showed that the ICA moduli values correlate well with the FWD moduli and laboratory resilient moduli that are obtained from field measurements. The correlation coefficient is more than 60% in each individual case which is encouraging if compared with the contemporary research.
- The system is able to generate as-built map that provides complete stiffness profile of the compacted subgrade as oppose to the traditional quality control methods which provide spot testing results.
- One important finding from this research is that the ICA can be used to identify and remedy under-compacted regions during the construction of pavements. In two subgrade compaction projects (I-35 near Main St. and I-35 Service Road projects), it was shown that the stiffness of the under compacted regions can be improved. The level of compaction in the entire project stretch was also more uniform when the ICA compaction procedure was followed.

6.2 Scope and Recommendations for Future Work

The research conducted in this dissertation was aimed at advancement of Intelligent Compaction (IC) technology to help facilitate the quality control process during compaction of asphalt pavement and the underlying subgrade. One of the long term targets of IC research is to automate the quality control procedure by providing feedback control of roller compaction effort so that the roller can alter its compaction force in real time based on the quality of the underlying pavement. Real time estimation of quality and consequent adjustment of vibratory force will be needed to accomplish

this goal. The implementation of real time feedback control requires understanding of the compaction dynamics and a computationally tractable representation of the system. The model developed in this dissertation can be used as a foundation for the research on feedback control.

The Interaction model was shown to be able to capture the dynamical behavior of the roller and the asphalt pavement during compaction. However, this model is based on some assumptions and its performance and applicability can be improved by addressing some of the following issues

- The model is developed considering a single layer of asphalt on top of a base layer. The compaction of multilayered pavement can be considered in future.
- For simplicity of computation, the contact area is assumed to be constant during compaction. In future research, studies can be performed to estimate contact area based on the roller and asphalt stiffness properties.
- Since during field compaction process the amplitude and frequency of compaction force remain constant, the model was simulated using compaction force with constant frequency and amplitude. The effect of variation of eccentric compaction force can be addressed in future research.
- The model incorporated the interaction of roller and asphalt pavement in the vertical and longitudinal direction only. The effect of lateral shear flow is not taken into account. Future research can be aimed at overcoming this limitation.

Field investigation results showed that the ICA developed in this dissertation can be used in conjunction with existing quality control methods for subgrade compaction. The following recommendations are made to leverage the results of this research.

- The ICA technology needs to be demonstrated on more construction sites with different soil and additive types to study the influence of these parameters on the ICA-estimated compaction quality parameter (ICA modulus of subgrade).
- The necessary specification or a special provision has to be developed for Intelligent Compaction of stabilized subgrades.
- Further research has to be carried out to study the long-term benefits of the Intelligent Compaction.

References

Åkesson, F. (2008). *Dynapac Compaction Analyzer and Optimizer*, Presentation, Dynapac, Dallas, TX: Transportation Pooled Fund Intelligent Compaction Systems initial-Task Working Group meeting.

Allen, D. L.; Schultz, D. B.; and Willett, D. A. (2003). *Evaluation of non-nuclear density gauges*. Research Rep. KTC-03-24/FR115-01-1F, KY. Transportation Center, Univ. of Kentucky, Lexington, KY.

American Association of State Highway and Transportation Officials (AASHTO, 2007). "Bulk Specific Gravity Of Compacted Bituminous Mixtures Using Saturated Surface-Dry Specimens." *AASHTO T-166*, Standard Method, Washington, DC: American Association of State Highway and Transportation Officials.

American Association of State Highway and Transportation Officials (AASHTO, 2009). *Rough Roads Ahead, Fix Them Now or Pay for It Later.* Report. National Transportation Research Group.

American Association of State Highway and Transportation Officials (AASHTO, 2014). "Standard Method of Test for Determining the Plastic Limit and Plasticity Index of Soils." *AASHTO T090*, National Research Council, Washington, DC.

American Association of State Highway and Transportation Officials (AASHTO, 2013). "Standard Method of Test for Determining the Liquid Limit of Soils." *AASHTO T089*, National Research Council, Washington, DC.

American Association of State Highway and Transportation Officials (AASHTO, 2012). "In-Place Density and Moisture Content of Soil and Soil-Aggregate by Nuclear Methods (Shallow Depth)." *AASHTO T307*, National Research Council, Washington, DC.

American Association of State Highway and Transportation Officials (AASHTO, 2010). "Standard Method of Test for Moisture -Density Relations of Soils using a 2.5-kg (5.5-lb) Rammer and a 305-mm (12-in) Drop." *AASHTO T99*, National Research Council, Washington, DC.

American Association of State Highway and Transportation Officials (AASHTO,2009). "Standard Method of Test for Determining the Resilient Modulus of Soils and Aggregate Materials." *AASHTO T307*, National Research Council, Washington, DC.

American Association of State Highway and Transportation Officials (*AASHTO, 1993).* "Guide for Design of Pavement Structures." *AASHTO, National Research Council, Washington, DC.*

American Society of Civil Engineers. (ASCE, 2014). *2013 Report Card For America's Infrastructure.*Reston, VA. http://www.infrastructurereportcard.org/a/#p/grade-sheet/gpa (April 6, 2016)

American Trucking Associations (ATA, 2015). *Forecast: ATA U.S. Freight Transportation Forecast to 2026*. http://www.trucking.org/article.aspx?uid=4caa8338-9128-40fe-ab45-c6fb0c24e417 (April 6, 2016)

AMMANN. (2016) "Ammann Compaction Expert." AMMANN, Switzerland. <http://www.ammann-group.com/en/home/technology/intelligent-ground-compaction/> (last accessed April 6, 2016).

Anderegg, R., and Kaufmann, K. (2004). "Intelligent Compaction with Vibratory Rollers: Feedback Control Systems in Automatic Compaction and Compaction Control." *Soil Mechanics 2004* (Transportation Research Record), no. 1868, 124-134.

Anderegg, R., Von, D., and Kaufmann, K. (2006). "Compaction Monitoring Using Intelligent Soil Compactors." *GeoCongress 2006: ASCE Geotechnical Engineering in the Information Technology Age.* Atlanta, GA.

ARA, Inc. (2004). *Guide for Mechanistic–Empirical Design of New and Rehabilitated Pavement Structures*, Final Report. NCHRP Project 1-37A.

Arasteh, M. (2007). "Innovations in Compaction Control and Testing." *Intelligent Compaction 2007 Construction Conference,* Federal Highway Administration, Bishmark, ND.

Barman, M., Imran, S.A., Nazari, M., Commuri, S. and Zaman, M. (2015) "Intelligent Compaction of Stabilized Subgrade of Flexible Pavement," *International Foundations Congress and Equipment EXPO, IFCEE-2015,* San Antonio, Texas. March 17-21, 2015, Published in the ASCE Geotechnical Special Publication No. 256, IFCEE 2015 © ASCE 2015, pp 2554-2566.

Beainy, F., Commuri, S., and Zaman, M. (2012). "Quality Assurance of Hot Mix Asphalt Pavements Using the Intelligent Asphalt Compaction Analyzer." *Journal of Construction Engineering and Management*, ASCE, 138(2), 178-187.

Beainy, F., Commuri, S., Zaman, M., and Imran, S. (2013a). "Viscoelastic-Plastic Model of Asphalt-Roller Interaction." *International Journal of Geomechanics*, ASCE, 13(5), 581-594.

Beainy, F., Commuri, S., and Zaman, M. (2013b). "Dynamical Response of Vibratory Rollers during the Compaction of Asphalt Pavements." *J. Eng. Mech.*, ASCE, 140(7).

BOMAG. (2016) "Systems for soil and asphalt compaction- Variocontrol." BOMAG, Boppard, Germany. http://www.bomag.com/world/en/variocontrol.htm (April_06, 2016).

Bonaquist, R., and Christensen, D. (2005). "Practical Procedure for Developing Dynamic Modulus Master Curves for Pavement Structural Design." *Journal of the Transportation Research Board* (Transportation Research Board of the National Academies), 1929, 208-217.

Bouc, R. (1967). "Forced vibrations of a mechanical system with hysteresis." *Proceedings of the 4th conference on non-linear oscillation*, Prague, Czechoslovakia, pp. 315.

Briaud, J. L., and Seo, J. (2003). "Intelligent compaction: Overview and research needs." Texas A&M Univ., College Station, TX.

Brown, E.; Kandhal, P. S.; Roberts, F. L.; Kim, Y.; Lee, D.; and Kennedy, T. (2009). "Hot Mix Asphalt Materials, Mixture Design, and Construction." *NAPA Research and Education Foundation*, Third Edition, pp. 60, 321-384, 459.

Burnham, T.R. (1997). *Application of the Dynamic Cone Penetrometer to Minnesota Department of Transportation Pavement Assessment Procedures.* Report No. MN/RD- 97/19. Minnesota Department of Transportation, St. Paul, M. N.

Camargo, F., Larsen, B., Chadbourn, B., Roberson, R., and Siekmeier, J. (2006). "Intelligent Compaction: A Minnesota Case History." *54th Annual University of Minnesota Geotechnical Conference*.

Chang, G., Xu, Q., Rutledge, J., Horan, R., Michael, L., White, D., and Vennapusa, P. (2011). "Accelerated Implementation of Intelligent Compaction Technology for Embankment Subgrade Soils, Aggregate Base, and Asphalt Pavement Materials." *FHWA-IF-12-002*. Federal Highway Administration, Washington D.C.

Chang, G., Xu, Q., Rutledge, J., and Garber, S. (2014). "A study on Intelligent Compaction and In-Place Density" *FHWA-HIF-14-017*. Federal Highway Administration, Washington D.C.

Chang, K.G. and Meegoda, J.N. (1997). "Micromechanical Simulation of Hot Mix Asphalt." *Journal of Engineering Mechanics*, Vol. 123, 495-503

Chen, J. (2011). *Discrete Element Method (DEM) Analyses for Hot-Mix Asphalt (HMA) Mixture Compaction.* PhD Dissertation, University of Tennessee.

Chen, J., and Huang, L. (2000). "Developing an Aging Model to Evaluate Engineering Properties of Asphalt Paving Binders." Journal of Materials and Structures (Springer), 33(9), 559-565.

Cominsky, R., Killingsworth, B., Anderson, M., Anderson, D., and Crockford, W. (1998). *Quality Control and Acceptance of Superpave-Designed Hot Mix Asphalt*. Washington, DC: National Research Council.

Commuri, S., and Zaman, M. (2008). "A novel neural network-based asphalt compaction analyzer." *International Journal of Pavement Engineering* (Taylor & Francis), 9(3), 177-188.

Commuri, S., and Zaman, M. (2010). "Method and apparatus for predicting the density of asphalt." *USPTO, 7,669,458*, March 02, 2010.

Commuri, S., Zaman, M., Barman, M., Nazari, M., Imran, S.A., Beainy, F. (2014*). Evaluation of Performance of Asphalt Pavements Constructed using Intelligent Compaction Techniques*, Final Report for project ODOT SP&R Item #2246, submitted to Oklahoma Department of Transportation, Oklahoma City, USA, December.

Connolly, C. (2008). *Asphalt Manager Intelligent Compaction.* Presentation, Bomag, Dallas, TX: Transportation Pooled Fund Intelligent Compaction Systems initial Task Working Group meeting.

CTC & Associates (CTC) (2006). *Intelligent Compaction of Soils.* Madison, WI: WisDOT Research & Communication Services Wisconsin Highway Research Program.

Dave, E.; Buttlar, W.; Paulino, G.; and Hilton, H. (2006). "Graded Viscoelastic Approach for Modeling Asphalt Concrete Pavements." *Proceedings of the International Conference FGM IX*, American Institute of Physics, 736-741, Oahu Island, Hawaii.

Davisch, P., Camargo, F., Larsen, B., Roberson, R., and Siekmeier, J. (2006). *Validation of DCP and LWD Moisture Specifications for Granular Materials.* Minnesota Department of Transportation Research Services Section, St. Paul, Minnesota.

Dubravka, S., and Davor, H. (2008). “Simulation on vibratory roller-soil interaction.” Int. J. Adv. Eng., 2(1), 137–146.

Dynapac (2016). “Dynapac Compaction Analyzer.” Dynapac, Wardenburg, Germany. http://www.intelligentcompaction.com/downloads/presentation/Akesson_Dynapac%20I.pdf (last accessed March. 21, 2016).

Dynapac (2009). “Dynapac CC422V ibratory Smooth Drum Roller.” Specification Sheet. http://www.admarsupply.com/filehandler.ashx?x=3035 (March 3, 2016).

Federal Highway Administration (FHWA, 2014). *Intelligent Compaction*. U.S. Department of Transportation. http://www.fhwa.dot.gov/construction/ictssc/pubs/hif13053.pdf (Feb. 05, 2016).

Federal Highway Administration (FHWA, 2015). *Traffic Volume Trends December 2015*. Washington, DC. https://www.fhwa.dot.gov/policyinformation/travel_monitoring/15dectvt/15dectvt.pdf (April 6, 2016)

Federal Highway Administration (FHWA, 1999). *Pavement Design Considerations.* Washington, DC. https://www.fhwa.dot.gov/pavement/cfr06261.cfm (April 6, 2016).

Goh, S., You, Z., Williams, C., and Li, X. (2011). "Preliminary Dynamic Modulus Criteria of HMA for Field Rutting of Asphalt Pavements: Michigan’s Experience." *ASCE Journal of Transportation Engineering*, 137(1), 37-45.

Guler, M.; Bosscher, P.J.; and Plesha, M.E. (2002). “A porous elasto-plastic compaction model for asphalt mixtures with parameter estimation algorithm.” *Geotechnical Spacial Publication*, 123, 126–143.

Herbert, W., and Jennette, R. (2011). *Benefit Analysis of Nondestructive Testing For Roadway Management*. Project Number: MQP-MGE-JMM-0411, Worcester, MA; Worcester Polytechnic Institute.

Hertz, H. (1895). *Über die Berührung fester elasticscher Körper, Gesammelte Werke*, Bd. 1. Leipzig.

Huerne, H.L. (2004). “Compaction of Asphalt Road Pavements.” *PhD Dissertation*, University of Twente, Netherlands.

Imran, S., Beainy, F., Commuri, S., and Zaman, M. (2014). “Dynamical Model of Asphalt-Roller Interaction During compaction.” *11th InternationalConference on Informatics in Control, Automation and Robotics,* 1, 559-567.

Imran, S., Commuri, S., and Zaman, M. (2015). “A 2 Dimensional Dynamical Model of Asphalt-Roller Interaction During Vibratory Compaction.” *Proceedings of the 12th International Conference on Informatics in Control, Automation and Robotics*, pp. 533-540, Colmar, Alsace, France.

Ingersoll Rand, (2007). *DD 118HF Large Asphalt Compactors.* Specification Sheet. http://www.volvoce.com/SiteCollectionDocuments/VCE/History/11C__asphalt%20compactors/03%20Ingersoll%20Rand/IR%20DD-118HA%20HF%20HFA/IR%20DD-118HF%202%2015-0022-07xx.pdf (March 23, 2016).

Kassem, E.; Scullian, T; Masad, E.; Chowdhury, A.; Liu, W.; Estakhri, C.; and Dessouky, S. (2012). Comprehensive evaluation of compaction of asphalt pavements and a practical approach for density predictions. Transportation Research Record: *Journal of the Transportation Research Boar*d, 2268, 98–107.

Kröber, W., Floss, R., and Wallrath, W. (2001). “Dynamic soil stiffness as quality criterion for soil compaction.” *Geotechnics for roads, rail tracks, and earth structures*, A. Gomes Correia and H. Brandl, eds., Balkema, Lisse, Netherlands.

Koneru, S.; Masad, E.; and Rajagopal, K.R. (2008). “A thermodynamical framework for modeling the compaction of asphalt mixes.” *Mechanics of Materials*, 40 (10), 846–864.

Krishnan, J.M., and Rao, C.L. (2000). “Mechanics of Air Voids Reduction of Asphalt Concrete Using Mixture Theory,” *International Journal of Engineering Science*, 38(12), 1331–1354.

Lavin, P. (2003). *Asphalt pavements: A practical guide to design, production and maintenance for engineers and architects*, Spon, New York.

Liu, Y., and You, Z. (2009). "Determining Burger’s Model Parameters of Asphalt Materials using Creep-recovery Testing Data." *Pavements and Materials: Modeling, Testing, and Performance*, Geotechnical Special Publication No. 184, 26-36.

Liu, Y., Qingli, D., and You, Z. (2009). "Viscoelastic Model for Discrete Element Simulation of Asphalt Mixtures." *Journal of Engineering Mechanics*, ASCE, 135(4), 324-333.

Lundberg, G. (1939). *Elastische Berührung zweier Halbräume, Forschung, auf dem Gebiete des Ingenieurwesens*, Band 10, Göteborg, 201–211.

Margreta, M.; Ford, C.; and Grube, R. (2014). *U.S. Freight on the Move: Highlights From the 2012 Commodity Flow Survey Preliminary Data*. Special Report. Bureau of Transportation Statistics. U.S. Department of Transportation. Washington, DC.

Masad, E., Koneru, S.; Scarpas, T., Kassem, E., and Rajagopal, R. (2010). *Modeling of Hot-Mix Asphalt Compaction: A Thermodynamics-Based Compressible Viscoelastic Model*. Final Report, Washington, DC: Federal Highway Administration.

Masad, E. , Scarpas, A. , Rajagopal, K. , Kassem, E. , Koneru, S. , and Kasbergen, C. (2014). "Finite element modeling of field compaction of hot mix asphalt. Part II: Applications." *Int. J. Pavement Eng.*, 1–15.

Mathworks (2013). "Simulink: Simulation and Model based Design". http://www.mathworks.com/products/simulink/ (March 23, 2016).

Maupin, G. W. (2007). *Preliminary field investigation of intelligent compaction of hot-mix asphalt.* Final Report No. VTRC-08-R7, Virginia Transportation Research Council, Virginia DOT, Charlottesville, VA.

Micaelo, R., Ribeiro, J., Azevedo, M., and Azevedo, N. (2009). "Discrete Element Modelling of Field Asphalt Compaction." *Sixth International Conference on Maintenance and Rehabilitation of Pavements and Technological Control*, Turin, Italy.

Mitra, S. K.(2006) "Digital Signal Processing A Computer Based Approach", 3rd ed., McGraw Hill, New York, NY, pp. 866 - 879

Mitsui, A. (2007). *Vibratory mechanism and vibratory roller*. United States of America Patent 7213479 B2. May 08, 2007.

Mooney, M. A., and Adam, D. (2007). "Vibratory Roller Integrated Measurement of Earthwork Compaction: An Overview." *Proceedings FMGM2007-International Symposium on Field Measurements in Geomechanics*. September 24-27, Boston.

Mooney, M. A., and Rinehart, R. V. (2009). "In-Situ Soil Response to Vibratory Loading and Its Relationship to Roller-Measured Soil Stiffness." *Journal of Geotechnical and Geoenvironmental Engineering*. ASCE, 135(8), 1022–1031.

Mooney, M. A., Facas, N. W., Musimbi, O. M., White, D. J., and Vennapusa, P. K. (2010). *Intelligent soil compaction systems.* NCHRP Rep. 676, National Cooperative Highway Research Program, Washington, DC.

Moore, W. (2006). "Intelligent Compaction: Outsmarting soil and asphalt." *Construction Equipment*, March 31, pp. 39-48.

National Asphalt Pavement Association (NAPA, 2014). *Asphalt Pavement Overview.* http://www.asphaltpavement.org/index.php?option=com_content&task=view&id=14&Itemid=33 (Mar 20, 2016).

Nazzal, M. D., and Mohammad, L. N. (2010). "Estimation of Resilient Modulus of Subgrade Soils Using Falling Weight Deflectometer." *Transportation Research Record: Journal of the Transportation Research Board, No. 2186,* Transportation Research Board of the National Academies, Washington, D.C., 1–10.

Nillson, R.; Hopman, P.; and Isacsson, U. (2002). "Influence of different rheological models on predicted pavement responses in flexible pavements." *Road Materials and Pavement Design: An International Journal*, 3, 117-149.

Pellinen, T. K., and Xiao, S. 2006. *Stiffness of Hot-Mix Asphalt*. Publication FHWA/IN/JTRP 2005/20. Joint Transportation Research Program, Indiana Department of Transportation and Purdue University, West Lafayette, Indiana.

Pellinen, T; and Witczak, M. (2002). "Use of Stiffness of Hot-Mix Asphalt as a Simple Performance Test." *Journal of the Transportation Research Board* (Transportation Research Board of the National Academies), 1789, 80-90.

Petersen, L. (2005). *Continuous Compaction Control MnROAD Demonstration.* Maplewood, MN: Minnesota Department of Transportation.

Peterson, L.; and Petersen, Ryan (2006). *Intelligent Compaction and In-Situ Testing at Mn/DOT TH53.* St. Paul, MN: Minnesota Department of Transportation.

Pietzsch, D. and Poppy, W. (1992). "Simulation of geomaterial compaction with vibratory roller", *Journal of Terramechanics*, 29(6), pp. 585-597.

Pisarski, A., and Reno, A.; (2016). "2015 AASHTO Bottom Line Report". Resport submitted to *American Association of State Highway and Transportation Officials (AASHTO),* NCHRP Project HR-20-24, Task 086. Washington, DC.

Pronk, A. (2005). "The Huet–Sayegh model: a simple and excellent rheological model for master curves of asphaltic mixes." *Proceedings of the R.Lytton symposiumonmechanics of flexible pavements.* Baton Rouge, LA.

Rahman, F. Hossain, M., and Romanoschi, S. A. (2008). *Intelligent Compaction Control of Highway Embankment Soil in Kansas*. Final report, K-TRAN: KSU-06-7, Kansas Department of Transportation, KS.

Rakowski, S. (2008). *Intelligent Compaction CCV IC.* Presentation, Sakai, Dallas, TX: Transportation Pooled Fund Intelligent Compaction Systems initial-Task Working Group meeting.

Rawls, D.; and Potts, D. (2008). *AccuGrade® Compaction GPS Mapping & Measurement System*. Presentation, Caterpillar, Dallas, TX: Transportation Pooled Fund Intelligent Compaction Systems initial-Task Working Group meeting.

Rinechart, R. V and Mooney, M. A.(2008). "Instrumentation of a Roller Compactor to Monitor Vibration Behavior During Earthwork Compaction." *Automation in Construction, Elseiver*, 17 (2008), 144-150.

Russell, H. S., and Hossain, M. (2000). "Design Resilient Modulus of Subgrade Soils from FWD Tests." *Pavement Subgrade, Unbound Materials, and Nondestructive Testing*, ASCE, 286(6), 87-103.

Sandstrom, A. (1998). *Control of a compacting machine with a measurement of the characteristics of the ground material.* USPTO # 5,727,900, March 17, 1998.

Sandström A. J., and Pettersson, C. B. (2004). "Intelligent Systems for QA/QC in Soil Compaction", *Proc., 83rd Annual Transportation Research Board Meeting*, January 11-14. Washington, DC.

Sakai. (2013). "Compaction Information System." Sakai, GA, USA. <http://www.sakaiamerica.com/technology/intelligent-compaction/> (March. 21, 2016).

Scherocman, J. (2000). *Compaction Hot-Mix Asphalt Pavemens:Part I. Roads & Bridges.* http://www.roadsbridges.com/compacting-hot-mix-asphalt-pavements-part-i (April 06, 2016).

Scherocman, J.; and Dwight, W. (2008). *Factors Affecting Asphalt Compaction.* Asphalt Institute.

Sebesta, S.; Estakhri, C.; Scullion, T.; and Liu, W. (2006). *New technologies for evaluating flexible pavement construction: Year 1 report.* Technical Rep. No. FHWA/TX-06/0-4774-1, Texas DOT, Austin, TX.

Shen, P., and Lin, S. (2008). "Mathematic modeling and characteristic analysis for dynamic system with asymmetrical hysteresis in vibratory compaction." *Meccanica(Springer)*, 43(5), 505-515.

Shenoy, A., and Romero, P. (2002). "Standardized procedure for analysis of dynamic modulus (E*) data to predict asphalt pavement distresses." *Journal of the Transportation Research Board (Transportation Research Board of the National Academies)*, 1789. 173-182.

Siekmeier, J. A., Young, D., and Beberg, D. (2000). "Comparison of the Dynamic Cone Penetrometer with other Tests During Subgrade and Granular Base Characterization in Minneosta, Nondestructive Testing of Pavement and Backcalculation of Moduli." *ASTM STP 1375*, 3, West Conshohocken, P.A.

Thompson, M. (2006). "Intelligent Soil Compaction for Assuring Subgrade Quality." *Greater Iowa Asphalt Conference.* Des Moines, IA: Iowa State University.

Thurner, H., and Sandström, Å. (2000). "Continuous Compaction Control." European Workshop Compaction of Soils And Granular Materials, 237-246, Paris, France.

Vennapusa, P., White, D.J., Morris, M. (2010). "Geostatistical analysis for spatially referenced roller-integrated compaction measurements," *J. of Geotech. and Geoenv. Engr*., ASCE, 136(6), 813-822.

Von Quintus, H. L., Rao, C., Bhattacharya, B. Titi, H., English, R.(2010). *Evaluation of Intelligent Compaction Technology for Densification of Roadway Subgrades and Structural Layers*. Final Report, WHRP Project ID 0092-08-07, Wisconsin Department of Transportation, Madison, WI.

Wen, Y. (1976). "Method for random vibration of hysteretic systems." *J Eng Mech*. 102, 249–263.

White, D. J., Jaselskis, E., Schaefer, V., Cackler, T. (2005). "Real-time compaction monitoring in cohesive soils from machine response." Transp. Res. Rec., 1936, *Journal of the Transportation Research Board*, Washington D.C., 173–180.

White, D. (2006). *Field evaluation of compaction monitoring technology*. Tech Transfer Summary, lowa Highway Research Board, lowa DOT Transportation, Ames, IA.

White, D.J., Vennapusa, P. (2009). Report of the Workshop on Intelligent Technologies for Earthworks, EERC Publication ER09-02, Earthworks Engineering Research Center, Iowa State University, Ames, Iowa.

White House (2014). *Economic Analysis of Transportation Infrastructure Investment.* Washington, DC. https://www.whitehouse.gov/sites/default/files/docs/economic_analysis_of_transportation_investments.pdf (April 6, 2016)

Wisdom, B. (2009). "RoadScience Tutorial: Want Optimum Density? Get Smart." *Road Science*, November 1, 2009.

Woo, W., Chowdhury, A., and Glover, C. (2008). "Field Aging of Unmodified Asphalt Binder in Three Texas Long-Term Performance Pavements." *Journal of the Transportation Research Board* (Transportation Research Board of the National Academies), 2051, 15-22.

Xu, Q.; and Solaimanian, M. (2009). "Modelling linear viscoelastic properties of asphalt concrete by the Huet–Sayegh model." *International Journal of Pavement Engineering*, 10(6), 401-422.

Young, C., and Oetken, N. "AccuGrade." Caterpillar, Illinois, USA. <http://www.intelligentcompaction.com/downloads/TPF/MSIC_OpenHouse_CAT.pdf> (April 6, 2016)

Zapata, C.; and Houston, W. (2008). *Calibration and Validation of the Enhanced Integrated Climatic Model for Pavement Design.* Washington, DC: Transportation Research Board.

Appendix : Notations

A_c = contact area of three asphalt blocks and drum;

C_{vi} , C_{pi} , C_1 , C_2 = constants of integration;

d = length of each block underneath the drum;

d_f = displacement between the i^{th} block and the $(i+1)^{\text{th}}$ block during interaction;

d_b = displacement between the i^{th} block and the $(i-1)^{\text{th}}$ block during interaction;

|E* | = dynamic modulus of asphalt mix;

F_a = reaction force of the asphalt layer;

F_{ec} = vibratory force of the roller;

F_{ecZ} = vertical eccentric force of the roller;

F_{ecX} = horizontal eccentric force of the roller;

F_{xi} = force generated by the shear spring component G_i between the current i^{th} grid element and $(i+1)^{\text{th}}$ grid element;

G_i= stiffness of shear spring component;

g = gravitational acceleration of earth;

K_{aei} = elastic stiffness coefficient of the i^{th} block;

K_{avi} = viscous stiffness coefficient of the i^{th} block;

k_{df} = drum-frame stiffness coefficient;

m_a = asphalt mass;

m_d = mass of the drum;

m_f = mass of the frame;

$m_{ec}r_{ec}$ = moment of the eccentric mass;

T = drum block contact period;

V_a = percentage of air voids in asphalt mix;

w = width of the drum;

z_{a_i} = total displacement of the i^{th} block;

z_d = displacement of the drum;

$\dot{z}_d$ = velocity of the drum;

$\dot{z}_f$ = velocity of the frame;

z_f = displacement of the frame;

$\ddot{z}_d$ = vertical acceleration of the drum;

$\ddot{z}_a$= vertical acceleration of the asphalt pavement;

$\ddot{z}_f$ = acceleration of the frame;

ε_{ei} = elastic deformation of the i^{th} block;

ε_{vi} = viscoelastic deformation of the i^{th} block;

ε_{pi} = plastic deformation of the i^{th} block;

ε_{vi_1} = visco-elastic deformation of the i^{th} block after the first step;

ε_{pi_1} = permanent deformation of the i^{th} block after the first step;

ε_{vi_2} = visco-elastic deformation of the i^{th} block after the second step;

ε_{pi_2} = permanent deformation of the i^{th} block after the second step;

ϕ = phase angle;

η_{df} = drum-frame damping coefficient;

η_{avi}= viscous damping coefficient of the i^{th} block;

η_{api}= plastic damping coefficient of the i^{th} block;

σ_i = force experienced by the i^{th} block;

ω_{ec} = angular frequency of rotation of eccentric mass;